

University of Louisville

ThinkIR: The University of Louisville's Institutional Repository

Electronic Theses and Dissertations

5-2016

The influence of miR-99a on mTOR signaling regulation in colorectal cancer cell lines.

Jonathan Rice

Follow this and additional works at: <https://ir.library.louisville.edu/etd>



Part of the [Digestive System Diseases Commons](#), [Medical Biophysics Commons](#), [Medical Physiology Commons](#), [Neoplasms Commons](#), [Surgery Commons](#), and the [Surgical Procedures, Operative Commons](#)

Recommended Citation

Rice, Jonathan, "The influence of miR-99a on mTOR signaling regulation in colorectal cancer cell lines." (2016). *Electronic Theses and Dissertations*. Paper 2412.
<https://doi.org/10.18297/etd/2412>

This Doctoral Dissertation is brought to you for free and open access by ThinkIR: The University of Louisville's Institutional Repository. It has been accepted for inclusion in Electronic Theses and Dissertations by an authorized administrator of ThinkIR: The University of Louisville's Institutional Repository. This title appears here courtesy of the author, who has retained all other copyrights. For more information, please contact thinkir@louisville.edu.

THE INFLUENCE OF MIR-99A ON MTOR SIGNALING REGULATION IN
COLORECTAL CANCER CELL LINES

By

Jonathan Rice

B.S. (Hons) – The University of Texas at Austin, Austin, TX (2007)

M.D. – The University of Texas Medical Branch, Galveston, TX (2011)

A Dissertation Submitted to the Faculty of the School of Medicine of the University of
Louisville for the Partial Fulfillment of the Requirement for the Degree of
Doctor of Philosophy in Physiology and Biophysics

Department of Physiology and Biophysics

School of Medicine

University of Louisville, KY

May 2016

Copyright © 2016 by Jonathan D. Rice

All rights reserved

THE INFLUENCE OF MIR-99A ON MTOR SIGNALING REGULATION IN
COLORECTAL CANCER CELL LINES

By

Jonathan Rice, M.D.

B.S. (Hons) – The University of Texas at Austin, Austin, TX (2007)
M.D. – The University of Texas Medical Branch, Galveston, TX (2011)

A Dissertation Approved on

May 22, 2015

By the following Dissertation Committee:

Susan Galandiuk, M.D., Dissertation Co-Director

Irving G. Joshua, Ph.D., Dissertation Co-Director

Claudio Maldonado, Ph.D.

Dale Schuschke, Ph.D.

Aruni Bhatnagar, Ph.D.

DEDICATION

This dissertation is dedicated to my parents, Sterling and Vicki, for believing, encouraging, and investing in me throughout my life, my mentor, Dr. Susan Galandiuk, who has given me her time to guide and teach me during my doctoral studies, and Dr. Hiram C. Polk, Jr., from whom I have learned more from during my doctoral studies than most people learn in a lifetime. Dr. Polk, I am forever grateful for our evening meetings to edit papers and review questions, thank you for the life lessons and guidance.

ACKNOWLEDGEMENTS

I am thankful for the opportunity I was given to work in the Price Institute of Surgical Research and to Dr. Irving Joshua for allowing me to undertake my doctoral studies in the Department of Physiology and Biophysics. I am grateful to Dr. Claudio Maldonado, Dr. Aruni Bhatnagar and Dr. Dale Schuschke for their valuable roles as committee advisors. I cannot express enough thanks and gratitude I have for Ms. Sarah Gardner, Mr. Rob Eichenberger, Mr. Henry Roberts and Mr. Michael McClain for their daily input, guidance, help and support with all aspects of my studies.

I would have not made it through these difficult years of my life without Ms. Ashley Ragsdale, Dr. Allison Nitsch, Ms. Kassie Pierce, Dr. Benjamin Stahl, Dr. Jason Younga, Mr. Alain Estephan and Mr. Karl Otto and for this I thank you all.

Finally I would like to thank Dr. Kelly McMasters for allowing me to take the time during my surgical residency to pursue a graduate degree in physiology. Your dedication to advancing surgical research is inspiring. Thank you for allowing me, previous and future residents with this unique opportunity to take dedicated time off from surgical training to pursue the answers to complex basic science questions.

ABSTRACT

THE INFLUENCE OF MIR-99A ON MTOR SIGNALING REGULATION IN COLORECTAL CANCER CELL LINES

Jonathan Rice

22nd May, 2015

Colorectal cancer (CRC) is the third most common cancer worldwide and the fourth most common cause of death. These are staggering statistics for a disease that can essentially be cured if caught early and the pathology is favorable to therapeutic intervention. There is currently a drastic decrease in five year survival as the cancer stage increases from locally confined disease to metastatic disease. These statistics suggest that although some strides have been made with colon cancer screening and early intervention, there is still much room for improvement in both screening and treatment of CRC.

One of the pathways that have been linked to CRC is the mammalian target of rapamycin (mTOR) pathway. Recently this has been the subject of intense study particularly with a view to better targeted drug therapy for colorectal cancer. Much is known about this pathway; however, multiple regulatory elements have yet to be elucidated. MicroRNAs (miRNAs) have been shown to influence some aspects of the mTOR pathway in other cancers, however their role in the mTOR pathway in CRC has

yet to be fully explored. The microRNA-99 (miR-99) family of miRNAs has recently been implicated in regulation of mTOR signaling in other diseases.

Studies were conducted using normal colon epithelial and CRC cell lines provided the following key findings:

1. Transfection of miRNA-99a mimic into CCD-841 (normal epithelium) and CRC cell lines, HT-29 (Dukes C), HCT-116 (Dukes D), results in a decrease in the amount of phosphorylated mTOR protein in all 3 cell.
2. miRNA-99a transfection also affected expression of downstream protein products, with a decrease phosphorylated S6K1 in HT-29 and CCD-841, while this same transfection showed an increase in this phosphorylated protein in cell line HCT-116. The opposite was observed for protein 4EBP1 after transfection, which showed an increase in phosphorylated 4EBP1 in cell lines HT-29 and CCD-841, but a decrease in phosphorylated protein the HCT-116 cell line.
3. Transfection of miRNA-99a mimic resulted in decreased motility and invasion in cell lines HT-29 and HCT-116 as compared to cell lines transfected with the negative control. Transfection with the miRNA-99a antagomir resulted in increased motility in both CRC cells lines but minimal changes or decrease in invasion.

The effects of miRNA-99a on mTOR protein, S6K1 and 4EBP1 were elucidated by this project providing further evidence as to the importance of mTOR inhibition for

possible regulation of CRC metastasis. This supports new avenues of study to further understand CRC metastasis as well as possible targets for therapeutic intervention.

TABLE OF CONTENTS

ACKNOWLEDGMENTS

ABSTRACT

LIST OF TABLES

LIST OF FIGURES

CHAPTER

- I. Colorectal Cancer: a Significant Clinical Problem
 - A. Epidemiology
 - B. Staging
 - C. Screening
 - D. Treatment Options (list first endoscopic, then surgical then for advanced disease)
 - E. Clinical Scenarios Illustrating Limitations of Current Screening Guidelines
 - F. Currently available plasma based biomarkers for colorectal cancer
- II. Preliminary Data : miRNA as Biomarkers for Colorectal Cancer
 - A. miRNA
 - B. Tissue and plasma miRNA in CRC, initial studies
 - C. Plasma miRNA used to detect premalignant lesions (adenomas)
 - D. Difficulties with assay reproducibility
 1. Systematic review
 2. Selection of miRNA for study

3. Patient population
4. Time to plasma extraction
5. Repeated Sample Acquisition
6. Method of RNA extraction
7. Cycle threshold bar setting
8. Intra-operator variability
9. Inter-operator variability
10. Selection of housekeeping gene
11. Discussion

E. Colon Cancer cell lines used to detect miRNA differences between cancers of differing growth rates and metastatic capability

III. Mammalian Target of Rapamycin Signaling Pathway (mTOR)

A. mTOR Complex 1 (mTORC1)

B. mTOR Complex 2 (mTORC2)

C. Regulators of mTORC1

D. Regulators of mTORC2

IV. Hypothesis & Specific Aims

V. Materials and Methods

A. Cell Lines

1. CCD841

2. HT-29

3. HCT-116

- B. Maintenance of Cell Lines
 - 1. Initial culturing of cells
 - 2. Sub-culturing
 - 3. Freezing of cell lines
- C. miRNA Transfection
- D. Harvesting cells for RNA or protein extraction
- E. Polymerase chain reaction
- F. Western Blot
- G. Cell Migration Assay
- H. Cell Invasion Assay

VI. Transfection

- A. Introduction
- B. Data and Results
- C. Discussion

VII. Western Blot Studies

VIII. Specific Aim 1- The effect of miRNA-99a on mTOR protein

- A. Introduction
- B. Data and Results
- C. Discussion

IX. Specific Aim 2- The effect of miRNA-99a on S6K1 and 4EBP1

- A. Introduction
- B. Data and Results

1. S6K1

2. 4EBP1

C. Discussion

X. Specific Aim 3- The effect of miRNA-99a on cell Migration and Invasion

A. Introduction

B. Migration Data and Results

C. Invasion Data and Results

D. Discussion

XI. Final Discussion and Overview

REFERENCES

APPENDIX

LIST OF ABBREVIATIONS

CURRICULUM VITAE

LIST OF TABLES

- Table 1. Colorectal Cancer Staging
- Table 2. 5 year Survival Rates of Colon and Rectal Cancer
- Table 3. Multiple sources of variability in microRNA data and literature search
- Table 4. Systematic review: 74 plasma miRNA publications July 1, 2013 - June 30, 2014.
- Table 5. Effect of Repeated Sample Acquisition. Comparison of mean $\Delta\Delta\text{CT}$'s for various plasma miRNA from plasma samples drawn from the same 7 individuals on the same day 12 hours apart.
- Table 6. Total RNA concentration and purity for Trizol LS and Qiagen miRNeasy with RNA yeast carrier.
- Table 7. Inter-operator variability with two different extraction methods. Differences in $\Delta\Delta\text{CT}$ between Qiagen miRNeasy with RNA carrier and no pre-amplification and Trizol LS with pre-amplification.
- Table 8. Intra-Operator Variability (Duplicates) for the Trizol LS RNA Extraction and Preamplicification Protocol.
- Table 9. Differences in ΔCT between operators with Trizol LS RNA extraction and pre-amplification (inter-operator variability).
- Table 10. Differences in ΔCT between operators with Qiagen miRNeasy with RNA Carrier and No Pre-amplification (Inter-Operator Variability).
- Table 11: Percentage of Housekeeping Gene (HGK) Samples Expressed within Each Group Investigated.
- Table 12. Mean and Standard Deviation of Housekeeping Genes with 100% expression.
- Table 13. Expression data for Housekeeping Genes RNU6 and miR520d-5p
- Table 14. Number of miRNAs expressed in screening array of cell lines ranging from Dukes A-Dukes D.

Table 15. Fold Change and Regulation of miRNA 99 Family in the screening array for colorectal cancer cell lines.

Table 16. Cell line criteria for each passage

Table 17. mTOR pathway proteins of interest with molecular weight and predicted Western Blot band detection size.

LIST OF FIGURES

Figure 1: 5 Year Survival and Distribution of Colorectal Cancer Based on Location of Disease

Figure 2: Colorectal Cancer Progression from Benign Polyp to Invasive Tumor

Figure 3: miRNA processing from nucleus to cytoplasm

Figure 4: A PRISMA flow diagram illustrating the search strategy used

Figure 5: Heat map showing expression of 11 miRNA in plasma of 16 patients with colorectal adenoma prior to treatment and in plasma of 16 controls

Figure 6: mTOR pathway

Figure 7: Cell migration diagram and experimental steps

Figure 8: Cell invasion diagram and experimental steps

Figure 9: HT-29 Fold Change of miRNA-99a Expression after Transfection (n=2)
Error bars = standard error of the mean

Figure 10: HCT-116 Fold Change of miRNA-99a Expression after Transfection (n=2)
Error Bars = Standard Error of the Mean

Figure 11: CCD-841 Fold Change of miRNA-99a Expression after Transfection (n=2)
Error Bars = Standard Error of the Mean

Figure 12: Mechanistic Target of Rapamycin Pathway focusing on AKT input into mTORC1

Figure 13: mTOR pathway focusing on mTORC1 output on S6K1 and 4EBP1 (enlarged central portion of Figure 11)

Figure 14: MTT assay dosing curve of increasing Rapamycin dosing concentrations in HT-29, HCT-116 and CCD-841. Two different concentrations of plated cell density denoted in the key.

Figure 15: Western blot and bar graph of total mTOR protein expression when miRNA-99a mimic is transfected in normal epithelial colon cell line CCD-841. Bar chart is expressed in relative density units.

- Figure 16: Western blot and bar graph of phosphorylated mTOR protein expression when miRNA-99a mimic is transfected in normal epithelial colon cell line CCD-841. Bar chart is expressed in relative density units.
- Figure 17: Western blot and bar graph of phosphorylated mTOR protein expression when miRNA-99a mimic is transfected in HT-29 CRC cell line. Bar chart is expressed in relative density units.
- Figure 18: Western blot and bar graph of total mTOR protein expression when miRNA-99a mimic is transfected in HCT-116 CRC cell line. Bar chart is expressed in relative density units.
- Figure 19: Western blot and bar graph of phosphorylated mTOR protein expression when miRNA-99a mimic is transfected in HCT-116 CRC cell line. Bar chart is expressed in relative density units.
- Figure 20: Western blot and bar graph of phosphorylated S6K1 (75 KDa) protein expression when miRNA-99a mimic is transfected in normal colon epithelial cell line CCD-841. Bar chart is expressed in relative density units.
- Figure 21: Western blot and bar graph of total S6K1 (70 KDa) protein expression when miRNA-99a mimic is transfected in HT-29 CRC cell line. Bar chart is expressed in relative density units.
- Figure 22: Western blot and bar graph of phosphorylated S6K1 (70 KDa) protein expression when miRNA-99a mimic is transfected in HT-29 CRC cell line. Bar chart is expressed in relative density units.
- Figure 23: Western blot and bar graph of phosphorylated S6K1 (70 KDa) protein expression when miRNA-99a mimic is transfected in HCT-116 CRC cell line. Bar chart is expressed in relative density units.
- Figure 24: Western blot and bar graph of phosphorylated 4EBP1 (15-20 KDa) protein expression when miRNA-99a mimic is transfected in normal colon epithelial control cell line CCD 841. Bar chart is expressed in relative density units.
- Figure 25: Western blot and bar graph of total 4EBP1 (15-20 KDa) protein expression when miRNA-99a mimic is transfected in normal colon epithelial control cell line CCD 841. Bar chart is expressed in relative density units.
- Figure 26: Western blot and bar graph of phosphorylated 4EBP1 (15-20 KDa) protein expression when miRNA-99a mimic is transfected in HT-29 cell line. Bar chart is expressed in relative density units.

Figure 27: Western blot and bar graph of total 4EBP1 (15-20 KDa) protein expression when miRNA-99a is transfected in HT-29 cell line. Bar chart is expressed in relative density units.

Figure 28: Western blot and bar graph of phosphorylated 4EBP1 (15-20 KDa) protein expression when miRNA-99a mimic is transfected in HCT-116 cell line. Bar chart is expressed in relative density units.

Figure 29: Western blot and bar graph of total 4EBP1 (15-20 KDa) protein expression when miRNA-99a mimic is transfected in HCT-116 cell line. Bar chart is expressed in relative density units.

Figure 30: HT-29 Migration Assay after transfection with miRNA-99a Mimic (Blue) and Antagomir (Red). All data is normalized to the negative control.

Figure 30b: Numerical Density Values for HT-29 migration assay

Figure 31: HCT-116 Migration Assay after transfection with miRNA-99a Mimic (Blue) and Antagomir (Red). All data is normalized to the negative control.

Figure 31b: Numerical Density Values for HCT-116 migration assay

Figure 32: HT-29 Invasion Assay after transfection with miRNA-99a Mimic (Blue) and Antagomir (Red). All data is normalized to the negative control.

Figure 32b: Numerical Density Values for HCT-116 invasion assay

Figure 33: HCT-116 Invasion Assay after transfection with miRNA-99a Mimic (Blue) and Antagomir (Red). All data is normalized to the negative control.

Figure 33b: Numerical values for HCT-116 Invasion Assay

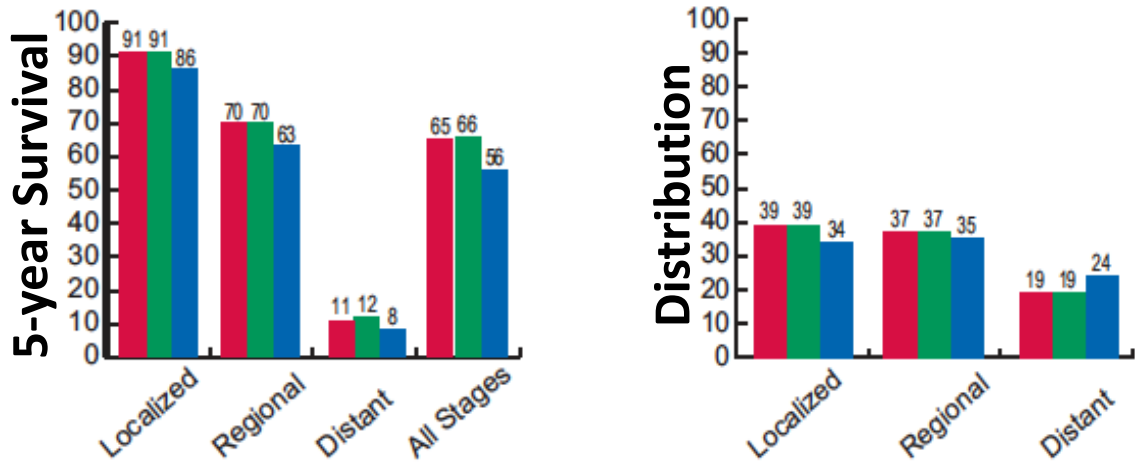
CHAPTER 1

COLORECTAL CANCER: A SIGNIFICANT CLINICAL PROBLEM

A. EPIDEMIOLOGY

Colorectal cancer is a major cause of morbidity and mortality. As of 2011, it was the third most common cancer worldwide and the 4th most common cause of death.¹ In the United States, in 2013, it was the third most common cancer among men and women accounting for 96,830 new cases of colon cancer and 40,000 new cases of rectal cancer and in turn 50,310 colorectal cancer deaths annually.¹ These statistics suggest that although some strides have been made with colon cancer screening and intervention, there is still much room for improvement in both screening and treatment.

Figure 1: 5 Year Survival and Distribution of Colorectal Cancer Based on Location of Disease



CA CANCER J CLIN 2010;60:277-300

B. STAGING

Table 1: Colorectal Cancer Staging

Colorectal Cancer Stage		
I	Dukes A	Tumor invades submucosa or muscularis propria
IIA		Tumor invades through the muscularis propria into pericorectal tissues
IIB	Dukes B	Tumor penetrates to the surface of the visceral peritoneum
IIC		Tumor directly invades or is adherent to other organs or structures
IIIA		Tumor invades submucosa. 1-6 regional lymph nodes
IIIB	Dukes C	Tumor invades with greater than 6 regional lymph nodes
IIIC		Tumor penetrates to the surface of the visceral peritoneum
IV	Dukes D	Distant Metastasis

C. SCREENING

Early screening appears to have led to a delayed but meaningful reduction in disease mortality. Although this is a significant advance for clinicians and their patients, the side effects and preoperative preparation that are involved in colon and rectal cancer screening leads to significant cost to the health care system and personal morbidity to the patient.²

Current recommendations for colon cancer screening for patients that are not a “high risk” for colon cancer begins at the age of 50 and continues until the age of 75.³ There are currently 3 accepted screening tests; each has its benefits and downsides, each occurring at different intervals. The first screening test is the high-sensitivity fecal occult blood test, which is recommended once yearly. The upside of this is the lack of invasive nature and no need to undergo bowel preparation; the downside of this test is it is not specific for colon cancer and detects any blood that is in one’s gastrointestinal tract. The second screening test is flexible sigmoidoscopy. The recommended interval of this test is every five years with the addition of fecal occult blood test done every three years. The advantage of this test is the clear visibility of the lower part of the colon and rectum, but the downside is its invasiveness and patient discomfort. In addition, the clinician is unable to visualize the entire colon. Colonoscopy is the currently accepted “best screening” method and most complete screening test. It is recommended every 10 years for patients who are not at high risk. The benefits of colonoscopy are complete visualization of the colon and potential intervention when polyps are detected. Downsides of colonoscopy include the laxative bowel preparation for this procedure, the risk of bowel perforation and operator skill set, both with respect to completeness and safety. To

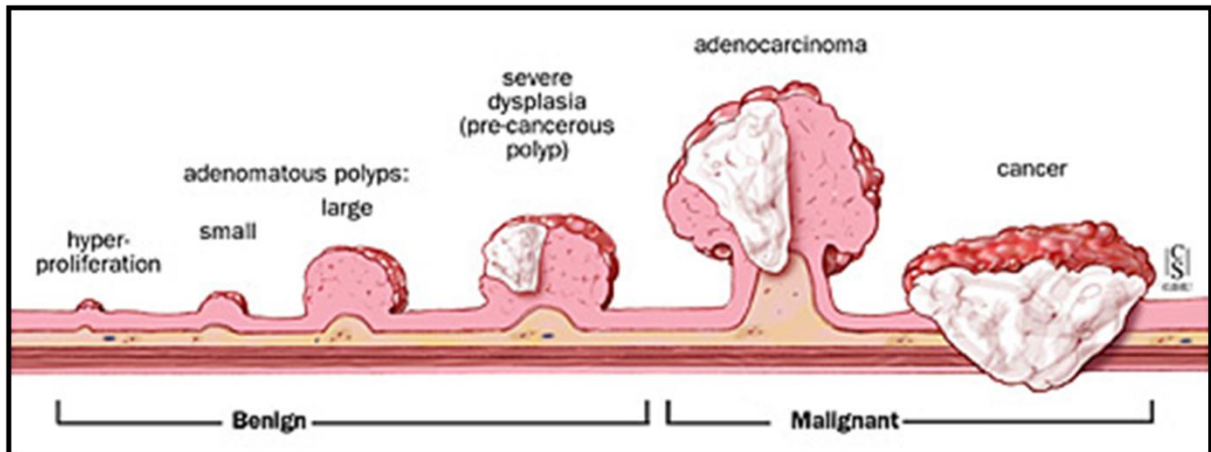
state the obvious, colonoscopy does not come without risk. The unpleasant nature of this bowel preparation leads to imperfect compliance and reduces the effectiveness of the colonoscopy itself.

D. TREATMENT OPTIONS

Current therapy focuses on endoscopic and surgical intervention.³ The additions of chemotherapy and radiation therapy come into play when regional or distant metastasis are a factor. Due to the advances over the last several decades in endoscopic surveillance, more cases of colon cancer are detected at an early stage prior to metastasis.³

Early stages of colon cancer are treated and may be cured with polyp removal. This is why screening colonoscopies are so important- because when a polyp is recognized and removed prior to the polyp converting to an invasive mass, it can be essentially “cured” at the time of endoscopy. If the polyp progresses to an invasive, cancer but has not metastasized to the lymph nodes, this also can be treated with surgical, often laparoscopic, resection (Figure 2). Colon cancers can be treated with segmental colectomy and anastomosis, frequently leading to patient cure.

Figure 2. Colorectal Cancer Progression from Benign Polyp to Invasive Tumor



E. CASE SCENARIOS ILLUSTRATING LIMITATIONS OF CURRENT SCREENING GUIDELINES

With a variety of screening tests whose goal is early intervention, there are still clinical scenarios where large bowel tumors are missed for several reasons. This can be illustrated in the following two clinical scenarios.

Case 1

A 48 year old woman presents to her primary care physician with a several week history of blood seen in her stool. She undergoes a focused history and physical. She does not have a family history of any cancer or disease processes. She denies weight loss but does state that her bowel movements have been somewhat irregular as of late. Upon physical exam, her doctor does notice some external hemorrhoids with some blood on them. Since she does not have a family history of colon cancer and she is 2 years away from recommended “normal screening” for colon cancer, the doctor attributes the blood seen in the stool to the current hemorrhoids and provides treatment for this.

The same patient returns 2 years later, now with weight loss and lack of energy. She has not had any other blood noticed in her stool since her visit 2 years prior. Now that she is 50, and due to the nature of weight loss and weakness, her physician now recommends a screening

colonoscopy, during which a large partially obstructing cancer is seen in her transverse colon. In her evaluation prior to resection, a liver lesion is noticed. She is optimized for her operation and upon elective operation is found to have a bulky transverse colon cancer which is resected with a primary anastomosis; the lesion in the right lobe of her liver is biopsied and the mass is found to be adenocarcinoma consistent with colon cancer. She now requires systemic chemotherapy and/or a major liver resection for this metastasis. Her likelihood of surviving 5 years is less than 40%.

Case 2

A 60 year old woman has a several day history of blood in her stool. She presents to her primary care physician who performs a history and physical examination. Her most recent colonoscopy was 10 years ago and no polyps or masses were observed at the time. Since her last colonoscopy was 10 years ago and she is “due” for a screening exam, her personal physician schedules her for this procedure. During the colonoscopy, she is noted to have a locally advanced cancer in her sigmoid colon. She is subsequently scheduled for further evaluation and operative resection of the cancer and primary anastomosis. She recovers from her operation and the pathology reports show adenocarcinoma that has penetrated the bowel wall but is free of metastasis in the 16 lymph nodes removed intraoperatively. At 6 month follow up, she remains well and her primary relatives are notified by the patient of these events, since all relative now have a “positive” family history.

Both of the above scenarios would benefit from a more accurate screening examination to determine if an individual needs colonoscopy sooner than the recommended interval screening. In Case 1, the individual is “two years too young” for the recommended screening age, yet if a simple blood based test could tell the clinician of a possible polyp or cancer, then intervention could presumably be undertaken prior to development of a distant metastasis. Intervention prior to metastasis is key, as the 5 year recurrence rate for colorectal cancer drastically increases once distant metastasis is present.

F. CURRENTLY AVAILABLE PLASMA-BASED BIOMARKERS FOR COLORECTAL CANCER

Carcinoembryonic antigen (CEA) assay is the most popular assay for clinical monitoring. It has been used for post-operative surveillance and for monitoring response to therapy. CEA, however, lacks sufficient sensitivity and specificity for screening or for detecting CRC recurrence.⁴ It also has been used as a prognostic marker. CEA is normally elevated during the fetal development period but beyond that, it is not normally found in the blood. CEA levels may increase with distant metastasis but this assay does not have high specificity or sensitivity in regards to detection of distant metastases. In addition, CEA can be elevated in many other types of cancer, as well as falsely elevated in smokers.

Carbohydrate antigen 19-9 (CA 19-9) has been used as a prognostic tumor marker, but it is less sensitive than CEA for CRC.⁵ Methylated septin 9 has been reported to have good sensitivity and specificity for CRC but does not have sufficient ability to detect colorectal adenomas.⁶ Markers in development include CSA (colon cancer specific antigen)-1, 2

and 3, colon-cancer-secreted-protein (CCSP)-2,^{7, 8} galectin-3-ligand and haptoglobin-related-glycoprotein.

Unfortunately, no accurate, broadly applicable test currently exists for colorectal adenomas that could identify candidates for intervention (colonoscopic removal) in order to prevent CRC or to diagnose CRC at an earlier stage (Table 2 a&b). This has been a focus of work in the Price Institute since 1995.

Table 2. 5 year Survival Rates of Colon and Rectal Cancer

A. Colon Cancer by Stage

5 Year Survival Rate	
Stage	Survival Rate (%)
I	92
II A	87
II B	63
III A	89
III B	69
III C	53
IV	11

B. Rectal Cancer by Stage

5 Year Survival Rate	
Stage	Survival Rate (%)
I	87
II A	80
II B	49
III A	84
III B	71
III C	58
IV	12

*National Cancer Institute's SEER database, looking at people diagnosed with colon and rectal cancer between 2004 and 2010

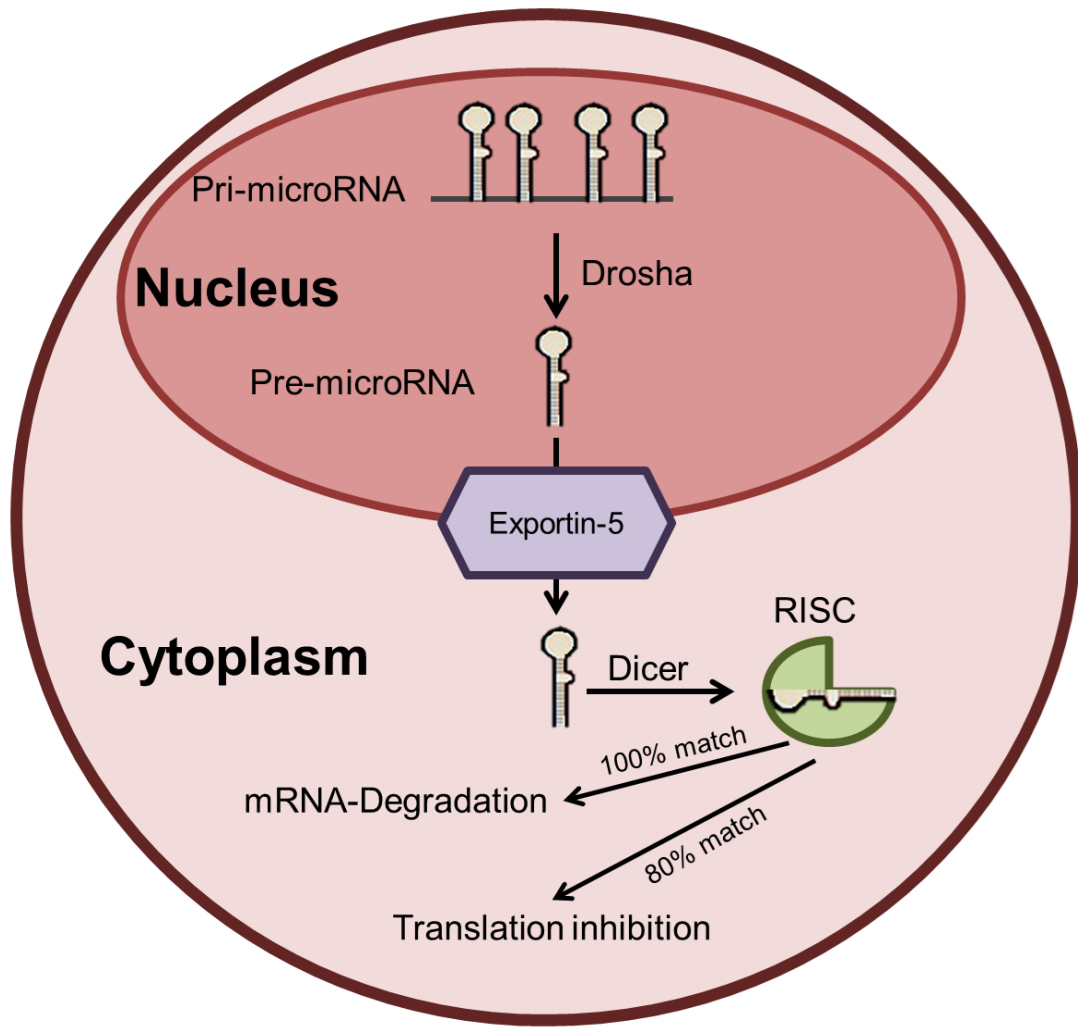
CHAPTER II

PRELIMINARY DATA : MIRNA AS BIOMARKERS FOR COLORECTAL CANCER

A. MIRNA OVERVIEW

miRNAs are short noncoding RNA molecules that range from approximately 19-23 nucleotides in length. They bind to complementary sequences on target messenger RNAs (mRNA). The affinity of binding can influence the effect of the miRNA on mRNA. miRNAs can cause translational repression, target sequence degradation and or gene silencing to name a few of their functions (Figure 3). miRNAs are a promising area to research because of their inherent stability intra- and extra-cellularly. Furthermore, they are known to be involved in numerous regulatory processes in the human body and have been shown to be sensitive and specific biomarkers in some cancers and other human diseases.

Figure 3. miRNA processing from nucleus to cytoplasm^{2,9}



Billeter et al. Semin Thorac Cardiovasc Surg. 2012¹⁰

B. TISSUE AND PLASMA MIRNA IN CRC, INITIAL STUDIES

Kanaan evaluated miRNA in both CRC tissue and normal mucosa. Levels of 380 miRNAs were determined using microfluidic array technology (Applied BioSystems) in a “training” set of 30 CRC patients from whom cancer and nearby normal tissue were collected. The 4 most dysregulated miRNAs ($P < 0.05$, False Discovery Rate (FDR): 10%) were then validated in a second blinded “test” set of 16 CRC patients from whom cancer and nearby normal tissue had also been collected. Nineteen of 380 miRNAs were dysregulated in CRC tissue in the tissue “training” set ($P < 0.05$, FDR: 10%). The 2 most upregulated (miR-31; miR-135b) and most down-regulated (miR-1; miR-133a) miRNAs identified CRC in our “test” set with 100% sensitivity and 80% specificity. MiR-31 was also more upregulated in stages III and IV compared with stages I and II ($P < 0.05$).¹¹ The most dysregulated tissue miRNAs were then validated in an independent new plasma test set consisting of 20 CRC patients with 20 age- and race-matched subjects without CRC. In the “plasma test” group, miR-21 differentiated CRC patients from controls with 90% specificity and sensitivity. Although these early results were promising, miR-21 has been described in other cancers. Thus, there is a need to develop a more specific plasma miRNA panel for CRC.

C. PLASMA MIRNA TO DETECT PREMALIGNANT LESIONS OF THE COLON (ADENOMAS)

We studied colorectal polyps or colorectal advanced adenomas (CAA) with the highest likelihood of malignant transformation over time. Advanced adenomas are defined as adenomas >0.75 cm, with a villous component or high-grade dysplasia and

represent a continuum from benign adenoma to invasive CRC. We screened 380 plasma miRNAs using microfluidic array technology (Applied BioSystems) in a screening cohort of 12 controls, 9 patients with CAA, and 20 patients with stage III & IV CRC. A panel of the most dysregulated miRNAs ($P < 0.05$, FDR 5%) was then validated in a blinded cohort of 26 controls, 16 patients with CAA, and 45 patients with CRC. After testing the 15 most dysregulated microRNAs in the validation group, a combined panel of miR-532-3p, miR-331, miR-195, miR-17, miR-142-3p, miR-15b, miR-532 and miR-652 identified CAA accurately. This 8-miRNA panel demonstrated an AUC of 0.868 [95% CI 0.76-0.98] in the plasma “validation” set, indicating good discriminative power. Additionally, in the validation set, miR-139-3p and miR-431 were significantly dysregulated differentiating controls from all CRC stages (AUC = 0.829 [95% CI: 0.73–0.93]) (Fig. 5). Receiver-operating-characteristic (ROC) curves of miRNA panels for CAA versus all CRC showed an AUC of 0.856 (95% CI: 0.75–0.97). miRNAs specific for CAA and CRC were explored and identified. Sensitivity and specificity values are based on the generated ROC curves for each miRNA panel.¹²

D. DIFFICULTIES WITH ASSAY REPRODUCIBILITY

miRNA expression profiles have been shown to be unique to both the source material (i.e. plasma, tissue, etc.) and the disease process being investigated. miRNA profiles have, therefore, emerged as prospective biomarkers for cancer and many other human diseases¹³⁻¹⁷.

This has led to a rapid proliferation of miRNA research. Unfortunately, many studies have been conducted without attention to standardization of methods or reproducibility of results, particularly with respect to studies of plasma miRNA. In many

reports, it is difficult to deduce the actual methods used for analysis. This has led to the use of different extraction protocols, and various methods of quantification and statistical analysis, which, in turn, are a source of variability (Table 3). In part, due to this lack of standardization, many different miRNAs have been reported to be associated with a given disease process¹⁵. There is ongoing controversy over the optimal analytic methods for studies of miRNA in plasma.¹⁸

Table 3. Multiple sources of variability in microRNA data and literature search ^{12, 19-93}.

Parameter		Source of Variability
Biologic Sample	Tissue	<ul style="list-style-type: none"> • Preservation Method <ul style="list-style-type: none"> - Formalin fixed-paraffin embedded - Snap Frozen • Collection Method <ul style="list-style-type: none"> - Laser caption microdissection - Macrodissection (includes stroma)
	Plasma	<ul style="list-style-type: none"> • Collection method (e.g. EDTA tube) • Method to isolate plasma
	Other body fluids (urine, cerebrospinal fluid, etc.)	<ul style="list-style-type: none"> • Collection method
RNA Extraction	Time to extraction*†	<ul style="list-style-type: none"> • Immediate (within 24 h) • Delayed
	Method of RNA extraction*†	<ul style="list-style-type: none"> • Guanidinium thiocyanate-phenol chloroform based (e.g. Trizol LS®, LifeTechnologies) • Glass fiber filter-based methods (e.g. miRVANA,™ Ambion) • Phenol/guanidine-based with and silica membrane based purification (e.g. miRNeasy®, Qiagen)
	Type of miRNA*	<ul style="list-style-type: none"> • Total • Fractional (e.g. exosomal)
miRNA Detection & Statistical Analysis	miRNA characterization	<ul style="list-style-type: none"> • Cyanine dye-based RT qPCR (SYBR® Green) detection • Fluorogenic 5' nuclease-based RT qPCR detection • Deep sequencing
	Quantification*	<ul style="list-style-type: none"> • Absolute (addition of exogenous miRNA e.g. <i>C. elegans</i> miRNA) • Relative (use of an internal reference e.g. RNU48, RNU44, RNU47, RNU6, miR-16)
	Cycle threshold bar*†	<ul style="list-style-type: none"> • Fixed threshold • Variable threshold
	Statistical analysis*†	<ul style="list-style-type: none"> • Paired t-Test • Wilcoxon Signed Rank test • Cycle Threshold ratios • Rank-based
	Reproducibility†	<ul style="list-style-type: none"> • Intra-operator comparisons • Inter-operator comparisons
Symbols: *Items investigated in systematic literature review. † Items investigated in our proposed standard methodologic technique.		

Since the discovery of miRNAs, their detection in blood has received much attention due to the ease of access and ready availability of peripheral blood as compared to tissue¹⁵. Initially, we performed a systematic review of publications focusing on plasma miRNA in order to ascertain what methods and reporting criteria were currently being utilized. We then we used a panel of 11 selected miRNA to study the effect of time to plasma extraction, method of RNA extraction, cycle threshold bar setting, intra-operator variability, inter-operator variability and selection of housekeeping gene on data obtained in plasma miRNA studies.^{94, 95} An in-depth description of our statistical analysis is found in the analysis section, however a full statistical model-based approach, such as analysis of variance or analysis of covariance (ANOVA or ANCOVA) was used to analyze the data.⁹⁴

1. SYSTEMATIC REVIEW

In order to determine the consistency and current status of methods reporting of clinical studies of plasma miRNA, we retrieved original manuscripts published from July 1, 2013, until June 30, 2014. We utilized a single search engine (PubMed) without language restriction using the following search words: plasma, microRNA, and human. We excluded review articles, case reports, or non-English language articles. Remaining articles were then obtained for review. These were then graded as to how many of the following criteria were clearly documented in the *Materials and Methods* sections: 1) time of plasma extraction, 2) method of RNA extraction, 3) type of miRNA used (total vs exosomal), 4) method of quantification (external vs internal reference), 5) cycle threshold bar setting, and 6) methods of statistical analysis (items denoted by * in Table 2).

Of the 220 retrieved abstracts, 130 were excluded because they were reviews, case reports, or non-English language manuscripts. Sixteen publications were unobtainable through our library, leaving 74 manuscripts available for review. A PRISMA flow diagram is shown in Figure 4 and data shown in Table 4.

Figure 4. A PRISMA flow diagram illustrating the search strategy used⁹⁴

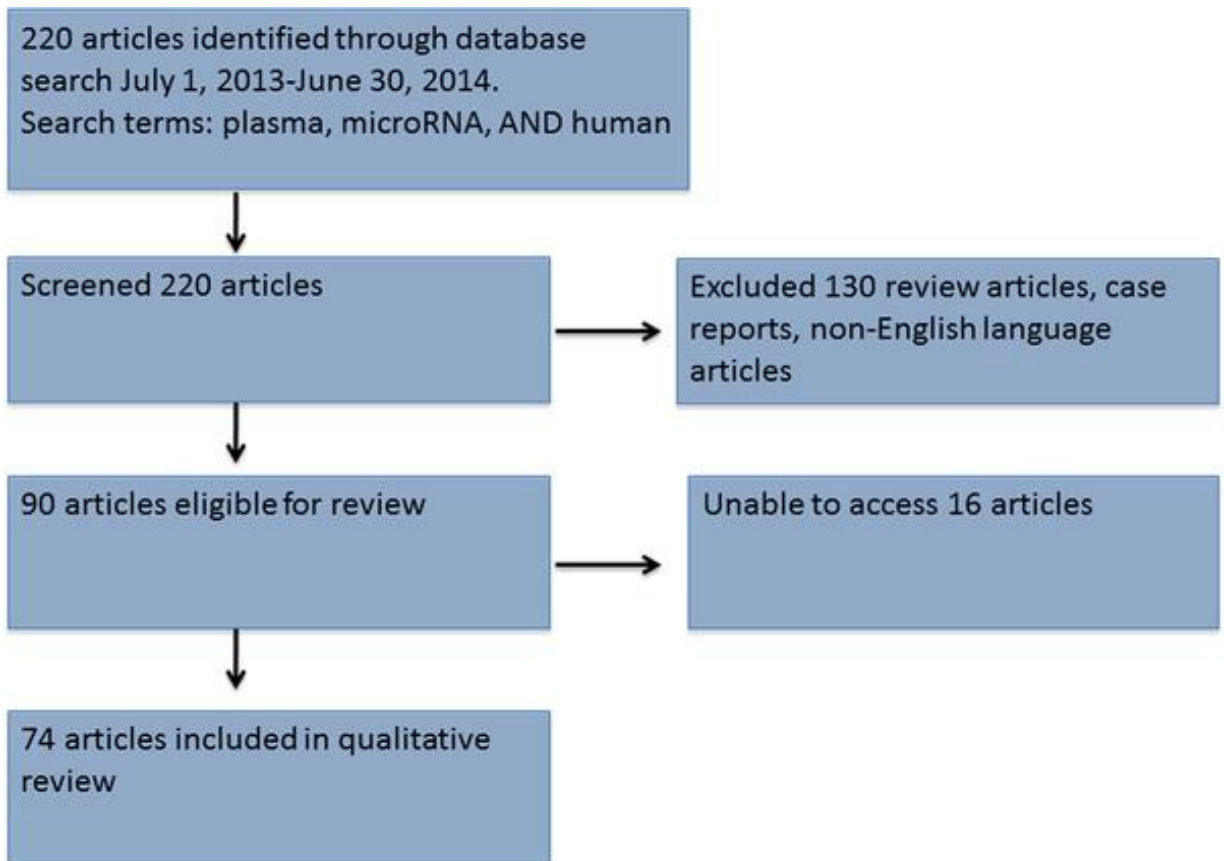


Table 4. Systematic review: 74 plasma miRNA publications July 1, 2013 - June 30, 2014.

Methodologic Parameter Assessed	Number of studies (% of total 74 manuscripts reviewed)
Time of Plasma Extraction	
≤ 2h	44 (59.5)
>2h	8 (10.8)
Not Stated	22 (29.7)
Method RNA Extraction+	
Trizol	13 (17.6)
miRNeasy	25 (33.8)
mirVana	30 (40.5)
Not Stated/Other	8 (10.8)
Type of miRNA used	
Total miRNA	72 (97.3)
Exosomal miRNA	2 (2.7)
Cycle Threshold Bar Setting	
Fixed	2 (2.7)
Variable	1 (1.4)
Not Listed	71 (95.9)
miRNA Quantification*	
External reference	31 (41.9)
Internal reference	32 (43.2)
Not specified	12 (16.2)
Statistical Analysis Described Ψ	74 (100)
t-test	30 (40.5)
Mann-Whitney	29 (39.2)
Receiver operating characteristic (ROC) curves	24 (32.4)
Wilcoxon	16 (21.6)
ANOVA	12 (16.2)
Other	14 (18.9)

+ Some manuscripts utilized more than one method of RNA extraction.

* Some manuscripts used both an internal and external reference.

Ψ Many manuscripts used multiple methods of statistical analysis.

Although nearly one-third of studies did not mention time to plasma, in the vast majority (nearly 58%), plasma extraction was completed ≤ 2 h after phlebotomy. Most authors used either Trizol, miRNeasy, or mirVana protocols for RNA extraction, and nearly all publications used total miRNA rather than exosomal miRNA. Equal proportions of manuscripts used internal and external references (43% and 42%, respectively). The most commonly utilized internal reference miRNAs were miR-16 (12 publications) and RNU-6 (7 publications). Seventy-one of the 74 reviewed publications did not describe the setting of the cycle threshold bar. All but 2 of the 74 (97%) papers stated at least some aspect of their statistical methods, with many using multiple, different testing methods as shown in Table 2. Among reviewed manuscripts, only 1 (1.4%) listed all 6 assessed criteria 27-102.

2. MICRORNA SELECTION

An eleven miRNA panel with RNU6 as an internal reference was used. These miRNAs were selected based upon unpublished data from our laboratory utilizing 380 miRNA arrays (Applied Biosystems, Carlsbad, California) to determine miRNA expression in the plasma of 20 colorectal cancer (CRC) patients, and 10 patients each with colorectal advanced adenoma (CAA)(adenomatous polyps > 0.6 cm in maximal diameter), breast cancer (BC), lung cancer (LC), pancreatic cancer (PC), and 10 controls.

In order to determine sample size, the most important aspect is adjustment of the significance level (alpha). For screening studies, we use Jung's procedure to adjust the alpha. Using the method of Jung to find about 5% of features to be significant at a false detection rate (FDR) of 5%, the adjusted alpha will be 0.0038. With any two groups, a

minimum of $n_1=10$ and $n_2=10$ using a two sample t test, we can detect at least 2.7 fold means (which we have observed in our preliminary data sets) using the common standard deviation at significance level of 0.0038 and power of 80%.

With respect to choice of number of miRNA in our panel, it was our expectation that no more than 10% of miRNA would be differentially expressed between cases and controls after adjusting the p values for multiple comparisons. Of these, in turn, one would not expect more than 0.5 to 3% of miRNA to be able to accurately identify cases and controls. Ten miRNA and one reference (housekeeping gene) miRNA were, therefore, chosen (approximately 3%). Statistical analysis using ANOVA identified 11 significantly dysregulated miRNAs specific for colorectal neoplasia (Table 2). Multiple test control was based on controlling the false discovery rate (FDR) at 10%. A logistic regression model was established using the top up-regulated miRNAs and used for predicting the adenoma and control groups for the validation data. The sensitivity and specificity for this prediction were calculated. The receiver operator characteristic (ROC) curves with area under the curve (AUC) values were microRNA-rated using current versions of SAS⁹⁶ and R⁹⁷⁻⁹⁹ (Figure 1a & b).

3. PATIENT POPULATION

The University of Louisville Institutional Review Board reviewed and approved this study. Written informed consent was obtained from all subjects who were treated at a single university-based colorectal surgery practice. The patient population consisted of 16 patients with colorectal advanced adenomas, and 16 patients without colorectal neoplasia (controls). The patient groups were age-, race-, and gender-matched. Prior to patient

treatment, 6 mL of peripheral whole blood was obtained in EDTA tubes (Becton-Dickinson, Franklin Lakes, NJ) via venipuncture from the adenoma group and from individuals in the “control” group at the time of routine screening colonoscopy. The latter group of individuals (n=16) had no colonic neoplasia or inflammatory bowel disease. Blood was stored at 4°C until plasma isolation. Plasma was isolated within 24 h of venipuncture, unless noted otherwise (see section below “*Time to Plasma Extraction*”). Patient demographics are displayed in Table 3 and did not differ between patient groups.

4. TIME TO PLASMA EXTRACTION

Five 6 mL aliquots of peripheral blood from 6 controls were obtained and stored at 4°C until extraction. Plasma was extracted at different time points: immediately (within 30 minutes after phlebotomy) and then at 12, 24, 48, and 72 h post-phlebotomy. Whole blood was centrifuged at 600 relative centrifugal force (rcf) for 15 minutes in order to isolate the plasma, which was then stored at -80°C for later use. Once plasma was isolated, it underwent downstream processing via the modified phenol/guanidine-based lysis and silica membrane-based extraction technique (miRNeasy, Qiagen, Venlo, Limburg).

Our proposed standard technique provided a comparison. When performing plasma extraction from whole blood at different time points, we found that 6 miRNAs showed no differences in Δ CT values. In contrast, 5 miRNAs expressed a statistically significant difference in Δ CT values between immediate plasma extraction and extraction ≥ 24 h for 1 miRNA (miR-122), between immediate extraction and extraction after ≥ 48 h for 2 miRNAs (miR 485-3p, miR-21), and for 2 miRNAs with extraction at 72 h (miR

523, miR 218) (Table 5.). Based upon these data using the representative miRNA we have analyzed, plasma extraction less than 12h after phlebotomy appears to provide equivalent results to immediate (within 30 minutes of phlebotomy) extraction.

5. EFFECT OF REPEATED SAMPLE ACQUISITION

In order to determine whether there was a difference between samples when plasma miRNA were analyzed in samples drawn at different times from the same individual, 6 mL peripheral blood was drawn from each of 12 healthy subjects without any neoplasia or inflammatory condition at 6:30 AM and 12 hours later at 6:30 PM on the same day. Plasma was extracted within 30 minutes of phlebotomy, and stored at -80°C for later use. Downstream processing was performed using the modified phenol/guanidine-based lysis and silica membrane-based extraction technique (miRNeasy, Qiagen, Venlo, Limburg) and methodology described below.

Repeated phlebotomy of the same individuals at 12-hour intervals showed no differences in miRNA expression values (Table 5).

Table 5. Effect of Repeated Sample Acquisition. Comparison of mean $\Delta\Delta\text{CT}$'s for various plasma miRNA from plasma samples drawn from the same 7 individuals on the same day 12 hours apart.

miRNA	$\Delta\Delta\text{CT}(\text{mean})$	p-value
miR-374	-0.4458	0.454
miR-142-3p	-0.4136	0.4322
miR-523	-0.5518	0.3424
miR-374-5p	-0.2611	0.6425
miR-376c	-0.4312	0.5867
miR-27a	-0.3863	0.4776
miR-520d-5p	-0.3081	0.7506
miR-122	-0.0856	0.9251
miR-485-3p	-0.2611	0.6392
miR-21	-0.3976	0.5261
miR-218	-1.332	0.1659
miR-374	-0.4458	0.454

6. METHOD OF RNA EXTRACTION

Total RNA was extracted from 250 μ L plasma samples using either the TRIzol® LS reagent protocol (Ambion, Austin, Texas), which was modified by addition of an extended overnight drying period, or by a modified miRNeasy (Qiagen, Venlo, Limburg) extraction technique with yeast carrier^{100, 101}. When using the TRIzol® LS total RNA extraction technique, pre-amplification was necessary, as the majority of samples yielded quantities of total RNA < 500 ng. In our experience, this is the minimum amount needed for adequate expression and amplification in qPCR. The Applied Biosystems protocol for producing custom reverse transcription and pre-amplification pools with TaqMan® miRNA assays was followed. Total RNA purity was assessed using a Nanodrop 2000 spectrophotometer (Thermo Scientific, Middlesex, MA).

The Qiagen miRNeasy extraction without pre-amplification resulted in a higher yield of RNA than Trizol LS extraction; therefore, pre-amplification was not necessary and could be omitted as a source of possible variation (Table 6). The average Δ CT was lower with miRNeasy, with fewer missing values than with Trizol purification and pre-amplification. Qiagen miRNeasy extraction without pre-amplification resulted in only 1 of 704 (0.14%) miRNAs not expressing; however, utilizing the Trizol LS extraction with pre-amplification, 109 of 704 (15%) of miRNAs investigated were not expressed (Table 7). A heat map showing miRNA expression for patient groups is shown in Figure 5. A Step-One Plus RT-PCR System (Life Technologies, Carlsbad, California), with default fast thermal cycling conditions, was used for RT-PCR. Individual Taqman probes (20x) were used during RT-PCR to bind to a complementary sequence in the target cDNA. These values were, in turn, normalized to the expression of the endogenous miRNA

RNU6 as internal reference to calculate ΔCT values for all studies except where indicated.

Table 6. Total RNA concentration and purity for Trizol LS and Qiagen miRNeasy with RNA yeast carrier.

Total RNA Extraction Method	Number of Samples	Mean Total RNA Concentration (\pm SD)	Mean Total RNA Amount	Average Purity (\pm SD) [A260/A280]	p-value*
Trizol LS	32	19 (\pm 12) ng/ μ L	380 ng	2.03 (\pm 0.72)	<0.0001
Qiagen miRNeasy with RNA Yeast Carrier	32	353 (\pm 85) ng/ μ L	7060 ng	1.95 (\pm 0.13)	

*p-value for mean total RNA concentration between methods

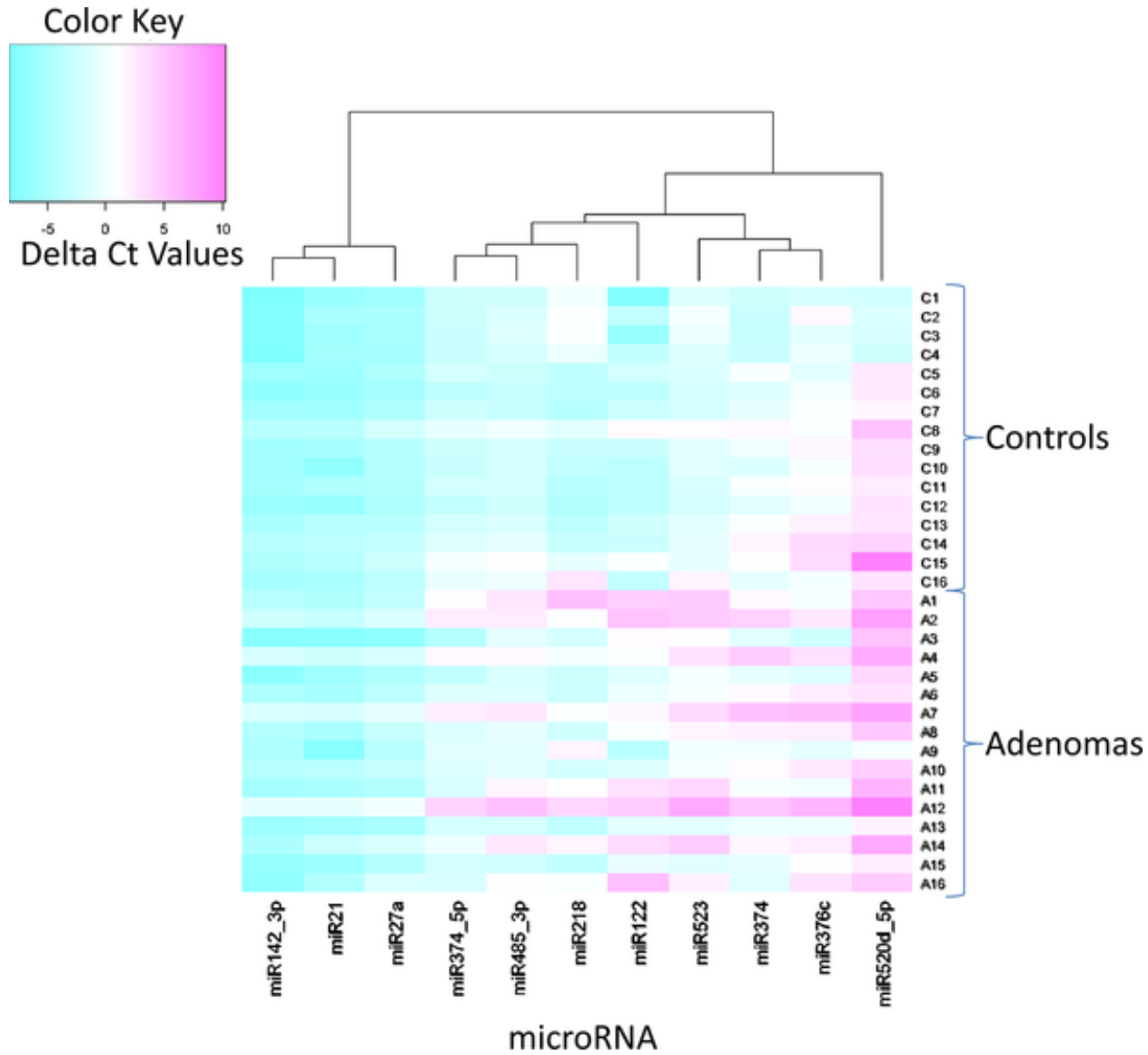
Table 7. Inter-operator variability with two different extraction methods. Differences in $\Delta\Delta CT$ between Qiagen miRNeasy with RNA carrier and no pre-amplification and Trizol LS with pre-amplification.

microRNAs	Trizol LS with Preamplification		Qiagen miRNeasy w/o Preamplification		p-value
	Mean $ \Delta\Delta CT ^*$ ($\pm SD$)	# miRNA Not Expressed	Mean $ \Delta\Delta CT ^*$ ($\pm SD$)	# miRNA Not Expressed	
miR-374	1.69 (± 1.32)	0	0.70 (± 0.78)	0	0.0006
miR-142-3p	1.69 (± 1.83)	0	0.91 (± 0.89)	0	0.0340
miR-523	1.45 (± 1.45)	0	1.38 (± 1.02)	0	0.8240
miR-374-5p	1.69 (± 1.73)	5	1.27 (± 1.06)	0	0.2461
miR-376c	2.42 (± 1.42)	22	0.76 (± 0.91)	0	<0.0001
miR-27a	1.29 (± 1.23)	6	0.98 (± 1.03)	0	0.2786
miR-520d-5p	2.05 (± 2.03)	31	1.20 (± 1.01)	1	0.0405
miR-122	1.82 (± 1.86)	13	1.11 (± 1.10)	0	0.0642
miR-485-3p	1.45 (± 1.45)	0	1.50 (± 1.01)	0	0.8734
miR-21	2.40 (± 1.82)	0	1.36 (± 1.00)	0	0.0062
miR-218	1.77 (± 1.79)	32	1.09 (± 1.06)	0	0.0692
Total	1.79 (± 1.63)	109/704 = 15% ^a	1.12 (± 0.99)	1/704 = 0.14% ^a	<0.0001
Comparison of Total Number of miRNAs Not Expressed by the Two Methods ^a					<0.0001

* $|\Delta\Delta CT|$ = Absolute Value [Operator 1 ΔCT – Operator 2 ΔCT].

Bold = statistically significant. a = chi-squared test comparing number of miRNA not expressed using Trizol LS with preamplification as compared to using Qiagen miRNeasy without preamplification

Figure 5. Heat map showing expression of 11 miRNA in plasma of 16 patients with colorectal adenoma prior to treatment and in plasma of 16 controls



7. SETTING OF CYCLE THRESHOLD

In order to compare cycle threshold (CT) values across plates, both fixed and variable thresholds were utilized. Since different miRNAs on the same plate may have different linear phases, a fixed threshold may not intersect across the linear phase. For this reason, the variable threshold is the default setting. The relative quantitation (RQ) manager from Applied Biosystems may use a different threshold (variable) within the same plate if one selects the option “automatic CT”. Different thresholds will be chosen for different miRNAs according to the linear phases. However, these CT values cannot be compared directly between different plates. The threshold needs to be considered in the analysis and adjustment of the CT values, if needed. In addition to this variable threshold setting, we examined the effect of fixed threshold settings of 0.01, 0.03, 0.05, or 0.5. CT values, threshold, and 40 cycles fluorescence intensities are miRNA-rated from RQ manager 1.2, Applied Biosystems.

Setting the cycle threshold bar at a fixed value of 0.03 was preferable to using the default “variable” threshold setting, provided that the number of missing values was less than 10%. Using the modified phenol/guanidine-based lysis and silica membrane-based extraction technique (mirNeasy), only 0.14% of values were missing. With this method of extraction, therefore, utilization of a fixed threshold of 0.03 yields reproducible results without the need for normalization required with the use of a variable threshold.

8. INTRA-OPERATOR VARIABILITY

Assays for individual miRNA for each patient sample were run in duplicate to permit assessment of intra-operator variability (comparison of duplicate samples).

There was no significant variability between duplicate samples performed by a single operator (Table 8). A paired t-test among duplicate samples was used to assess statistical significance.

Table 8. Intra-Operator Variability (Duplicates) for the Trizol LS RNA Extraction and Preamplicification Protocol

Colorectal Advanced Adenoma (n=16) + Control (n=16)				
microRNAs	Mean CT Value Duplicate A (\pm SD)	Mean CT Value Duplicate B (\pm SD)	$ \Delta$ CT [†]	p-value
miR-374	25.98 (\pm 1.80)	26.00 (\pm 1.93)	0.02	0.9518
miR-142-3p	28.48 (\pm 2.77)	28.74 (\pm 3.05)	0.27	0.6177
miR-523	20.48 (\pm 2.08)	20.21 (\pm 1.71)	0.27	0.4240
miR-374-5p	29.47 (\pm 3.53)	29.81 (\pm 3.61)	0.34	0.6186
miR-376c	32.27 (\pm 2.63)	31.68 (\pm 2.33)	0.58	0.3265
miR-27a	28.62 (\pm 2.25)	29.24 (\pm 2.99)	0.62	0.2216
miR-520d-5p	35.61 (\pm 1.90)	35.24 (\pm 1.77)	0.36	0.4806
miR-122	28.88 (\pm 2.40)	29.11 (\pm 2.82)	0.23	0.6814
miR-485-3p	29.32 (\pm 3.06)	29.44 (\pm 3.32)	0.12	0.8320
miR-21	26.97 (\pm 2.58)	26.96 (\pm 2.81)	0.01	0.9833
miR-218	35.90 (\pm 2.38)	35.83 (\pm 2.08)	0.07	0.9206

[†] $|\Delta$ CT| = absolute value (mean cycle threshold value for duplicate 1 for the miRNA of interest – mean cycle threshold value for duplicate 2 for the miRNA of interest).

9. INTER-OPERATOR VARIABILITY

In order to assess inter-operator variation following total RNA extraction, two experienced operators separately performed subsequent sample processing, including reverse transcription, preamplification (for samples extracted using TRIZOL LS), and qPCR. Each operator used the same thermocycler (Mastercycler, Eppendorf, Hamburg, Germany) and Step-One Plus RT-PCR System, but at different times on different days. The cycle threshold (CT) values were exported with the CT bar set at 0.03.

Inter-operator variability was assessed using two different miRNA extraction techniques. Inter-operator variability using the Trizol LS purification and pre-amplification showed one miRNA miR-21 to be significantly different between operators. In addition, a large number of samples were noted to have no miRNA expression for 6 of the 11 evaluated miRNA (Table 9). The large number of samples with no miRNA expression again highlighted the importance of selecting the best extraction technique, since this was not seen with the other method (see also data Table 7). Inter-operator variability using the Qiagen miRNeasy technique yielded 2 miRNAs (miR-485-3p and miR-21) with statistically significantly different Δ CT values (p-values comparing the Δ CT of the two different operators, 0.0191 and 0.0500, respectively) (Table 10). It was believed that these differences in miRNA expression data between operators were within the range of experimental error. Indeed, when these experiments were repeated, these differences were not observed (data not shown). In order to determine whether any inter-observer differences would have a significant impact upon observed group differences we utilized an ANOVA model to examine variations in both miR-21 and RNU6. The group effect remained significant, even when there was an effect of inter-

operator variability. The coefficient of variation for RNU6 was 9.1398, and 8.1211 for miR-21. In addition, we determined the mean and standard deviation of 64 measurements of miR-21 performed in plasma samples of patients with adenoma (mean 26.3 ± 1.8 , median 25.9) as well as 64 measurements of miR-21 performed in plasma samples of controls (mean 27.6 ± 3.2 , median 28.4).

Table 9. Differences in Δ CT between operators with Trizol LS RNA extraction and pre-amplification (inter-operator variability).

Colorectal Advanced Adenoma (n=16) + Control (n=16)						
Unpaired t-test - Cycle Threshold = 0.03						
microRNAs	Operator 1		Operator 2		p-value [‡]	Mean $ \Delta\Delta$ CT [*] (\pm SD)
	Mean Δ CT [†] (\pm SD)	# miRNA Not Expressed	Mean Δ CT [†] (\pm SD)	# miRNA Not Expressed		
miR-374	-1.95 (\pm 2.53)	0	-1.53 (\pm 2.39)	0	0.4974	1.69 (\pm 1.32)
miR-142-3p	0.84 (\pm 1.99)	0	1.23 (\pm 3.06)	0	0.5478	1.69 (\pm 1.83)
miR-523	-7.01 (\pm 3.11)	0	-7.78 (\pm 2.17)	0	0.2551	1.45 (\pm 1.45)
miR-374-5p	2.02 (\pm 2.59)	2	2.83 (\pm 2.85)	3	0.2577	1.69 (\pm 1.73)
miR-376c	5.83 (\pm 2.21)	11	5.48 (\pm 2.71)	11	0.6490	2.42 (\pm 1.42)
miR-27a	1.25 (\pm 1.46)	1	1.50 (\pm 1.77)	5	0.5580	1.29 (\pm 1.23)
miR-520d-5p	8.57 (\pm 3.39)	14	7.00 (\pm 2.73)	17	0.1587	2.05 (\pm 2.03)
miR-122	2.41 (\pm 4.23)	5	2.21 (\pm 3.98)	8	0.8632	1.82 (\pm 1.86)
miR-485-3p	1.48 (\pm 2.35)	0	1.34 (\pm 2.50)	0	0.8182	1.45 (\pm 1.45)
miR-21	-1.83 (\pm 2.60)	0	0.05 (\pm 2.01)	0	0.0019	2.40 (\pm 1.82)
miR-218	8.01 (\pm 2.88)	13	8.93 (\pm 2.62)	19	0.3650	1.77 (\pm 1.79)
					Total Average	1.79 (\pm 1.63)

[†] Δ CT = miRNA of interest cycle threshold value - U6 cycle threshold value.

^{*} $|\Delta\Delta$ CT = Absolute Value [Operator 1 Δ CT – Operator 2 Δ CT].

[‡] = p value of mean Δ CT operator 1 vs operator 2.

Bold = statistically significant.

Table 10. Differences in Δ CT between operators with Qiagen miRNeasy with RNA Carrier and No Pre-amplification (Inter-Operator Variability).

Colorectal Advanced Adenoma (n=16) + Control (n=16)						
Unpaired t-test - Cycle Threshold = 0.03						
microRNAs	Operator 1		Operator 2		p-value [‡]	Mean $ \Delta\Delta$ CT [*] (\pm SD)
	Mean Δ CT [†] (\pm SD)	# miRNA Not Expressed	Mean Δ CT [†] (\pm SD)	# miRNA Not Expressed		
miR-374	-1.80 (\pm 1.75)	0	-1.69 (\pm 1.99)	0	0.8151	0.70 (\pm 0.78)
miR-142-3p	-7.16 (\pm 1.57)	0	-6.60 (\pm 1.81)	0	0.1910	0.91 (\pm 0.89)
miR-523	-3.21 (\pm 2.82)	0	-2.12 (\pm 2.92)	0	0.1339	1.38 (\pm 1.02)
miR-374-5p	-3.27 (\pm 1.94)	0	-2.33 (\pm 1.87)	0	0.0529	1.27 (\pm 1.06)
miR-376c	-0.04 (\pm 1.74)	0	0.05 (\pm 1.98)	0	0.8475	0.76 (\pm 0.91)
miR-27a	-6.12 (\pm 1.56)	0	-5.52 (\pm 1.79)	0	0.1579	0.98 (\pm 1.03)
miR-520d-5p	5.54 (\pm 2.54)	0	6.27 (\pm 2.91)	1	0.2925	1.20 (\pm 1.01)
miR-122	-2.69 (\pm 2.96)	0	-2.05 (\pm 3.58)	0	0.4387	1.11 (\pm 1.10)
miR-485-3p	-2.60 (\pm 2.02)	0	-1.31 (\pm 2.26)	0	0.0191	1.50 (\pm 1.01)
miR-21	-7.59 (\pm 1.75)	0	-6.69 (\pm 1.85)	0	0.0500	1.36 (\pm 1.00)
miR-218	-3.73 (\pm 2.28)	0	-2.90 (\pm 2.23)	0	0.1460	1.09 (\pm 1.06)
					Total Average	1.12 (\pm 0.99)

[†] Δ CT = miRNA of interest cycle threshold value - U6 cycle threshold value.

^{*} $|\Delta\Delta$ CT = Absolute Value [Operator 1 Δ CT - Operator 2 Δ CT].

[‡] = p value of mean Δ CT operator 1 vs operator 2. **Bold** = statistically significant

10. SELECTION OF HOUSEKEEPING GENE (HKG)

We determined expression of the following housekeeping genes (HKGs): Let-7a, Let-7d, Let-7g, miR-16, RNU6, RNU48, miR-191, miR-223, miR-484, and miR-520d-5p. The cycle threshold (CT) was fixed at 0.03 for all samples. Once RT-PCR was performed for all samples, for each potential HKG, the mean CT and standard deviation was calculated for all sample groups, allowing for comparison among HKGs.⁹⁵

Following identification of the HKGs with uniform expression in all samples, and the narrowest standard deviation, we then used these HKGs alone or in combination as reference to determine their utility in comparing differences in miRNA expression between groups. Only miRNA which were expressed in $\geq 50\%$ of subjects in each groups were analyzed.

The number of samples in which these HKGs were expressed by patient groups is shown in Table 11. Let-7a, Let-7d, Let-7g, and RNU48 were only expressed in 26%, 7%, 10%, and 8% of these samples, respectively. Only miRNAs with uniform expression in all samples were included in the subsequent analysis.

Table 11. Percentage of Housekeeping Gene (HKG) Samples Expressed within Each Group Investigated.

HGKGene (HKG)	Patient Groups (Number and Percent of Samples Expressing HKG)					
	Colorectal Cancer n=20	Colorectal Adenoma n=11	Breast Cancer n=10	Lung Cancer n=10	Pancreatic Cancer n=10	Control n=12
Let-7a	17 (85)	9 (82)	9 (90)	6 (60)	7 (70)	6 (50)
Let-7d	19 (95)	10 (91)	10 (100)	7 (70)	10 (100)	12 (100)
Let-7g	19 (95)	9 (82)	10 (100)	8 (80)	9 (90)	12 (100)
RNU48	19 (95)	11 (100)	10 (100)	8 (80)	7 (70)	12 (100)
miR-16	20 (100)	11 (100)	10 (100)	10 (100)	10 (100)	12 (100)
mir-191-5p	20 (100)	11 (100)	10 (100)	10 (100)	10 (100)	12 (100)
miR-223	20 (100)	11 (100)	10 (100)	10 (100)	10 (100)	12 (100)
miR-484	20 (100)	11 (100)	10 (100)	10 (100)	10 (100)	12 (100)
miR-520d-5p	20 (100)	11 (100)	10 (100)	10 (100)	10 (100)	12 (100)
RNU6	20 (100)	11 (100)	10 (100)	10 (100)	10 (100)	12 (100)

Shaded areas indicate all samples expressing HKG of interest

RNU6, miR-520d-5p, miR-16, miR-191, miR-223, and miR-484 were expressed in all samples. The mean CT and standard deviation for each of these remaining 6 potential HKGs that were expressed in all samples are listed in Table 1. Figure 1 is an example of PCR output showing CT values of HKG U6 and miR-520d-5p. RNU6, a commonly used HKG, was consistently expressed in all samples with a narrow standard deviation (Table 12).

Table 12. Mean and Standard Deviation of Housekeeping Genes with 100% expression.

	Mean CT (+/- Standard Deviation)					
	RNU6*	miR-16	miR-191	miR-223	miR-484	miR-520d-5p*
Colorectal Cancer (n=20)	22.4 +/- 3.8	19.4 +/- 4.7	18.4 +/- 4.5	15.0 +/- 4.2	15.6 +/- 2.8	29.5 +/- 0.8
Breast Cancer (n=10)	25.8 +/- 3.2	20.8 +/- 4.4	19.3 +/- 4.5	16.1 +/- 4.4	17.4 +/- 3.7	29.7 +/- 1.3
Lung Cancer (n=10)	26.8 +/- 2.4	22.6 +/- 4.6	22.2 +/- 4.6	19.3 +/- 4.7	19.7 +/- 4.3	29.0 +/- 0.6
Pancreatic Cancer (n=10)	27.3 +/- 2.2	25.2 +/- 2.1	21.3 +/- 4.7	19.8 +/- 3.2	17.8 +/- 3.1	30.4 +/- 0.8
Colorectal Adenoma (n=11)	22.6 +/- 2.5	20.2 +/- 3.7	18.0 +/- 3.0	14.7 +/- 3.0	15.0 +/- 1.6	30.7 +/- 0.9
Comparison (n=12)	22.0 +/- 2.2	21.2 +/- 1.8	20.1 +/- 2.7	17.5 +/- 2.7	17.2 +/- 1.6	30.5 +/- 1.0

* Data for RNU6 and miR520d-5p shown in shaded areas showed the narrowest standard deviation, with least variability between groups

In addition, our data indicated that a gene that has not been previously reported as an HKG (miR-520d-5p) had a remarkably stable expression over a variety of samples. Of all the HKGs we investigated, miR-520d-5p exhibited the narrowest range of expression (29.0-30.7) and the smallest standard deviation among samples as well as being expressed in all samples. Although we could find no reports describing use of miR-520d-5p as an HKG, due to the reliable expression and narrow standard deviation, we suggest that it could be used reliably in plasma miRNA research.

miRNA expression data using both HKG's (RNU6 and miR-520d-5p) with the highest expression and narrowest standard deviation are shown in table 13. Overall use of RNU6 seems generally to be superior to using either miR520d-5p alone or the average of RNU6 and miR520d-5p; however because of greater variability within the same sample with RNU6, we would recommend using a combination of RNU6 and miR520d-5p. RNU6 has a higher expression than miR520d-5p. HKG with different expression than the miRNA of interest is recommended. Sample size does appear to play a role. For example in our comparison of controls vs all other groups, or in the comparison of CRC vs CRAd our sample sizes are small and/or unequal (unbalanced). In this scenario results are less clear, than where sample sizes are more equal and where results are more consistent between RNU6, miR520d-5p and the combination of the two. ^{99, 102-107}

Table 13. Expression data for Housekeeping Genes RNU6 and miR520d-5p

Comparator Groups	No. miRNA Expressed in >50% of samples in each group	No. miRNA with raw p<0.05	No. miRNA with FDR adjusted p<0.25	No. miRNA with FDR adjusted p<0.1	No. miRNA with AUC >0.7	No. miRNA present in all samples in all groups	No. miRNA with FDR adjusted p<0.1 AND present in >80 of samples in both groups
Control vs All Others*							
RNU6	173	147	164	156	156	26	102
520d-5p	173	0	0	0	5	26	0
RNU6 & miR520d-5p	173	63	117	26	82	27	9
(CRC & Crad) vs (BC,LC,PC)							
RNU6	219	107	138	114	82	27	58
520d-5p	176	110	141	120	80	27	82
RNU6 & miR520d-5p	176	40	45	28	29	27	19
CRC vs Crad							
RNU6	219	2	2	2	8	43	1
520d-5p	219	1	1	1	17	43	0
RNU6 & miR520d-5p	219	3	1	1	11	43	0

* All others includes colorectal cancer (CRC), colorectal adenoma (Crad), breast cancer (BC), lung cancer (LC), and pancreatic cancer (PC)

11. DISCUSSION

With the growing field of miRNA research and the potential use of miRNAs as biomarkers for cancer and other human diseases, the lack of standardization and reproducibility among studies is becoming more apparent. Such variations in methodology can lead to large variability in results reported from one research group to another. Six different sources of variation in experimental technique were examined with respect to their effect on miRNA expression data: 1) time of plasma extraction, 2) method of RNA extraction, 3) cycle threshold setting, 4) intra-operator variability 5) inter-operator variability and 6) selection of housekeeping gene. Our brief literature review of a 1-year time frame, was not meant to be an exhaustive review, but rather to provide a “snap-shot” of current practices of performing experiments and analyzing data. Our literature review has shown, that many publications focusing on plasma miRNA do not carefully describe their experimental methods, that there is wide variation in performing such studies and analyzing resulting data.

There has been discussion as to whether plasma or serum is better for study of circulating miRNA. While some report comparable data others report differences between the two sources¹⁰⁸⁻¹¹⁰. We chose to focus on plasma, due to the concerns that miRNAs might be released from blood cells into the serum during the coagulation process as suggested by Wang et al¹⁰⁹.

Our data regarding the timing of plasma extraction suggest that plasma needs to be isolated rapidly, within hours after phlebotomy. With blood samples that were stored at 4°C, even with a modest sample size, we observed statistically significant different Δ CTs for select miRNA beginning as early as plasma extraction at 24 h. This is in

agreement with prior reports linking hemolysis to altered miRNA expression¹¹¹. Due to the limited sample size and small number of miRNA investigated, we suggest that plasma be isolated within 12 h following phlebotomy in order to avoid falsely elevated or reduced miRNA expression levels.

The three most widely used methods of total RNA extraction from plasma or serum are guanidinium thiocyanate-phenol chloroform-based methods (e.g., Trizol LS, Life Technologies, Carlsbad, CA), phenol with glass fiber filter-based (e.g. miRVANA, Ambion®, Life Technologies), and phenol/guanidine with silica membrane based purification (e.g. miRNeasy, Qiagen, Venlo, The Netherlands). Moret et al.¹⁰¹ compared all three methods and found that a modified phenol/guanidine lysis with silica membrane-based RNA extraction method yielded enhanced quantity, purity, and performance on assays. Although we did not assess the glass-fiber filter-based method here, our data agree with those of Moret et al.¹⁰¹ and suggest that the Qiagen miRNeasy with yeast carrier isolation method yields a very reproducible result. The high concentration of 353 +/- 85 ng/ μ L total RNA obtained with this technique as compared to Trizol LS, which resulted in concentration of 19 +/- 12 ng/ μ L, allows for pre-amplification to be omitted prior to qPCR, omitting yet another source of data variability. In using this technique, we were able to reduce the number of “missing” samples (miRNA that did not express) from 15% to 0.14%.

Analysis of various fixed as well as of variable threshold settings indicated that a fixed Ct setting of 0.03 produced the most reproducible data provided that < 10% of data were missing. This has the significant advantage of not requiring the additional statistical

adjustment that is required when a variable threshold is utilized (Rai et al., unpublished data, 2014).

We demonstrated a lack of significant intra-operator variability. In view of this, triplicates are not necessary, and if there are few missing values (<10%), one could even question the need to perform duplicates given the very low $\Delta\Delta CT$. Inter-operator variation was also low. Using the phenol/guanidine-based lysis and silica membrane-based purification technique resulted in a narrowing of $\Delta\Delta CT$ values between operators as compared to guanidinium thiocyanate-phenol chloroform purification. In fact, when these experiments were repeated, the differences in miRNA expression between operators for miR-21 and miR-485-3p were not seen, leading us to conclude that this was within the range of experimental error and not a significant issue.

When determining CT values and normalizing miRNA expression of samples of interest to an internal HKG, it is imperative that the HKG be reproducible and express at similar values across all samples. An ideal HKG should meet the following criteria: 1) Expressed in all samples, 2) Have medium-to-high levels of expression in the specimens analyzed and 3) Have consistent levels of expression with narrow standard deviation. When applying these three criteria to our data, Let-7a, Let-7d, Let-7g and RNU48 were eliminated since they were not expressed in all samples. Of the 6 remaining potential HKGs, two had a very narrow standard deviation as well as consistent expression: RNU6 and miR-520d-5p. Based upon our data, due to the narrow standard deviation and less variability among groups, we propose that both RNU6 and miR520d-5p should be used as HKGs.

Based upon our studies, rapid plasma extraction is essential. A modified phenol/guanidine-based lysis and silica membrane-based purification RNA extraction is preferred due to the extremely low rate of missing values and high RNA yield, allowing the investigator to avoid using pre-amplification, another source of variability. If there is a low number of missing values (<10 %), a fixed threshold setting of 0.03 provides the most reliable, consistent data without the need for data normalization. With this setting, there is no significant intra-operator variability, i.e. replicates can be restricted to duplicates, rather than triplicates, resulting in cost and labor savings. RNU6 and miR-520d-5p are the most reliable of the 10 studied HKGs for studies of plasma miRNA. The use of plasma miRNA as biomarkers of human disease is evolving and expanding. Data reproducibility is essential prior to clinical application. Standardization of analytic methods and reporting is necessary to permit accurate data comparison and validation.

A. COLON CANCER CELL LINES USED TO DETECT MIRNA DIFFERENCES BETWEEN CANCERS OF DIFFERING GROWTH RATES AND METASTATIC CAPABILITY

The Price Institute at The University of Louisville allows for a unique situation to study tissue and plasma samples on patients that are followed clinically by the lead investigator. This gives a large range of pathology, but has limitations due to heterogeneity among patients with respect to preoperative treatment, race, gender, immune factors and other variables. Studies using commercially available colon cancer cell lines offer several advantages. First and foremost is the reproducibility of cell lines. When minimizing the pass rate (the amount of times the cells are divided), early passes of cell lines behave nearly the same within that cell line across different experiments. This is important when

dealing with cancer cells that tend to divide rapidly and already behave differently than non-cancerous cells. With meticulous study and observation, after a few weeks, we know the behavior of the different cell lines under investigation. This is important because once their “normal” growth rate and behavior is known; it allows us to use external means to manipulate these cells to study different states to which cancer cells could possibly be exposed to in a patient. Although use of such cell lines is widely accepted they do have disadvantages. Cell lines are immortalized cancer cells. No matter what the conditions are; this will add caution to interpreting the results until these results are in turn tested in animal models or verified in a human clinical trial.

Not only do cell lines allow us to manipulate cancer pathology to investigate different aspects of cancer pathway progression, but they also allow us to study these pathways in different stages of cancer. By utilizing well established immortalized CRC cell lines, we can examine different cancer stages. It allows us to look at benign non-cancerous epithelial cell lines as well as cancer cell lines.

Prior to developing a hypothesis, screening arrays were performed utilizing Taq-Man[®] microfluidic technology array cards. In this screening, the overall goal was to establish which miRNAs were differentially dysregulated between cell lines of different cancer stages. The use of both an “A” card and “B” card was utilized, each assessing 384 unique human miRNA (760 total miRNAs). Dukes A-D cell lines were screened and had a high number of these miRNAs expressed in each cell line (Table 14). Of the miRNAs expressed miRNA-99a and miRNA-100 had a unique expression that no other set of miRNAs had (Table 15). This differential expression led us to further investigate miRNA-99 and miRNA-100.

Not to our surprise an extensive amount has been published regarding the miRNA-99 family, which includes miRNA-99a, -99b and -100. Specifically, a large amount of work has been done investigating the role of the miRNA 99 family and its suppression of prostate-specific antigen and cancer proliferation in prostate cancer.¹¹² We investigated different pathways with which the miRNA 99 family was associated and noted its involvement in the mammalian target of rapamycin (mTOR) pathway. Although some work has been done previously with respect to the role of mTOR in colorectal cancer, there are few reports examining the effect of miRNA-99a mTOR protein expression and its ultimate effect on downstream targets of the mTOR pathway.

Table 14. Number of miRNAs expressed in screening array of cell lines ranging from Dukes A-Dukes D.

Number of miRNAs Expressed				
TLDA Card	Duke's A (SW1116)	Duke's B (SW480)	Duke's C (HT-29)	Duke's D (HCT116)
1st 384 microRNAs	293	335	314	313
2nd 384 microRNAs	262	219	209	210

Table 15. Fold Change and Regulation of miRNA 99 Family in the screening array for colorectal cancer cell lines.

microRNAs	Fold Change				Fold Regulation			
	Dukes' A vs. Control	Dukes' B vs. Control	Dukes' C vs. Control	Dukes' D vs. Control	Dukes' A vs. Control	Dukes' B vs. Control	Dukes' C vs. Control	Dukes' D vs. Control
miR-100	0.03	0.14	0.02	4.91	-39.5	-7.1	-52.3	4.9
miR-99a	0.02	0.14	0.03	4.85	-45.4	-7.0	-34.2	4.8

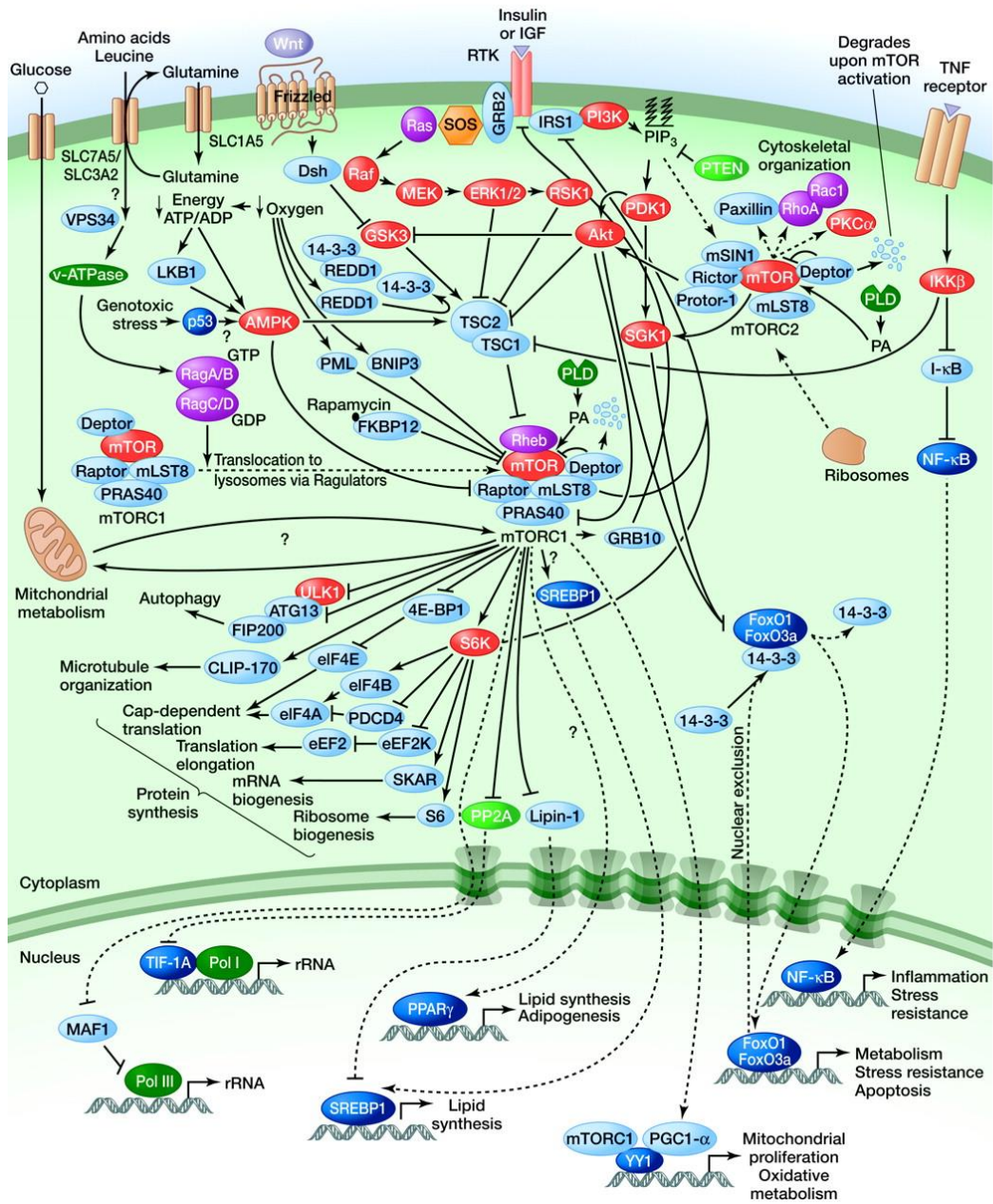
CHAPTER III

MAMMALIAN TARGET OF RAPAMYCIN (MTOR) SIGNALING PATHWAY

miRNAs have been shown to be involved in multiple pathways in all types of cancers; this is no different with colorectal cancer. One of the pathways that have been shown to influence cancer behavior, especially in prostate cancer, is the mTOR signaling pathway. Although much is known about this pathway and its two protein complexes, mTORC1 and mTORC2, there is still much to learn in regards to its relationships to CRC and its influence on CRC progression.

Over the past several decades the mTOR, which is now referred to as the *mechanistic* target of rapamycin, mTOR signaling pathway (Figure 6) has been shown to play an integral role in the regulation of organ growth and homeostasis. Due to its regulation of multiple cellular processes, it has been shown to influence multiple cancer pathways, obesity and type 2 diabetes to name a few. This has led to much interest in further understanding this pathway in various disease states and particularly interest with respect to potential for pharmaceutical intervention in the mTOR pathway.

Figure 6. mTOR pathway



Mathieu Laplante, and David M. Sabatini Cold Spring Harb Perspect Biol 2012;4:a011593

TOR1 and TOR2 genes were identified in the early 1990s during genetic screening in budding yeast. These were shown to be mediators of the toxic effects of rapamycin on yeast. Rapamycin is a naturally occurring macrolide produced by *Streptomyces hygroscopicus* bacteria. mTOR itself is a serine/threonine protein kinase that is part of the phosphoinositide 3-kinase (PI3K)-related kinase family and interacts with several proteins to form two distinct complexes aptly named mTOR complex 1 (mTORC1) and complex 2 (mTORC2). Not yet completely understood, the mechanism of action of rapamycin's effect on mTOR is thought to occur by a gain-of-function complex when rapamycin binds intracellularly with the 12-kDa FK506-binding protein. It is believed that this rapamycin-FK506 complex will then interact with and inhibit mTOR protein when a part of the mTORC1 complex but does not inhibit the function of mTOR when it is a part of mTORC2. Although rapamycin-FK506 is implicated in this inhibition process, the exact binding process of this complex to mTORC1 has yet to be discovered.

A. MTOR COMPLEX 1 (MTORC1)

mTORC1 is composed of six protein components:

1. mTOR protein
2. mammalian lethal with sec-13 (mLST8, also called GBL)
3. DEP domain containing mTOR-interacting protein (DEPTOR)
4. Tti1/Tel2 complex
5. Regulatory-associated protein of mammalian target of rapamycin (RAPTOR)
6. proline-rich Akt substrate 40kDa (PRAS40)

RAPTOR and PRAS40 are the two proteins that are unique to mTORC1, and are not a part of mTORC2.

mTORC1 is involved in multiple key processes needed for health, not limited to but including protein synthesis, autophagy and lipid synthesis. This complex helps regulate downstream proteins that are key in protein synthesis. One of these being the eukaryotic initiation factor 4E (eIF4E)-binding protein 1 and the p70 ribosomal s6 Kinase 1 (S6K1). Previously described, the phosphorylation of 4E-BP1 inhibits its binding to eIF4E, which then in turn promotes cap-dependent translation. In addition S6K1 is stimulated by mTORC1 and leads to its involvement in mRNA development, cap-dependent translation and regulation of many other protein activities.

Apropos autophagy, which is the degradation of cellular components by lysosomes, mTORC1 increases autophagy when it is inhibited. The opposite is true also, as when mTORC1 is stimulated by upstream inputs autophagy will decrease. This suggests that inhibition of TORC1 can lead to unregulated cell growth.

B. MTOR COMPLEX 2 (MTORC2)

mTORC2 is composed of seven protein components:

1. mTOR protein
2. mLST8
3. DEPTOR
4. Tti1/Tel2 complex
5. Rapamycin-insensitive companion of mTOR (RICTOR)
6. Mammalian stress-activated map kinase-interacting protein 1 (mSin 1)
7. Protein observed with rictor 1 and 2 (protor 1/2)

RICTOR, mSin1 and protor 1/2 are the 3 unique proteins that are a part of mTORC2.

C. REGULATORS OF MTORC1

mTORC1 has multiple inputs from various upstream pathways. These currently include but are not limited to, growth factors, stress, energy status, oxygen availability and amino acids. These inputs lead to mTORC1's control on protein/lipid synthesis and autophagy.

mTORC1 is regulated by growth factors that initially increase the phosphorylation of TSC2 via the protein kinase B (PKB) activation cascade. The activation of TSC2 in turn leads to inactivation of mTORC1. In addition extracellular-signal-regulated Kinase 1/2 and S6K1 have the opposite effect and inhibit or deactivate the TSC1/2 complex that in turn leads to activation of TORC1.

D. REGULATORS OF MTORC2

Compared to mTORC1, all aspects of the mTORC2 pathway, including its regulators are less well understood. Due to the inability of FKBP-12-rapamycin to bind to the intact mTORC2, it was originally thought that this complex was completely insensitive to rapamycin, however, recently it has come to light that this is not the case.¹¹³ The complex nature of mTORC2 is shown by the fact that some cells over time reduce mTORC2 signaling via suppression of mTORC2 assembly, by an as yet not understood mechanism.¹¹³ Unlike mTORC1, mTORC2 is insensitive to upstream nutrients, yet responds to certain growth factors, including insulin. The mechanism of this is currently not known, but ribosomes are known to be necessary for this signaling to occur.¹¹³

One facet of mTORC2 activity that is known is its effect upon AKT, which helps regulate certain cellular processes such as metabolism, growth, proliferation, metabolism and cellular survival. Sarbassov et al, in 2005 showed that mTORC2 phosphorylates

AKT at its hydrophobic motif, which results in its activation.¹¹⁴ In addition, it has been shown that silencing components of mTORC2 impairs the phosphorylation of some targets of AKT, whereas other targets of AKT are unaffected.^{115, 116}

CHAPTER IV

HYPOTHESIS AND SPECIFIC AIMS

Several pathways that influence colorectal cancer have been shown to interact with the mTOR pathway such as the wnt pathway, PI3/AKT, P53 and RAS/RAF. These pathways influence normal cell life progression including apoptosis, tumor suppression, protein activation and cell binding to name only a few of their functions. Although mTOR has been shown to influence colorectal cancer, the link between the miRNA 99 family and mTORs and its influence on CRC is not clear. It has been shown that certain miRNAs bind to mTOR, however, changes in the cells' activity, and downstream protein expression have not yet been fully described.

Preliminary work in our laboratory has shown the miRNA 99 family miRNA to be differentially expressed among colon cancer cell lines of different metastatic potential, suggesting that these miRNA may play a role in invasiveness and metastasis in CRC.

This was investigated with the following hypothesis:

Hypothesis: miR-99a decreases cell proliferation, migration and possibly invasion of colorectal cancer cell lines by decreasing mTORC1 and mTORC2 expression.

3 Specific Aims will be investigated:

1. To determine the effect of miRNA-99a on mTOR protein phosphorylation

2. To determine miRNA-99a's influence on the phosphorylation of mTOR pathway's downstream proteins: S6K1 and 4EBP1
3. To determine if transfection of HT-29, HCT-116 and CCD841 cell lines with miRNA-99a will inhibit cell migration and invasion

CHAPTER V

MATERIALS AND METHODS:

A. CELL LINES

In this study, three relevant cell lines (Table 1) acquired from American Type Culture Collection (ATCC, Manassas, Virginia) were reinitialized from frozen (-80°C) material, then either allowed to grow for future testing, i.e. Western blot analysis, polymerase chain reactions (PCR) or immunohistochemistry (IHC), or grown for harvesting to be used at a later time. All cell lines were adhesive in nature and are not free floating cell lines, i.e. when cells are growing and dividing they adhere to the cell culture flasks.

1. CCD 841 CoN (ATCC® CRL-1790™)

Normal epithelial colon cells were harvested from a human female fetus at the 21 week gestation period and cultured in Eagle's Minimum Essential Medium (EMEM) supplemented with 0.5% mixture of penicillin, streptomycin, amphotericin B, 0.5% L-glutamine, and 10% Fetal Bovine Serum (FBS).

2. HT-29 (ATCC® HTB-38™)

Dukes' type C primary colorectal adenocarcinoma epithelial cells were harvested from a 44 year-old woman and cultured in McCoy's 5A medium supplemented with 0.5% mixture of penicillin, streptomycin, amphotericin B, 0.5% L-glutamine, and 5% FBS.

3. HCT-116 (ATCC® CCL-247™)

Dukes' type D, primary colorectal carcinoma epithelial cells were harvested from a man (age not stated), and cultured in McCoy's 5A medium supplemented with

0.5% mixture of penicillin, streptomycin, amphotericin B, 0.5% L-glutamine, and 5% FBS. Notably it has come to light that this cell line is not a typical adenocarcinoma Dukes' D cell line but from a patient with Hereditary Nonpolyposis Colorectal Cancer (HNPCC), which is a type of cancer that is defective in DNA mismatch repair, which will lead to microsatellite instability. Depending on the sub-classification of HNPCC, there have been up to 7 different genes implicated.¹¹⁷⁻¹²²

B. MAINTENANCE OF CELL LINES

Each cell line was maintained in a cell culture hood, which was swabbed down with 70% ethanol (EtOH) before and after each use and the hood was run for 10 minutes prior to working to establish protective air flow. All items, including gloved hands, entered the hood only after being cleansed with 70% EtOH. Only one cell line and appropriate culture medium were placed in the cell culture hood at any given time and the hood was cleaned with 70% EtOH in between cell line transfers.

1. INITIAL CULTURING OF CELLS

For each cell line, 8mL of appropriate culture media was first added to a 15mL tube. Then 9mL of appropriate culture media was added to a 25 mL cell culture flask. The flask was incubated to allow temperature equilibration of the culture media prior to placing the freshly thawed cells into the flask. The vial of frozen cells was then rapidly thawed in a 37°C water bath, keeping the O-ring and cap out of the water to reduce contamination. After the cells were thawed, the external surface of each vial was cleansed with 70% EtOH, placed in the hood and transferred to the 15mL tube with appropriate

culture media. Finally, the flask with the thawed cells is rinsed using 1 mL of appropriate culture media and added to the 15 mL tube. The contents of the 15mL tube were centrifuged at 125g, at 37°C for 6 minutes, until a cell pellet was formed. The cell pellet was aspirated and then resuspended using 1mL of appropriate culture media via a micropipette tip to obtain cell suspension. The cells were then added to the pre-warmed 25 mL flask with 9 mL of appropriate culture media which was gently rocked in order to disperse cells and then was placed back in the incubator at 37°C, where they were left to grow with daily monitoring.

2. SUB-CULTURING/SPLITTING CELLS

Prior to sub-culturing or splitting cell lines, the current flask of actively growing cell lines was viewed at 10x magnification to determine whether the cells were 70-90% confluent and ready to be divided. When the cells were determined to be proper confluent, they were then transferred from the incubator into the cell culture hood. For each cell line the appropriate culture media and a 3 mL aliquot of trypsin-EDTA were then set into a 37°C water bath to thaw. Once thawed, the 15 mL tube of trypsin-EDTA and bottle of cell culture medium were vortexed and homogenized, then the containers were cleaned with 70% EtOH and placed in the cell culture hood. With the culture flask inside the cell culture hood, the next step was to remove the old culture medium from the flask and discard it into the waste beaker. The flask was then washed with 0.5mL of trypsin for 2-3 seconds and then emptied into the waste beaker. Next, 2.5 mL of trypsin was added to the flask, gently rocked and the flasks were observed through an inverted microscope to determine when the cells had rounded up into the trypsin media off the bottom of the flask. The type of cell line, as well as confluence of the cells, has an effect

on how fast the trypsin works. While the trypsin acted on the old culture flask, the appropriate cell culture medium was added to a new 75 mL flask(s) and incubated at 37°C. Once the trypsin exerts its effect, the cells are rounded up and suspended; 8mL of appropriate culture media was added to the flask. This cell suspension was added to a 15mL tube and then centrifuged at 125g, at 37°C for 6 minutes, until a new cell pellet was formed. This 15mL tube was then cleaned with 70% EtOH and placed back into the cell culture hood. The supernatant was discarded and the cell pellet was re-suspended using 1mL of appropriate culture media via a micropipette tip to obtain a single-cell suspension.

At this point, cells were counted using a hemocytometer for further experiments or divided in pre-determined ratios for sub-cultivation. The split ratios for each cell line are detailed in Table 16.

Table 16. Cell line criteria for each passage

Cell Line:	Subcultivation* Ratio	Medium Renewal per week:	Number of cells per 75mL flask:
<u>CCD841</u> Normal fetal	1:2 – 1:3	2-3 times	2×10^6
<u>HT29</u> Dukes C	1:3 – 1:8	2-3 times	$\geq 1-2 \times 10^6$
<u>HCT116</u> Dukes D	1:3 – 1:10	2-3 times	$\geq 1-2 \times 10^6$

*Sub-cultivation refers to the multiple passes or generations of each cell line.

The calculated amount of cells was then added to the new 75 mL flask with pre-warmed (37°C) culture media. Finally, the flask with cells in suspension was labeled with cell line name, passage number and date, then gently rocked and returned to the incubator.

3. SUBSEQUENT FREEZING OF CELLS

The appropriate cryo-medium was created by taking a cell lines' respective medium and adding 5% sterile dimethyl sulfoxide (DMSO) to the final concentration. Similar to the sub-culturing/splitting protocol, the cells were treated with trypsin-EDTA, collected in media, and the cell suspension centrifuged into a pellet. However, as opposed to re-suspending the cell pellet in normal cell culture media, cryo-media was used. The cells were counted and the concentration of cells was adjusted to 4×10^6 cells/2mL of cryo-media. 2mL of the suspension was added to cryo-flasks that were specifically labeled. The cryo-flasks were stored in an ethanol-bath at -80°C overnight and then transferred into liquid nitrogen the next day. The earliest possible passage to obtain freezes is passage number 3.

C. MIRNA TRANSFECTION

Once the cell suspension's concentration was determined, the cells were plated into separate wells on a 6-well plate at a concentration of 250,000 cells/2mL culture media and then allowed a 24-hour period to adhere to the plate prior to transfection. At 24 hours, transfection of the following was performed:

- miR-99a mimic
- miR-99a antagomir

- mimic negative control
- antagomir negative control
- mimic positive control
- antagomir positive control

These were introduced to different individual wells using the Lipofectamine[®] 3000 Transfection Reagent Protocol. Each cell line was incubated for 72 hours after transfection prior to cell harvesting.

D. HARVESTING CELLS (FOR RNA OR PROTEIN)

After isolated cell populations had been transfected or treated with rapamycin, they were harvested for either total RNA or protein content. The medium was aspirated carefully and discarded. The cells were rinsed once with ice cold phosphate-buffered saline (PBS) and cells were then treated with trypsin-ethylenediaminetetraacetic acid (EDTA). This allows for them to round up in the appropriate media when added to the plate. The cell suspension was then centrifuged at 125g for 6 minutes at 37°C until a pellet was formed. The cell pellet was re-suspended with 1mL of 1x PBS and centrifuged into a pellet. If harvesting for total RNA, the cells were re-suspended using 0.4 mL of ice cold lysis buffer. If harvesting for protein, the cells were re-suspended using 0.15 mL of ice-cold radio immune-precipitation assay (RIPA) buffer. The cells and buffer are mixed thoroughly by pipetting and then stored at -80°C until needed.

E. POLYMERASE CHAIN REACTION

Cell samples in lysis buffer were prepared first via reverse transcription for microRNA quantification using a Step-One™ RT-PCR® System with default long thermal cycling conditions. Using the TaqMan miRNA reverse transcription kit and TaqMan microRNA-specific primer pool (5x), targeted RNA was converted into cDNA in a thermal cycler. TaqMan probes (20x) were used to bind to complementary sequences on target cDNA during quantitative RT-PCR. The levels of miRNA-99a were normalized to miRNA RNU6, an endogenous internal reference, in order to calculate Δ CT values. Δ CT values of samples transfected with miRNA-99a mimic and antagomir were compared to the Δ CT values of corresponding positive and negative controls.

F. WESTERN BLOT

For protein quantification, western blots (n=4 for each protein) were performed for target proteins in the mTOR pathway (Table 16). After the sample was thawed on ice from its -80°C storage, 0.001 mL of protease inhibitors were added. The cells were then sonicated to disrupt cellular membranes. The cell debris was centrifuged into a pellet. To determine the total concentration of protein in the sample, a bicinchoninic acid (BCA) assay was performed. The supernatant of the sample was then diluted by a factor of 20 with double distilled water in a 96 well plate. For reference, concentration standards from 0 to 1000ng/ μ L were added to appropriate wells. All wells were then treated with 0.16mLs of BSA assay and allowed to incubate at 37°C for 30 minutes. After incubation, the plates were then analyzed using Titertek Multiskan MCC/340® microplate reader which produced protein concentration of the samples in question.

An appropriate percentage Bolt[®] Bis-Tris Plus Gel was placed in the Bolt[®] Mini Gel Tank which was then filled half-way with running buffer. The wells were then loaded with molecular marker standards and cell protein samples ranging from 40 to 100 micrograms. Finally the remainder of the tank was filled with running buffer. The gels were run at 165mV for 35-90 minutes to run the molecular markers off the gel depending on the size of the protein of interest.

Proteins of interest in the mTOR pathway, their molecular weight (MW), and predicted band sizes are listed in Table 17.

Table 17. mTOR pathway proteins of interest with molecular weight and predicted Western Blot band detection size.

Protein	Observed Molecular Weight (kDa)	Predicted Band Size (kDa)
mTOR	289	>250
RAPTOR	149	149
RICTOR	192	192
eIF4g1	175	220
S6K1	70	70 and 85 ¹²³
eIF4EBP1	13	20,22, and 25

The completed gel with separated proteins is then transferred onto a Polyvinylidene difluoride (PVDF) membrane using the iBlot[®] Gel Transfer Device (protocol reference). The PVDF membrane was then cut to an appropriate size, covered in 5% milk, and rocked for 1 hour at room temperature in order to block proteins. Primary antibodies for target proteins were prepared in 5% milk and poured over the membrane which was then rocked for another 1 hour at room temperature. The membrane was washed for 10 minutes with Tris-buffered Saline and Tween 20 (TBS-T), and then covered with the secondary antibody which was also prepared in 5% milk and rocked for 1 hour at room temperature. The membrane was again washed for 10 minutes with TBS-T.

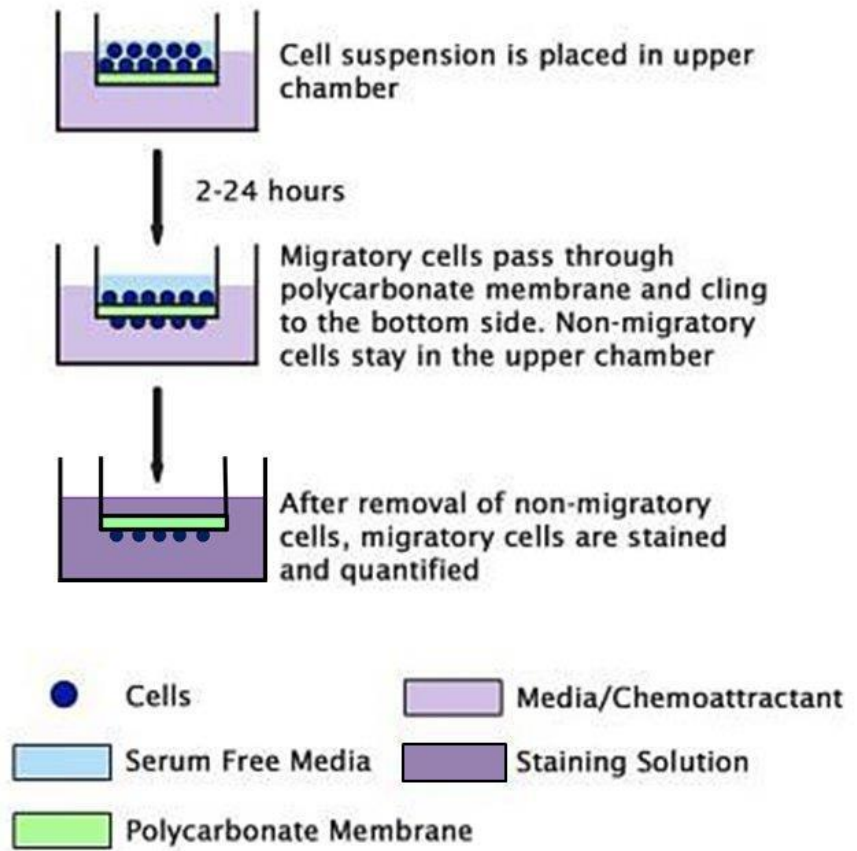
1-1.5mL of Enhanced chemiluminescence (ECL) reagents A and B, which react with the horseradish peroxidase (HRP) enzyme on the secondary antibody to produce light, was applied to each membrane in order to detect the target protein. The membrane and ECL substrates were left in the dark room for 2 minutes before the excess ECL was removed and the membrane was placed in a plastic cassette and left in the dark room.

G. CELL MIGRATION ASSAY

To determine the migration properties of the cell lines themselves Boyden chamber assays were utilized. Five assays were performed for each cell line. First described by Boyden in 1962, these assays allow for the cells chemotactic behavior to be determined.¹²⁴ This assay separates two chambers with a microporous membrane (8 μm pore size). After transfection has occurred the cells under study are then seeded into in the upper chamber. In this step the cells can be “starved” to a certain degree. In all assays

used in my studies, the FBS percentage was reduced from 10%, which is the percentage we use in day to day maintenance, down to 1% in this assay. This helps to promote cells' movement, once they have been starved for a period of time. They are allowed to settle in this chamber for 24 h without chemoattractant added to the bottom chamber. 24 hours after plating the cells into the upper chamber the addition of media with 20% FBS is added to the bottom chamber. Then the cells are allowed to migrate for 12 h. (Figure 7) At the 12 h mark the cells are observed under light microscopy and then stained to allow for quantification in a plate reader. The cells were stained with Blue Cell Stain Solution (Cell Biolabs, Inc.) and then extracted to read at 560nm in the plate reader.

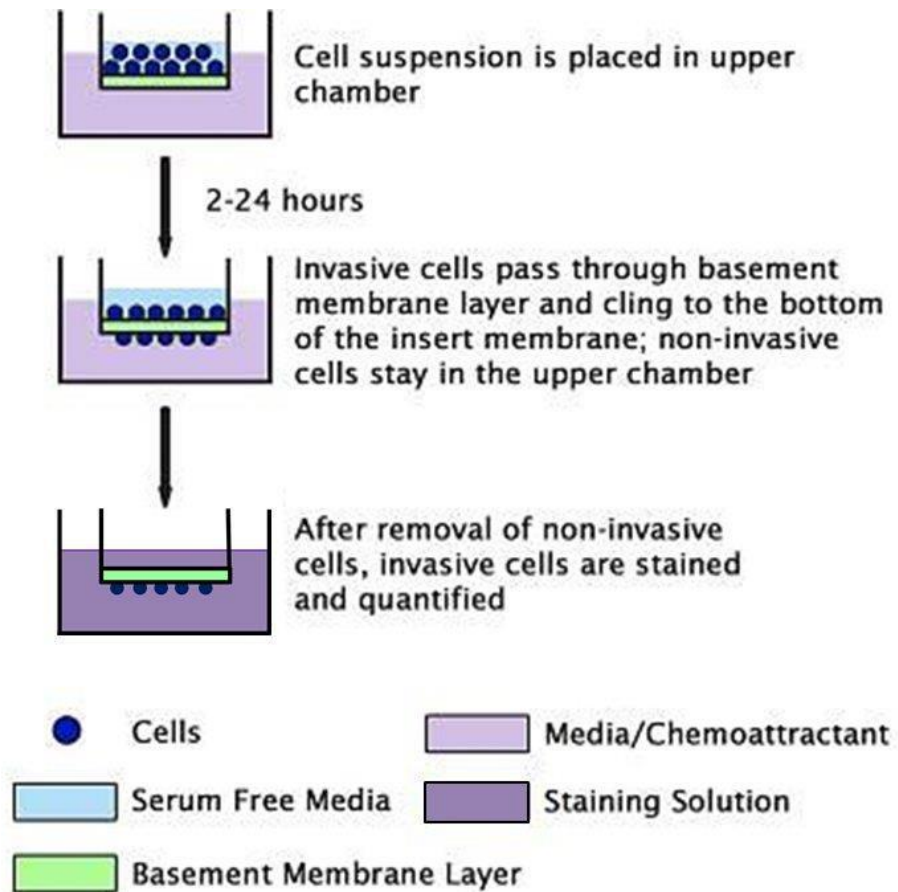
Figure 7. Cell migration diagram and experimental steps



H. CELL INVASION ASSAY

Similar to the Boyden migration assay, the invasion assay now coats the microporous membrane (8 μm pore size) with a uniform layer of dried basement membrane matrix solution. This layer allows for discrimination between invasive and non-invasive cells. If the cells have invasive properties then they will be able to degrade this matrix membrane solution and then migrate through the 8 μm pores that are present in the polycarbonate membrane inserts. (Figure 8) Similar to the migration assay, the cells are allowed 24 hours to settle after plating into the upper chamber. The upper chamber cells are once again “starved” with 1% FBS containing media. At the 24 hour time point, 20% FBS containing media is added to the bottom chamber. At the 12 hour mark the cells that have migrated are stained and the utilization of the plate reader at 560nm is used to determine the amount of cells that migrated. Five assays were performed for each cell line.

Figure 8. Cell invasion diagram and experimental steps



I. STATISTICAL ANALYSIS

To analyze statistical significance of the Western blot assays and migration/invasion studies we utilized the unpaired t-test. All data was analyzed in SPSS, (SPSS Inc. Released 2007. SPSS for Windows, Version 16.0. Chicago, SPSS Inc.) using a two tailed analysis. All sample sizes were equal and had a normal distribution. Statistical significance was defined as a $p < 0.05$.

For Western Blot samples all data had a sample size equal to four, unless noted. These were four cell culture samples that were each grown from new freezes, transfected at the same pass generation and transfected in the same fashion to give a true sample size of four. The same was done for the migration/invasion assay, except the sample size was increased to five.

CHAPTER VI

TRANSFECTION OVERVIEW, PRELIMINARY RESULTS AND DISCUSSION

A. INTRODUCTION

Transfection is the process of introducing an external nucleic acid into the normal functioning cell. In our experiments we utilize two types of non-viral transfection. The use of mimic and antagomirs were used to accomplish our goals. Mimic transfections occur when the investigator introduces more of what we are trying to upregulate. In our experiments with miRNA-99a, by introducing miRNA-99a mimics we are increasing the amount of active miRNA-99a into the cell's cytoplasm. The opposite occurs when we introduce an antagomir into the cell's cytoplasm. miRNA-99a antagomir ultimately down regulates the available amount of active miRNA in question.

Transfecting antagomirs tend to be more finicky and less successful than mimic reactions as it is more difficult to completely eliminate a resource from a cells environment than it is to add to it.

The use of miRNA mimics and antagomirs in transfection experiments allows us to manipulate cell line behavior and protein expression. Once transfection had occurred the first step is to verify the success or failure of the transfection.

B. DATA AND RESULTS

Real time polymerase chain reaction (qRT-PCR) is used to verify successful or unsuccessful transfection. Initially HT-29 cell line was investigated. HT-29 was allowed to grow and when appropriate amounts of cells were available seeded into 6 well culture plates. After 24h, after proper seeding and settling of transfection with miRNA-99a mimic, mimic negative control, antagomir and antagomir negative control was performed. We used Lipofectomine 3000[®] following manufacture's protocol. This was repeated with CCD841 and HCT116 cell lines.

Data regarding transfection of HT-29 is shown in Figure 9. The mi-RNA99a mimic transfection was associated with a fold change of miRNA 99a expression of 8750 as compared to the antagomir transfection which was associated with a miRNA 99a fold change of 0.065 (fold regulation of 15.2).

Next HCT-116 cell line was transfected, and verified via qRT-PCR. HCT-116 showed an increase in miRNA-99a expression as compared to the non-transfected control, however, the antagomir was closer to baseline expression and not down regulated (Figure 10).

After successful transfection of HT-29 and HCT-116, our attention turned to the transfection of CCD 841 (normal colon epithelial cells). Once again successful transfection was verified via qRT-PCR, and is shown in Figure 11. Similar to HCT-116 transfection, CCD 841 cells exhibited a fold change in miRNA 99a expression of 34 with transfection of miRNA-99a mimic. Transfection with the antagomir was not as successful. We observed a fold change of 1.4 in miRNA 99a expression, which is

opposite of what we would expect, ie. a down regulation with the introduction of an antagomir. All data was corrected for cell number in the analysis of fold change and fold regulations.

Figure 9. HT-29 Fold Change of miRNA-99a Expression after Transfection (n=2)
Error bars = standard error of the mean

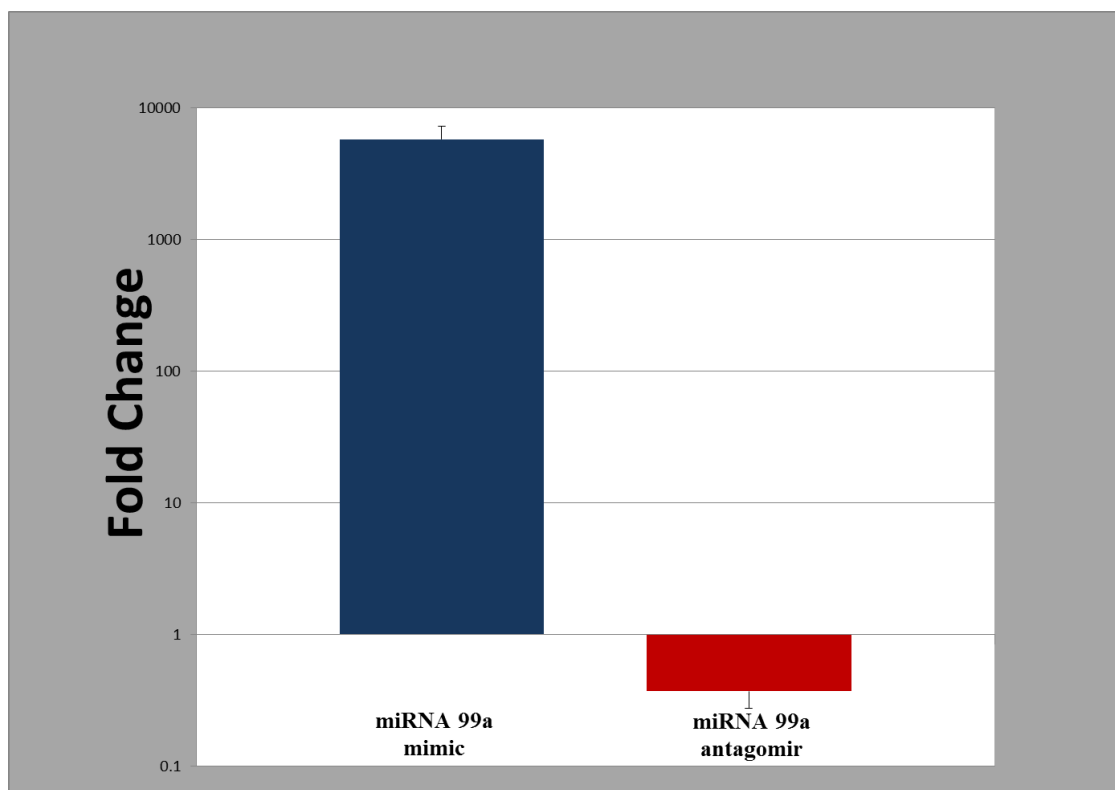


Figure 10. HCT-116 Fold Change of miRNA-99a Expression after Transfection (n=2)
Error Bars = Standard Error of the Mean

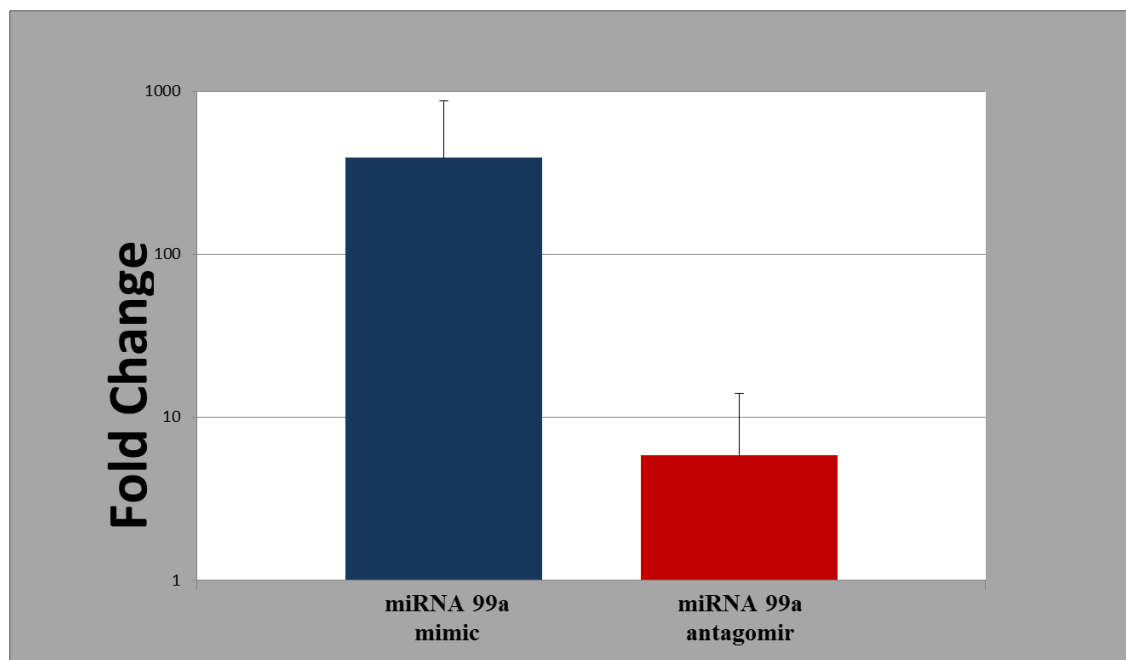
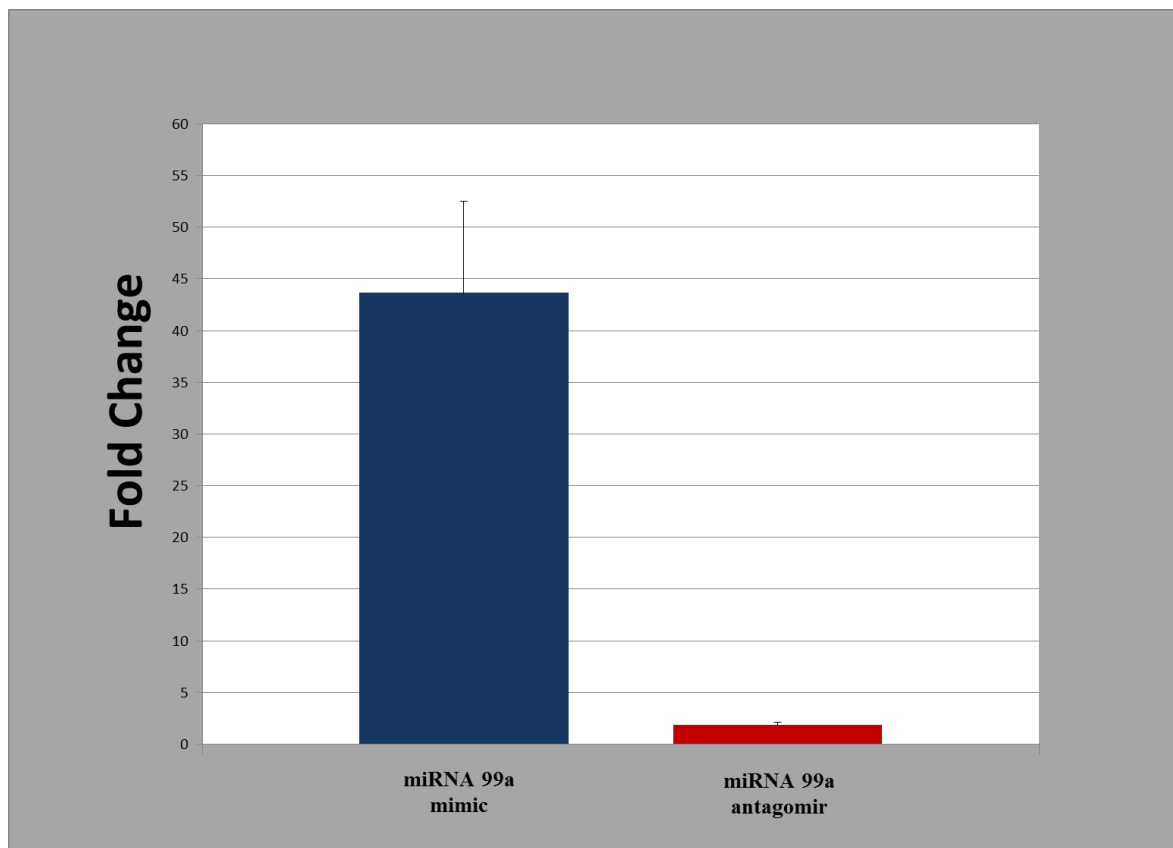


Figure 11. CCD-841 Fold Change of miRNA-99a Expression after Transfection (n=2)
Error Bars = Standard Error of the Mean



C. DISCUSSION

The process of transfection allows the investigator to up- or down-regulate certain elements of cell lines so we can investigate the effects they have on the cells. In this case, we wish to investigate how the expression of miRNA-99a affects cell protein expression and ultimately motility and invasion. Key to this process is verification that successful transfection has occurred.

These data suggest that in HT-29, transfection of miRNA-99a was successful with both the mimic and antagomir. The fold change for the mimic was well over 1000. In addition, the antagomir transfection of miRNA-99a in HT-29 resulted in down regulation of miRNA 99a expression. This was the only cell line in which the antagomir actually showed downregulation as compared to the negative control.

Although the fold change observed in HCT-116 was not to the same degree as with HT-29, it was also upregulated in comparison to the negative control. The antagomir did not show down-regulation of miRNA 99a expression when compared to the negative control.

When investigating the CCD 841 (normal epithelial cell line), the transfection data were not as satisfactory as for HT-29 and HCT-116. While transfection with the miRNA 99a mimic did result in a mild upregulation in miRNA 99a expression as compared to the negative control, this was relatively small, only a fold change of 38. This is the trend that we expected but when compared to the CRC cell lines the transfection did not demonstrate an impressive fold change.

However, successful transfection of the mimic occurred in all three cell lines allowing us to proceed with further analyses. Less promising results occurred with the antagomir. Although, HT-29 showed a negative fold regulation, CCD-841 and HCT-116 minimally exceeded zero. This is not surprising as it is somewhat difficult to completely block the activity of naturally occurring miRNAs in the cell. One possible solution to this is, in future studies, not covered in this thesis, would be to utilize miRNA knock out experiments.

CHAPTER VII

WESTERN BLOT STUDIES

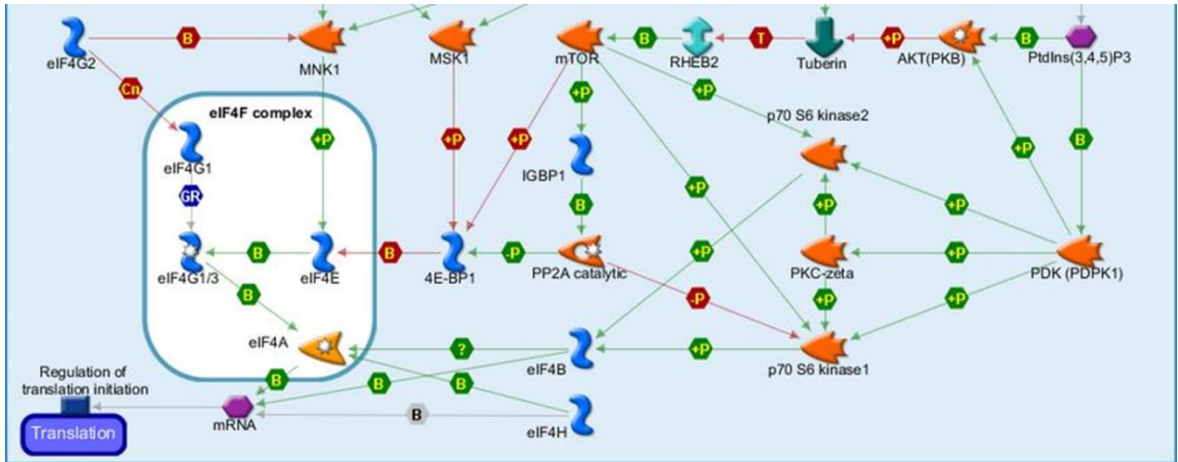
In order to study the effect of miRNA 99a upon the mTOR pathway it is necessary to study proteins that mTOR has an effect on. We chose to do this utilizing western blot analysis. The mTOR pathway has several proteins of interest that can be investigated, mTOR itself along with RAPTOR, RICTOR, S6K1, ieF4EG-1 and eiF4EBP-1 to name a few. The complexity of the mTOR pathway can be seen in Figure 12, which only shows the input of AKT into mTORC1. As stated in the introduction, mTOR has many pathways that converge on mTORC1 and which ultimately influence several vital processes in protein production and cell motility.

Part of the difficulty, when investigating the mTOR pathway, is dealing with the active forms of the protein. In some cases, the phosphorylation will activate the protein whereas in other cases, phosphorylation will inactivate the protein. This is demonstrated with the phosphorylation of 4EBP1. When 4EBP1 is phosphorylated directly via mTORC1, it inactivates 4EBP1. The same occurs when 4EBP1 is phosphorylated directly by MSK1. This becomes confusing as 4EBP1 can also be inactivated by PP2A catalytic, as shown in Figure 13.

PP2A catalytic is somewhat of a regulator between 4EBP1 and p70 S6 Kinase 1 (S6K1). mTORC1 phosphorylates both proteins, but in each case acts differently. 4EBP1

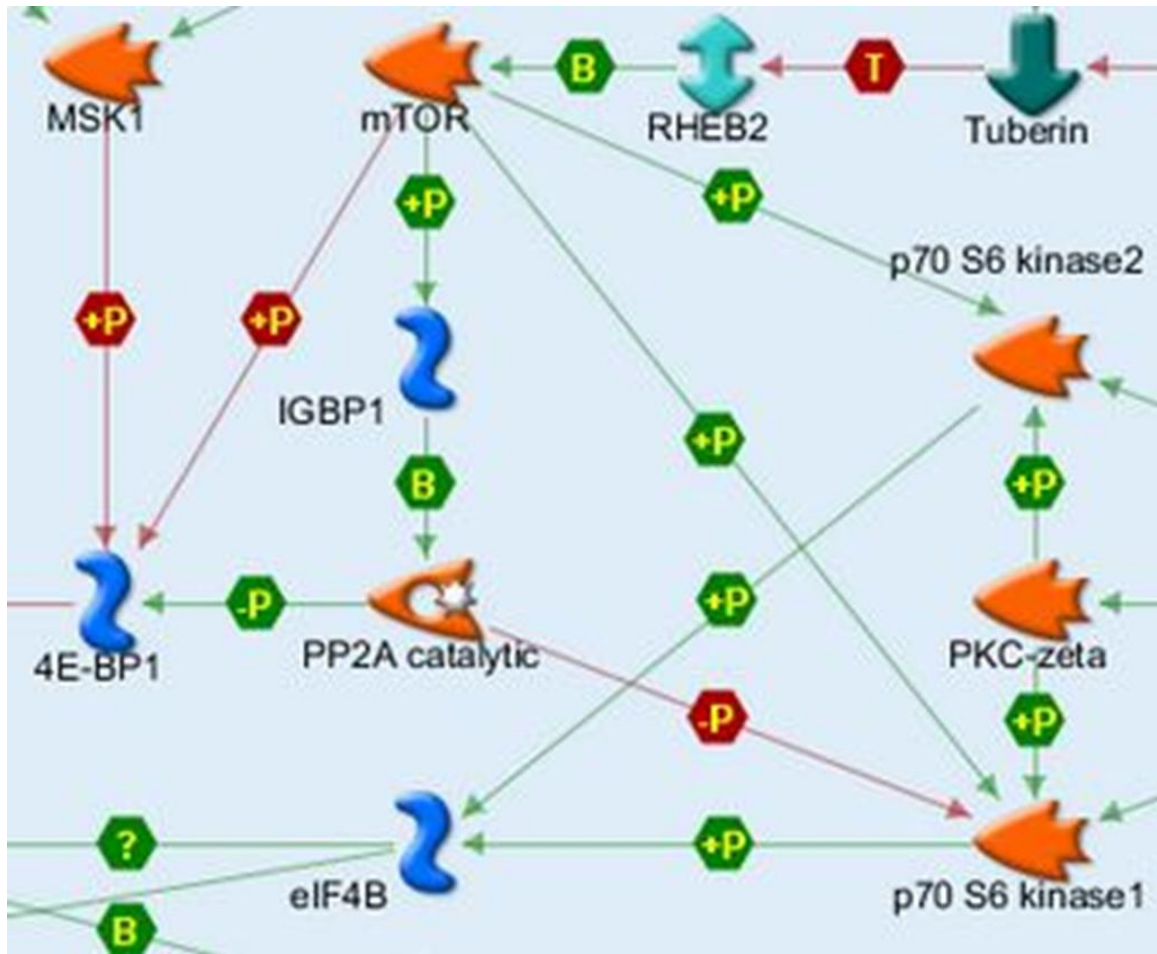
when phosphorylated is inactivated, but when TORC1 phosphorylates S6K1 it is activated. Then PP2A catalytic comes into play. It dephosphorylates both S6K1 and 4EBP1, but when it does this it activates 4EBP1 and inactivates S6K1. This is seen in Figure 13, where the red +P indicates that phosphorylation inactivates the protein and the green -P indicates that dephosphorylation activates the protein. In addition the red - P indicates that dephosphorylation inactivates the S6K1.

Figure 12. Mechanistic Target of Rapamycin Pathway focusing on AKT input into mTORC1



*Modified from <https://portal.genego.com/cgi/imagemap.cgi?id=496>

Figure 13. mTOR pathway focusing on mTORC1 output on S6K1 and 4EBP1 (enlarged central portion of Figure 11)



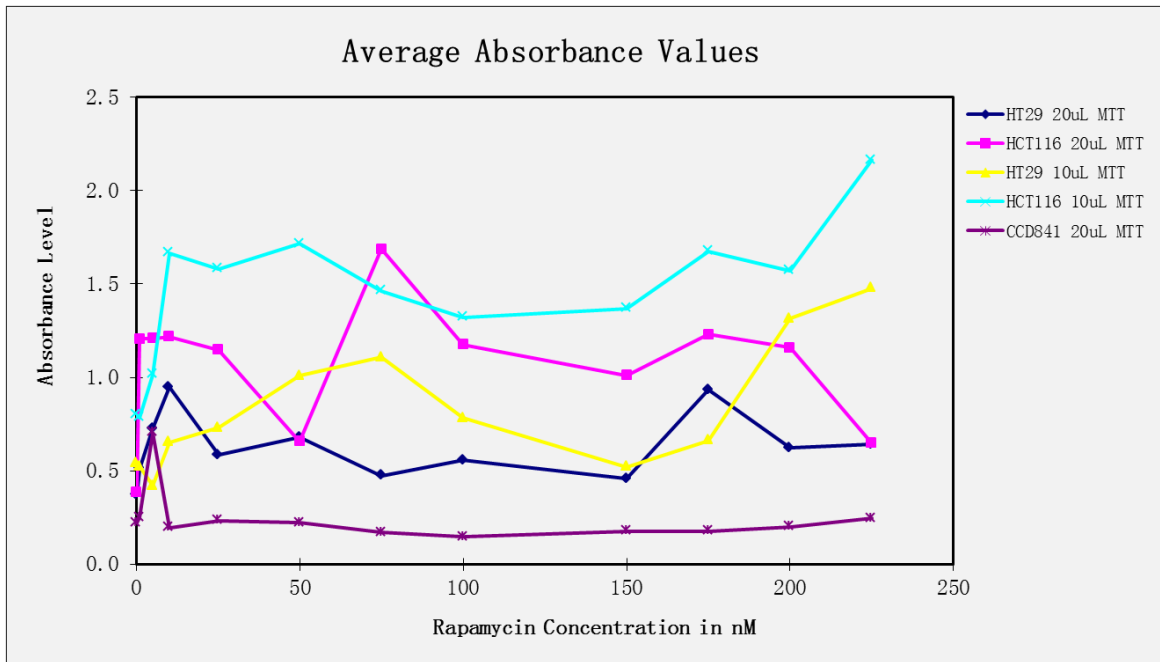
*Modified from <https://portal.genego.com/cgi/imagemap.cgi?id=496>

RAPAMYCIN STUDIES

Prior to investigating the effects that miRNA-99a had on the mTOR pathway itself, we wanted to witness what the cells response to direct rapamycin dosing would do. To initially do this we wanted to establish a dosing curve to recognize the optimum dose of rapamycin that would kill 50% of the cells alive in culture.

We utilized MTT assay to establish this curve and the results are shown in Figure 14. After multiple attempts with different concentrations of rapamycin to decrease the cell culture growth, we found that rapamycin directly did not reliably decrease the cellular concentration and this finding had been reported previously but in a different cancer cell line.¹²⁵

Figure 14. MTT assay dosing curve of increasing Rapamycin dosing concentrations in HT-29, HCT-116 and CCD-841. Two different concentrations of plated cell density denoted in the key.



CHAPTER VIII

SPECIFIC AIM 1: TO DETERMINE THE EFFECT OF MIRNA-99A'S ON MTOR PROTEIN PHOSPHORYLATION

A. INTRODUCTION

Initially we intended to investigate mTOR, RICTOR and RAPTOR proteins and determine if transfection with miRNA-99a would change their expression. However as the RICTOR and RAPTOR proteins are part of the mTOR complex, we chose instead to focus our investigations on the levels of mTOR itself and not the individual proteins of these complexes. It has not, to our knowledge, been shown whether the phosphorylation or dephosphorylation of RICTOR or RAPTOR changes the activity of mTORC1 or mTORC2. It has however been shown that miRNA-99a directly binds to and inhibits mTOR protein itself.¹²⁶

The decision was made to investigate direct levels of mTOR protein and several of the downstream proteins that the mTOR pathway has been shown to influence. These proteins include S6K1, 4EBP1 and eIF4G1. These proteins were investigated in HT-29, HCT-116 and CCD-841 cell lines. We chose to limit our study to cell lines derived from cancers with regional and distant metastasis as this would allow us to study changes in protein expression that may correlate with significant survival differences seen in these cancer stages clinically and therefore be possible targets for therapeutic intervention.

B. DATA AND RESULTS

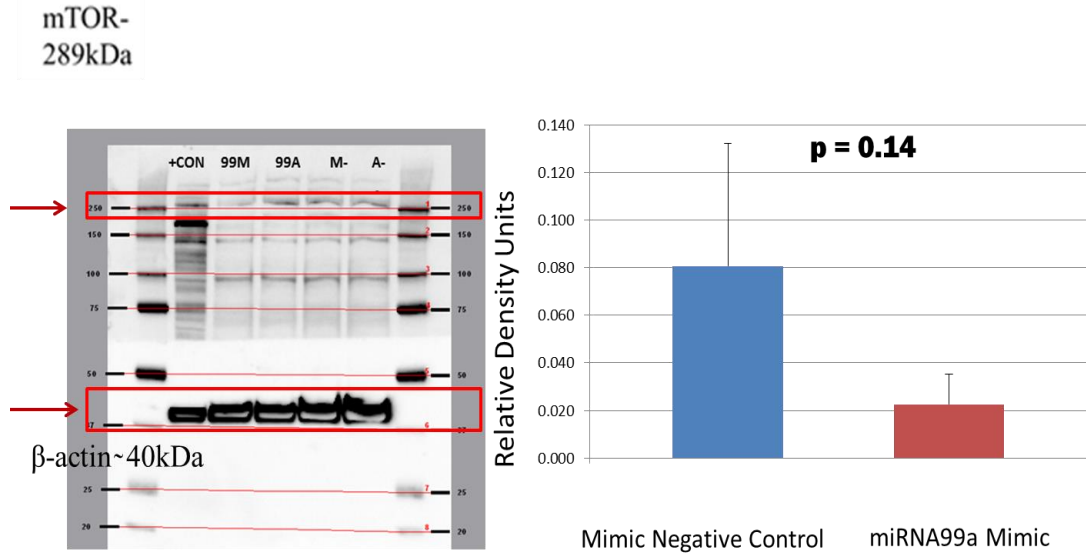
To answer specific aim 1, we needed to determine the effect of miRNA-99a upon mTOR protein itself. To do this we utilized Western blot assay after transfection of the 3 cells lines with miRNA-99a mimic.

Initially CCD-841 (normal epithelial CRC cells) underwent Western Blot analysis. Both antibodies for total mTOR and phosphorylated only had a similar trend showing downregulation after transfection compared to the negative control.

When the Western Blots were analyzed for mTOR total after transfection with miRNA99a, the CCD-841 showed a relative density of 0.022 ± 0.013 (Figure 15). When compared to the negative control which resulted in a relative density of 0.081 ± 0.051 . This was not statistically significant with $p = 0.14$.

Similarly, CCD-841 relative density from Western Blot analysis of phosphorylated mTOR after miRNA-99a mimic was transfected resulted in a value of 0.04 ± 0.01 (Figure 16). This is compared to the negative control after transfection which resulted in a value of 0.06 ± 0.01 . This was not statistically significant with a p value equal to 0.19. Although not statistically significant, with $n=4$ all Western Blots studied had the same trend. When investigation the normalized percentage of total antibody and phosphorylated compared to the negative control, this resulted in 27% and 73% respectively.

Figure 15. Western blot and bar graph of total mTOR protein expression when miRNA-99a mimic is transfected in normal epithelial colon cell line CCD-841. Bar chart is expressed in relative density units.

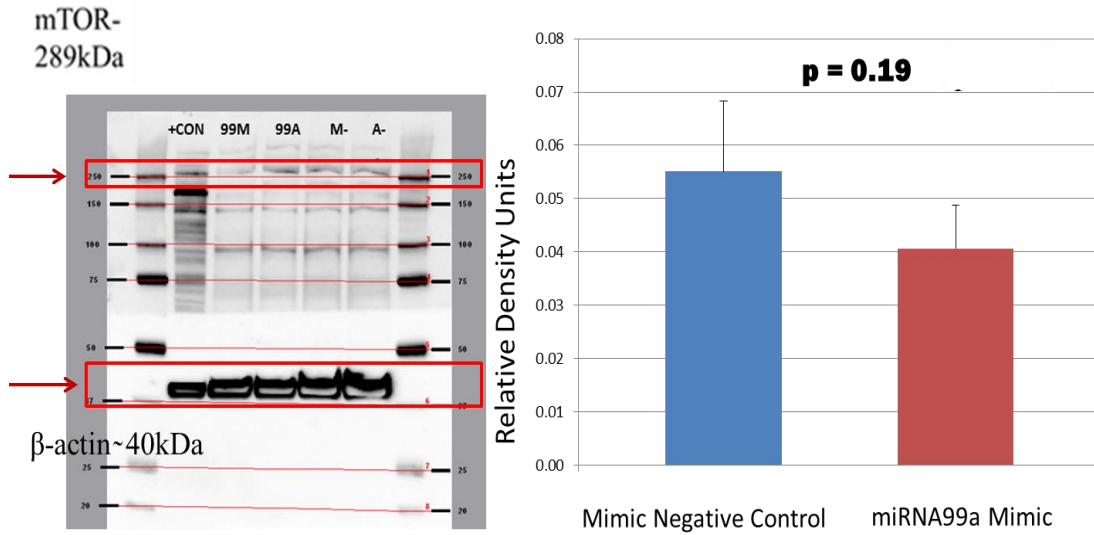


M = Mimic
A = Antagomir

	Mimic Negative Control	miRNA99a Mimic
AVG	0.081	0.022
SEM	0.051	0.013

99M	miR 99a Mimic transfected			
99A	miR 99a Antagomir transfected			
M-	miR 99a negative mimic transfected (Mimic Sham)			
A-	miR 99a negative antagomir transfected (Antagomir Sham)			
CON+	Purchased positive control cell lysate			

Figure 16. Western blot and bar graph of phosphorylated mTOR protein expression when miRNA-99a mimic is transfected in normal epithelial colon cell line CCD-841. Bar chart is expressed in relative density units.



N=4

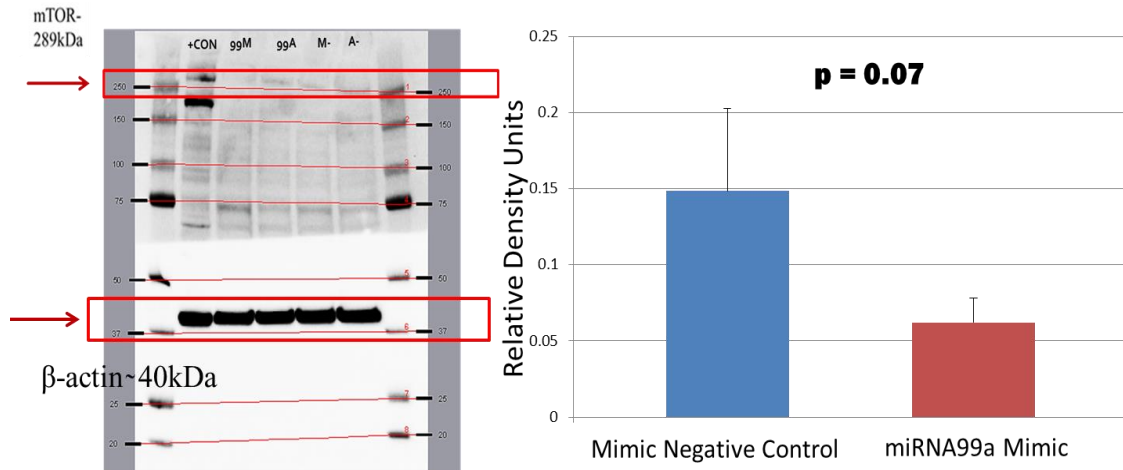
	Mimic Negative Control	miRNA99a Mimic
AVG	0.06	0.04
SEM	0.01	0.01

M = Mimic
A = Antagomir

99M	miR 99a Mimic transfected			
99A	miR 99a Antagomir transfected			
M-	miR 99a negative mimic transfected (Mimic Sham)			
A-	miR 99a negative antagomir transfected (Antagomir Sham)			
CON+	Purchased positive control cell lysate			

HT-29 was then investigated. We probed the transfected cells for both phosphorylated and total mTOR protein expression. We observed a relative density expression of 0.06 ± 0.02 relative density units for phosphorylated mTOR when compared to beta actin following transfection with miRNA-99a. This was not statistically significant ($p = 0.07$) when compared to the negative control (0.15 ± 0.05), yet with an $n = 4$ the trend of downregulation was consistent. These results are shown graphically in Figure 17. Probing for total expression of mTOR in HT-29 cell line was unsuccessful despite using 16 different mTOR antibodies; this could be due to non-specific binding of antibodies to other proteins. When investigation the normalized percentage of total antibody and phosphorylated compared to the negative control, this resulted in 42% and 186% respectively.

Figure 17. Western blot and bar graph of phosphorylated mTOR protein expression when miRNA-99a mimic is transfected in HT-29 CRC cell line. Bar chart is expressed in relative density units.



N=4

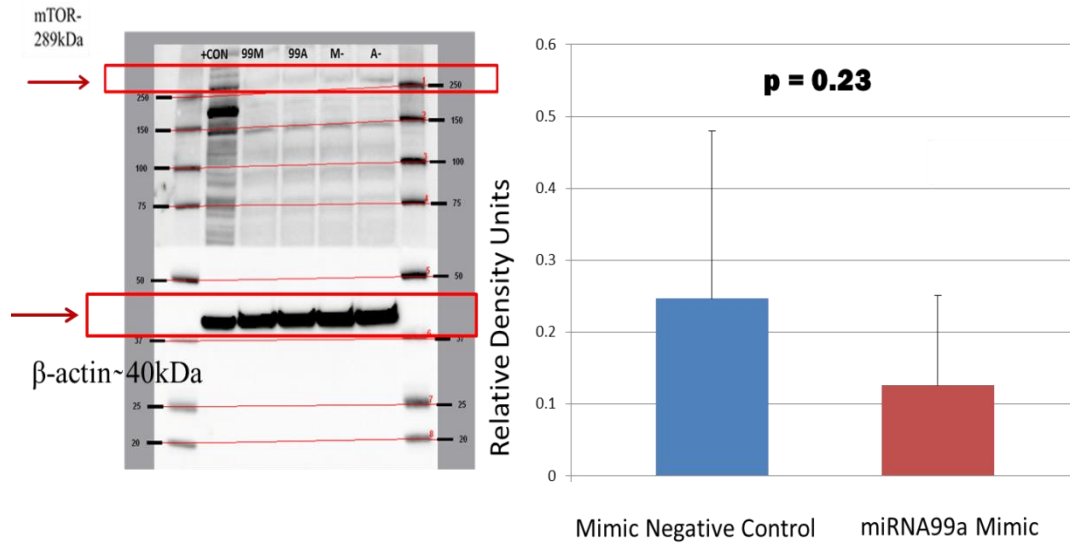
M = Mimic
A= Antagomir

	Mimic Negative Control	miRNA99a Mimic
AVG	0.15	0.06
SEM	0.05	0.02

99M	mIR 99a Mimic transfected		
99A	mIR 99a Antagomir transfected		
M-	mIR 99a negative mimic transfected (Mimic Sham)		
A-	mIR 99a negative antagomir transfected (Antagomir Sham)		
CON+	Purchased positive control cell lysate		

Finally we investigated phosphorylated and total mTOR expression after miRNA-99a transfection in the HCT-116 cell line. Although not significant, probing for mTOR total had the same trend as when we probed for the phosphorylated only mTOR (Figure 18). Similarly to HT-29, transfected cells with miRNA99a were downregulated compared to the negative control. This downregulation was statistically significant when probing for phosphorylated mTOR but not total mTOR (Figure 18-19). When investigating the normalized percentage of total antibody and phosphorylated compared to the negative control, this resulted in 51% and 640% respectively.

Figure 18. Western blot and bar graph of total mTOR protein expression when miRNA-99a mimic is transfected in HCT-116 CRC cell line. Bar chart is expressed in relative density units.



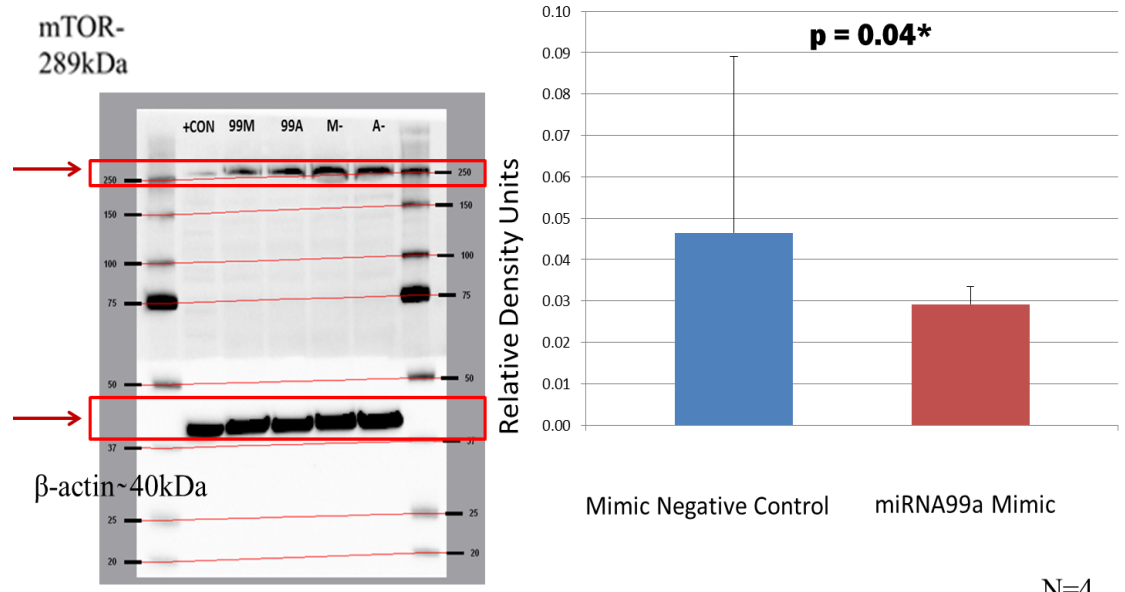
N=4

	Mimic Negative Control	miRNA99a Mimic
AVG	0.25	0.13
SEM	0.23	0.13

M = Mimic
A= Antagomir

99M	mIR 99a Mimic transfected			
99A	mIR 99a Antagomir transfected			
M-	mIR 99a negative mimic transfected (Mimic Sham)			
A-	mIR 99a negative antagomir transfected (Antagomir Sham)			
CON+	Purchased positive control cell lysate			

Figure 19. Western blot and bar graph of phosphorylated mTOR protein expression when miRNA-99a mimic is transfected in HCT-116 CRC cell line. Bar chart is expressed in relative density units.



M = Mimic
A = Antagomir

	Mimic Negative Control	miRNA99a Mimic
AVG	0.05	0.03
SEM	0.04	0.00

99M	mIR 99a Mimic transfected			
99A	mIR 99a Antagomir transfected			
M-	mIR 99a negative mimic transfected (Mimic Sham)			
A-	mIR 99a negative antagomir transfected (Antagomir Sham)			
CON+	Purchased positive control cell lysate			

C. DISCUSSION

In order to answer specific aim 1, we needed to limit our focus to miRNA-99a's effect on the total and phosphorylated mTOR protein levels after transfection. We expected, with the introduction of miRNA-99a mimic, the expression of phosphorylated mTOR protein would decrease in comparison to the mimic negative control. This trend was observed in all three cell lines under study.

HCT-116 when probing for phosphorylated only mTOR was the only cell line statistically significant. Although this may be the case, all of the above studies had a similar trend which was promising for future experiments.

We then investigated total mTOR protein expression after transfection of miRNA-99a mimic. This was successful in HCT-116 and normal epithelial cell line CCD-841, but we were unable to optimize an antibody for Western Blot detection with the HT-29 cell line. This could be due to lack of interaction with that particular primary antibody or mTOR not being expressed readily in that particular cell line. The latter is unlikely as phosphorylated mTOR was detected in this same cell line. The data for HCT-116 and CCD-841 reaffirmed our results from the phosphorylated-mTOR data and suggest that when miRNA-99a is introduced into the cell culture environment, there is a resulting down-regulation of both phosphorylated and total mTOR protein expression.

CHAPTER IX

SPECIFIC AIM 2: THE EFFECT OF MIRNA-99A'S EFFECT ON S6K1 AND 4EBP1

A. INTRODUCTION

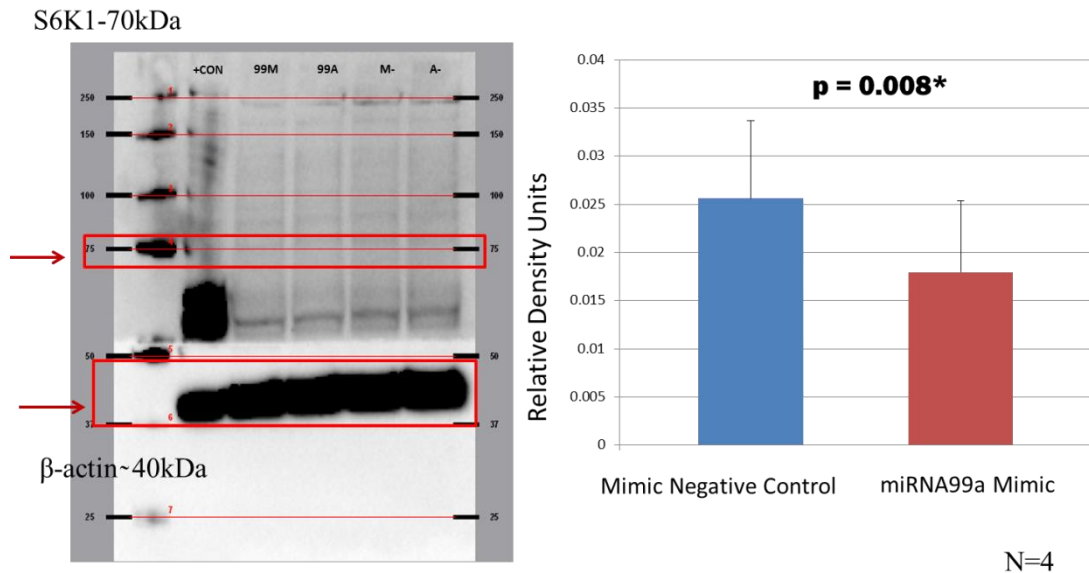
Our attention now focused on downstream proteins of the mTORC1 complex. The ultimate goal being to answer specific aim two, which was to determine the effect of miRNA-99a on the phosphorylation of mTOR pathway's downstream proteins. Initially, we performed Western blot analysis of phosphorylated S6K1 and total S6K1 expression in HT-29 cell line, followed by evaluation of cell lines HCT-116 and CCD-841. The same was then performed for 4EBP1.

B. DATA AND RESULTS

1. S6K1

Initially CCD-841, normal epithelial cell line, showed the expected result of downregulation after transfection with miRNA-99a. After transfection, S6K1 relative density expression was 0.018 ± 0.007 compared to the negative control 0.026 ± 0.008 (Figure 20). This comparison was statistically significant with a p value equal to 0.008. When investigation the normalized percentage of total antibody and phosphorylated compared to the negative control, this resulted in 70% and 75% respectively.

Figure 20. Western blot and bar graph of phosphorylated S6K1 (75 KDa) protein expression when miRNA-99a mimic is transfected in normal colon epithelial cell line CCD-841. Bar chart is expressed in relative density units.



M = Mimic
A = Antagomir

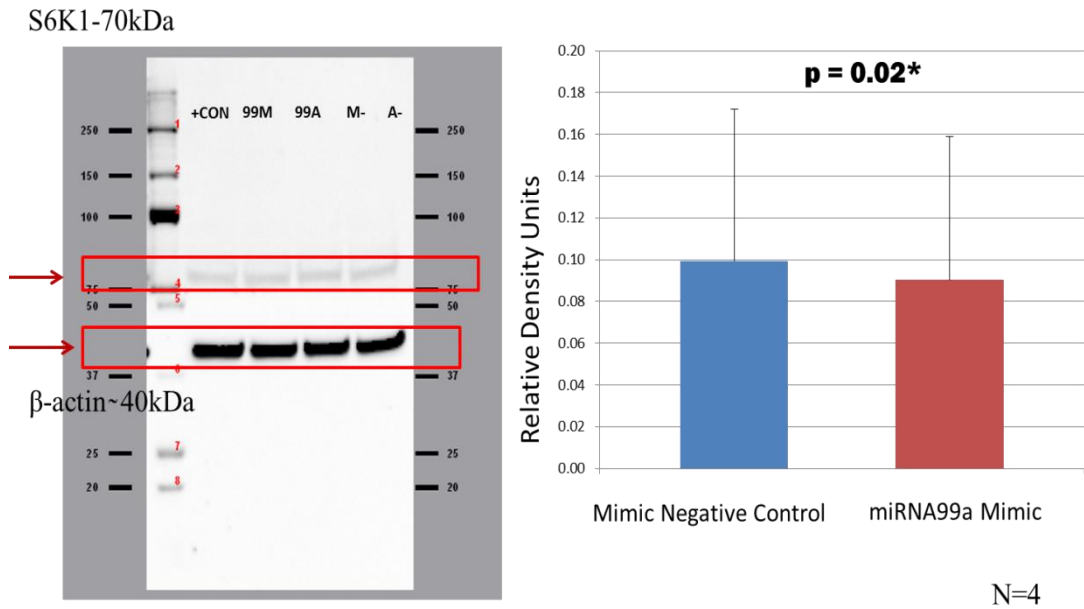
	Mimic Negative Control	miRNA99a Mimic
AVG	0.026	0.018
SEM	0.008	0.007

99M	miR 99a Mimic transfected			
99A	miR 99a Antagomir transfected			
M-	miR 99a negative mimic transfected (Mimic Sham)			
A-	miR 99a negative antagomir transfected (Antagomir Sham)			
CON+	Purchased positive control cell lysate			

HT-29 cell line was then transfected with miRNA-99a, and then mTOR total was probed for in the Western Blot studies. This resulted in a significant difference ($p = 0.02$) between miRNA-99a mimic and its transfected negative control (Figure 21). Once again the same pattern was observed after transfection, a downregulation of S6K1 compared to negative control.

Finally, HT-29 cell line was transfected with miRNA-99a and probed for phosphorylated only S6K1. This resulted in Western Blot analysis that showed a relative density measurement of 0.19 ± 0.04 . This was compared to the transfected negative control which resulted in a relative density of 0.22 ± 0.07 (Figure 22). This was not statistically significant ($p = 0.15$) but all samples had the expected downregulation of S6K1 after transfection when compared to the negative control. When investigation the normalized percentage of total antibody and phosphorylated compared to the negative control, this resulted in 90% and 86% respectively.

Figure 21. Western blot and bar graph of total S6K1 (70 KDa) protein expression when miRNA-99a mimic is transfected in HT-29 CRC cell line. Bar chart is expressed in relative density units.

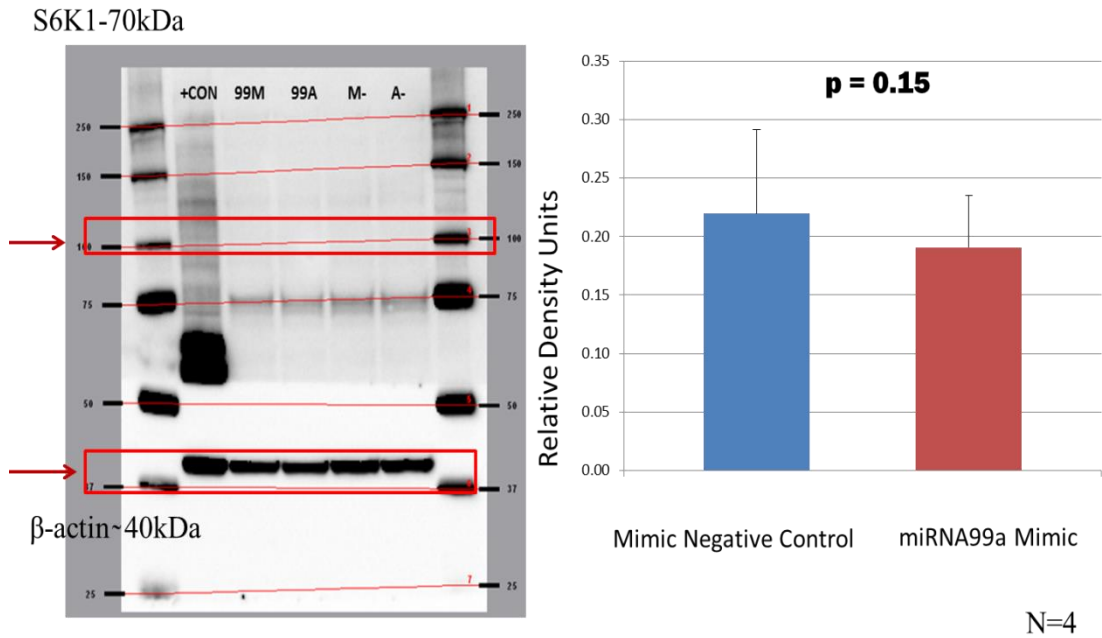


M = Mimic
A = Antagomir

	Mimic Negative Control	miRNA99a Mimic
AVG	0.10	0.09
SEM	0.07	0.07

99M	mIR 99a Mimic transfected			
99A	mIR 99a Antagomir transfected			
M-	mIR 99a negative mimic transfected (Mimic Sham)			
A-	mIR 99a negative antagomir transfected (Antagomir Sham)			
CON+	Purchased positive control cell lysate			

Figure 22. Western blot and bar graph of phosphorylated S6K1 (70 KDa) protein expression when miRNA-99a mimic is transfected in HT-29 CRC cell line. Bar chart is expressed in relative density units.

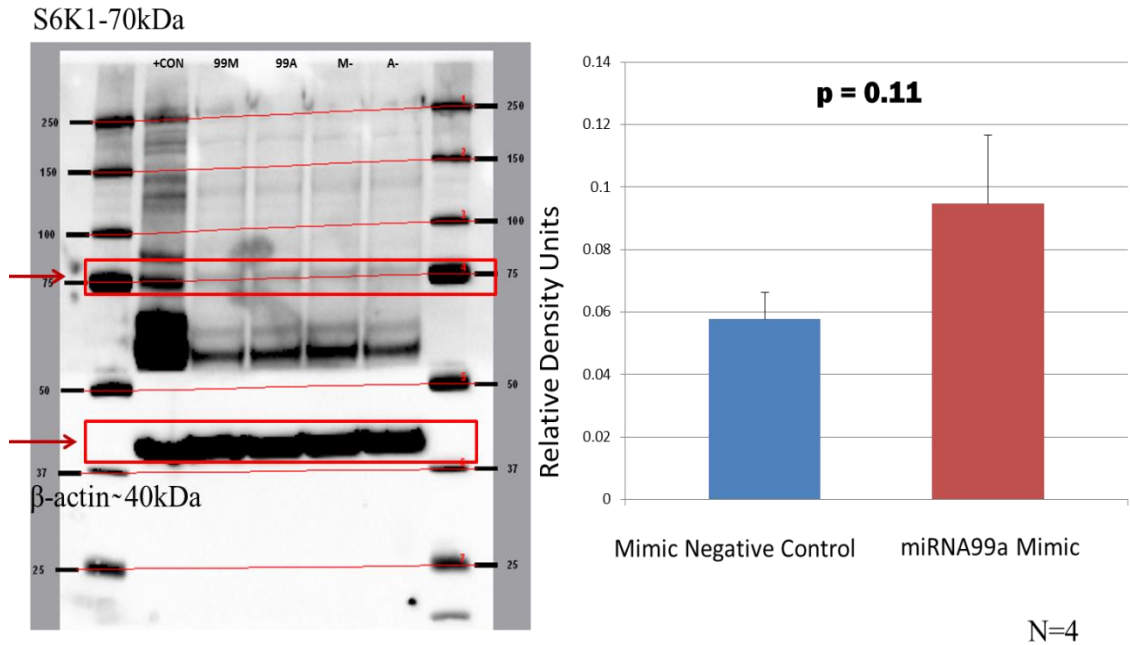


M = Mimic
A = Antagomir

99M	mIR 99a Mimic transfected			
99A	mIR 99a Antagomir transfected			
M-	mIR 99a negative mimic transfected (Mimic Sham)			
A-	mIR 99a negative antagomir transfected (Antagomir Sham)			
CON+	Purchased positive control cell lysate			

Once again we investigated both HCT-116 and CCD-841 for S6K1. The antibody probes were successful only when probing for phosphorylated antibodies and were not successful for total expression. HCT-116 phosphorylated resulted in a different pattern than expected. When transfected with miRNA-99a mimic it was upregulated (0.09 ± 0.02) compared to the negative control (0.06 ± 0.02 , Figure 23). Although not statistically significant ($p = 0.11$) this was an interesting result as it happened in all 4 samples and was the first experiment that showed this type of pattern after transfection. When investigation the normalized percentage of total antibody compared to the negative control, this resulted in 164% change.

Figure 23. Western blot and bar graph of phosphorylated S6K1 (70 KDa) protein expression when miRNA-99a mimic is transfected in HCT-116 CRC cell line. Bar chart is expressed in relative density units.



M = Mimic
A = Antagomir

	Mimic Negative Control	miRNA99a Mimic
AVG	0.06	0.09
SEM	0.01	0.02

99M	mIR 99a Mimic transfected		
99A	mIR 99a Antagomir transfected		
M-	mIR 99a negative mimic transfected (Mimic Sham)		
A-	mIR 99a negative antagomir transfected (Antagomir Sham)		
CON+	Purchased positive control cell lysate		

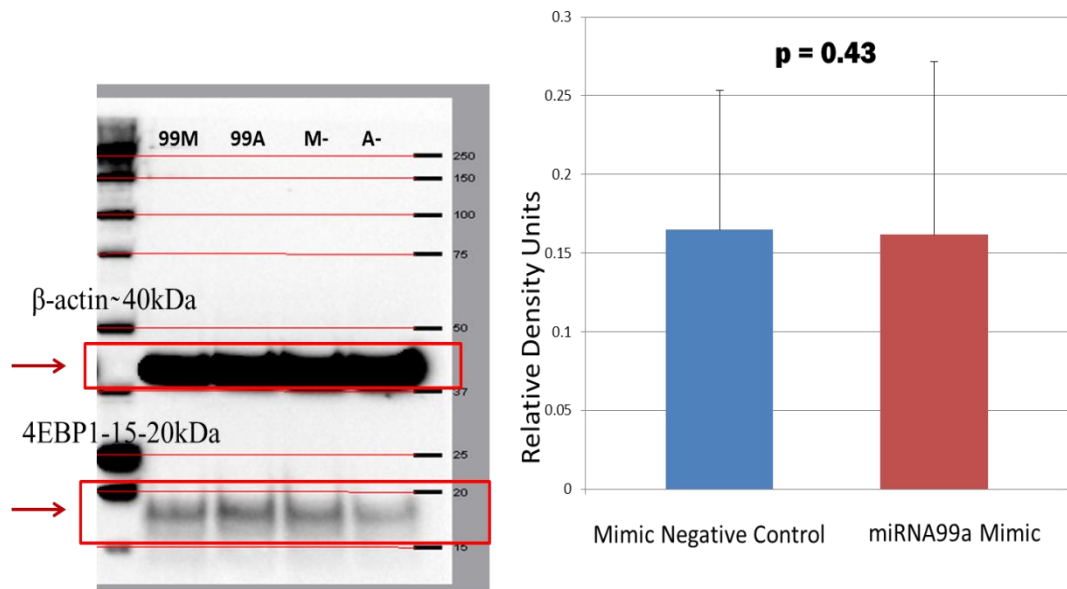
2. 4EBP1

Figure 12 shows the mTORs pathway direct interaction with 4EBP1. When mTOR is active and phosphorylates 4EBP1 it turns 4EBP1 off, this is the opposite of what mTOR does to the protein S6K1. Now that S6K1 was elucidated in the cell lines under study, we next wanted to see how miRNA-99a would influence the phosphorylation of 4EBP1.

First CCD-841 underwent Western blot analysis for 4EBP1 after transfection with miRNA-99a. The phosphorylated only Western Blots resulted with the same average across 4 samples (Figure 24). Both the negative control (0.16 ± 0.09) and transfected cell lines (0.16 ± 0.11) basically showed no difference.

Investigating total expression we saw upregulation of 4EBP1 after transfection with miRNA-99a compared to negative control (Figure 25). After transfection with miRNA-99a, a relative density of 0.14 ± 0.12 resulted compared to the negative control equal to 0.18 ± 0.14 . Once again the p value was not statistically significant but it was approaching significance ($p = 0.06$). When investigating the normalized percentage of total antibody and phosphorylated compared to the negative control, this resulted in 78% and 98% respectively.

Figure 24. Western blot and bar graph of phosphorylated 4EBP1 (15-20 KDa) protein expression when miRNA-99a mimic is transfected in normal colon epithelial control cell line CCD 841. Bar chart is expressed in relative density units.

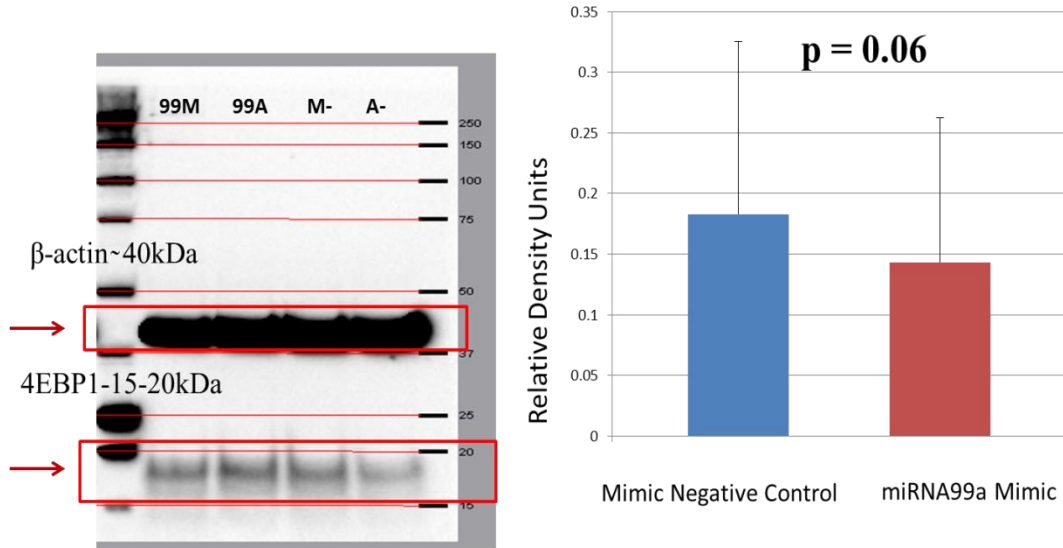


M = Mimic
A = Antagomir

	Mimic Negative Control	miRNA99a Mimic
AVG	0.16	0.16
SEM	0.09	0.11

99M	miR 99a Mimic transfected			
99A	miR 99a Antagomir transfected			
M-	miR 99a negative mimic transfected (Mimic Sham)			
A-	miR 99a negative antagomir transfected (Antagomir Sham)			
CON+	Purchased positive control cell lysate			

Figure 25. Western blot and bar graph of total 4EBP1 (15-20 KDa) protein expression when miRNA-99a mimic is transfected in normal colon epithelial control cell line CCD 841. Bar chart is expressed in relative density units.



M = Mimic
A = Antagomir

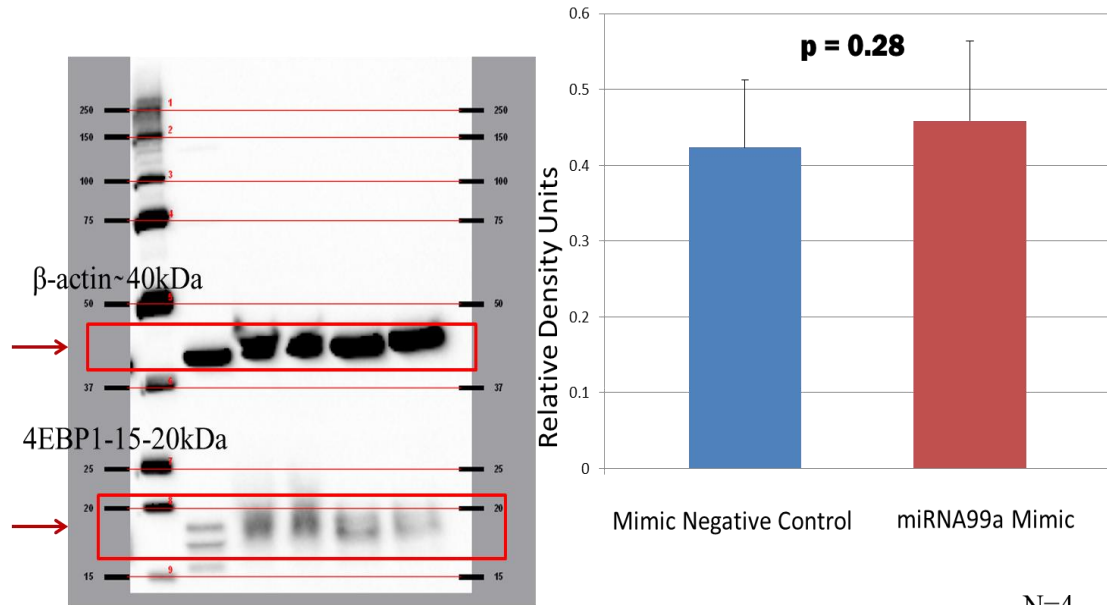
	Mimic Negative Control	miRNA99a Mimic
AVG	0.18	0.14
SEM	0.14	0.12

99M	mIR 99a Mimic transfected			
99A	mIR 99a Antagomir transfected			
M-	mIR 99a negative mimic transfected (Mimic Sham)			
A-	mIR 99a negative antagomir transfected (Antagomir Sham)			
CON+	Purchased positive control cell lysate			

After this, HT-29 was transfected with miRNA-99a and then underwent Western Blot analysis for total and phosphorylated only relative density measurements of 4EBP1. Figure 26 shows the results of phosphorylated only 4EBP1, which is 0.46 ± 0.11 for miRNA-99a mimic compared to the negative control, 0.42 ± 0.09 . This was not a statistically significant comparison with $p = 0.28$ for our 4 samples but once again all had a similar trend.

Next, probing for total expression of 4EBP1 shows a similar upregulation compared to negative control trend, although it is still not statistically significant ($p = 0.28$). After miRNA-99a transfection the relative density average was 1.17 ± 0.87 compared to the negative control average of 0.87 ± 0.60 (Figure 27). When investigation the normalized percentage of total antibody and phosphorylated compared to the negative control, this resulted in 135% and 108% respectively.

Figure 26. Western blot and bar graph of phosphorylated 4EBP1 (15-20 KDa) protein expression when miRNA-99a mimic is transfected in HT-29 cell line. Bar chart is expressed in relative density units.

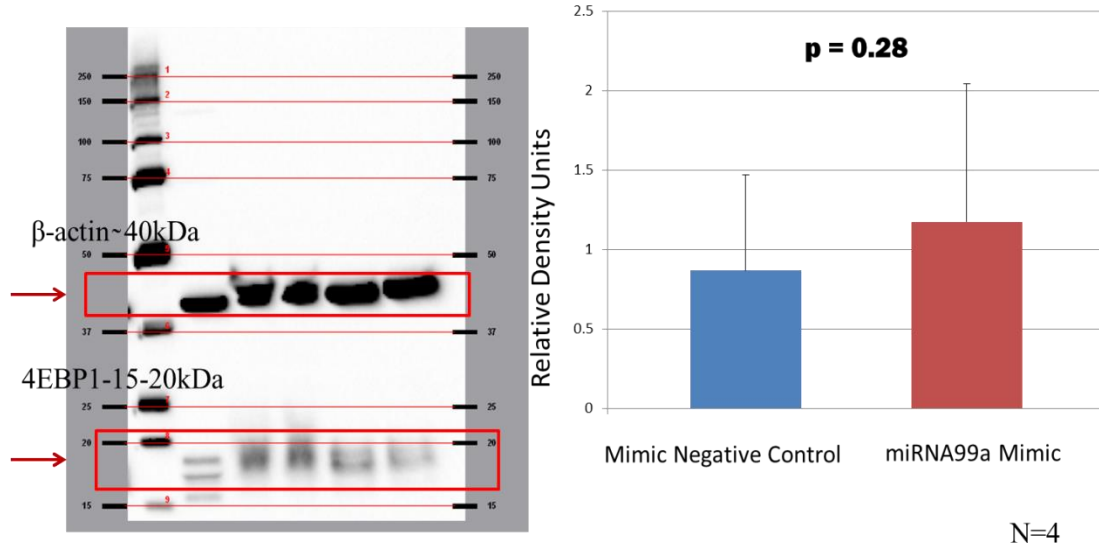


M = Mimic
A = Antagomir

	Mimic Negative Control	miRNA99a Mimic
AVG	0.42	0.46
SEM	0.09	0.11

99M	mIR 99a Mimic transfected		
99A	mIR 99a Antagomir transfected		
M-	mIR 99a negative mimic transfected (Mimic Sham)		
A-	mIR 99a negative antagomir transfected (Antagomir Sham)		
CON+	Purchased positive control cell lysate		

Figure 27. Western blot and bar graph of total 4EBP1 (15-20 KDa) protein expression when miRNA-99a is transfected in HT-29 cell line. Bar chart is expressed in relative density units.



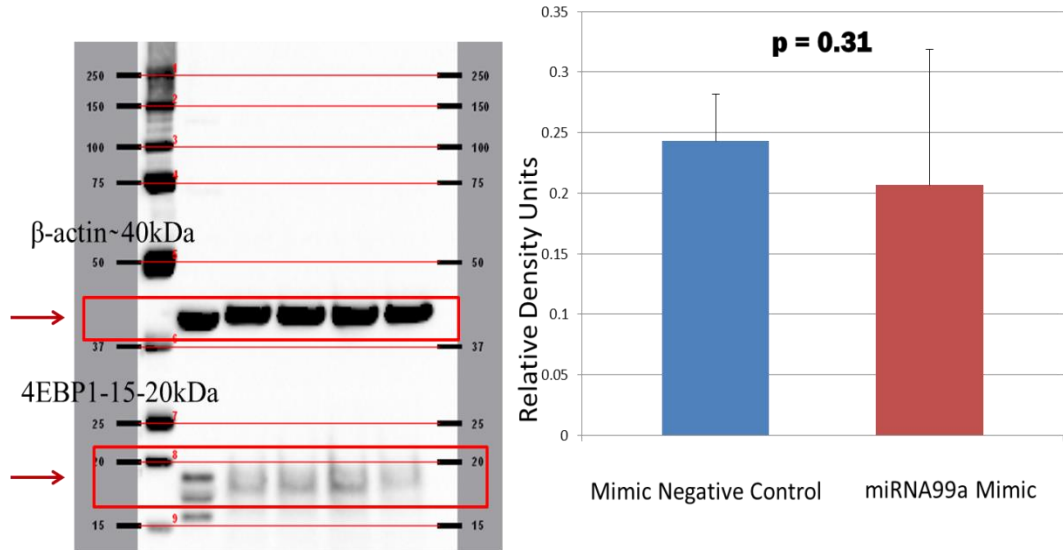
	Mimic Negative Control	miRNA99a Mimic
AVG	0.87	1.17
SEM	0.60	0.87

M = Mimic
A = Antagomir

99M	miR 99a Mimic transfected			
99A	miR 99a Antagomir transfected			
M-	miR 99a negative mimic transfected (Mimic Sham)			
A-	miR 99a negative antagomir transfected (Antagomir Sham)			
CON+	Purchased positive control cell lysate			

Once again after elucidating the trend in Dukes C CRC cell line, our attention next focused on HCT-116, Dukes' D cell line. After transfection, Western Blot analysis showed a relative density of 0.21 ± 0.11 compared to the negative control 0.24 ± 0.04 (Figure 28). Similarly the antibodies that detected total protein expression and not just phosphorylated had a similar trend with the mimic being downregulated (1.61 ± 0.27) compared to the negative control (1.78 ± 0.36 , Figure 29). Both of these sets of Western Blots were not statistically significant with p values of 0.31, 0.25 respectively but all had a similar trend. This is interesting because this trend is the exact opposite of the Dukes' C and normal epithelial cell lines when probing for not only 4EBP1 but also S6K1. Finally, when investigating the normalized percentage of total antibody and phosphorylated compared to the negative control, this resulted in 91% and 85% respectively.

Figure 28. Western blot and bar graph of phosphorylated 4EBP1 (15-20 KDa) protein expression when miRNA-99a mimic is transfected in HCT-116 cell line. Bar chart is expressed in relative density units.

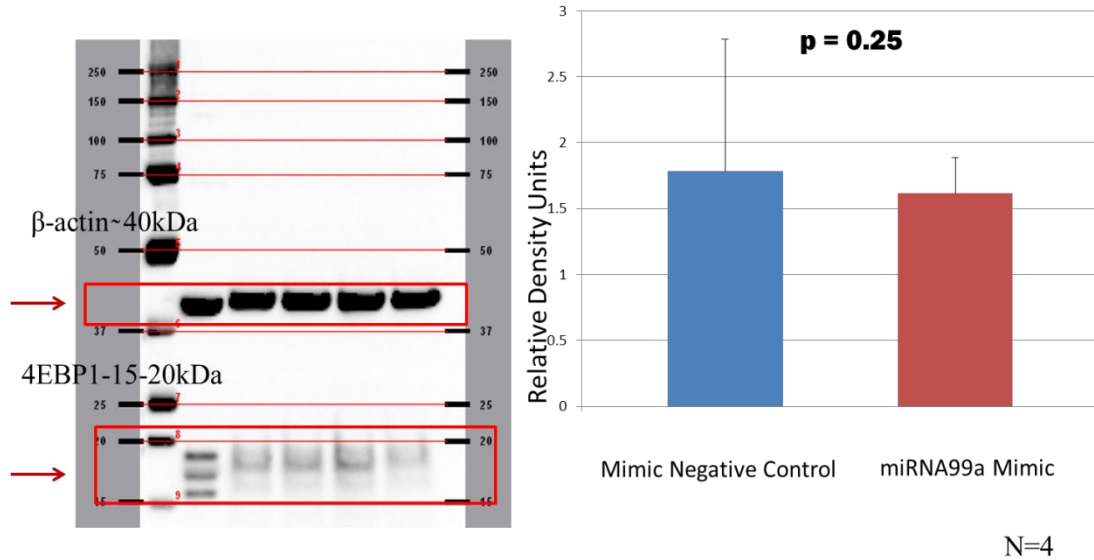


M = Mimic
A = Antagomir

	Mimic Negative Control	miRNA99a Mimic
AVG	0.24	0.21
SEM	0.04	0.11

99M	miR 99a Mimic transfected		
99A	miR 99a Antagomir transfected		
M-	miR 99a negative mimic transfected (Mimic Sham)		
A-	miR 99a negative antagomir transfected (Antagomir Sham)		
CON+	Purchased positive control cell lysate		

Figure 29. Western blot and bar graph of total 4EBP1 (15-20 KDa) protein expression when miRNA-99a mimic is transfected in HCT-116 cell line. Bar chart is expressed in relative density units.



M = Mimic
A = Antagomir

	Mimic Negative Control	miRNA99a Mimic
AVG	1.78	1.61
SEM	0.36	0.27

99M	miR 99a Mimic transfected			
99A	miR 99a Antagomir transfected			
M-	miR 99a negative mimic transfected (Mimic Sham)			
A-	miR 99a negative antagomir transfected (Antagomir Sham)			
CON+	Purchased positive control cell lysate			

C. DISCUSSION

In our study, we focused only on HT-29 and HCT-116 cell lines as well as one normal colon epithelial cell line. This decision to limit our study to these two cell lines can be justified as our ultimate goal is to uncover the mTOR pathways' influence on CRC metastatic potential. By focusing on these two cell lines, it allows us to limit our study to cell lines that are defined by their metastatic properties, HT-29 being derived from a cancer characterized by regional metastasis and HCT-116 derived from a cancer characterized by distant metastasis.

Our first step when investigating the mTOR pathway is to initially see if mTOR protein itself is affected when miRNA-99a is transfected into the cell line. It has been shown that miRNA-99a directly interacts with mTORC2 complex.¹²⁶ miRNA-99a has been shown to directly bind to this complex and repress its expression. We showed through Western blot analysis that transfection of miRNA-99a does indeed reduce the amount of both total and phosphorylated mTOR protein in all studied cell lines. Once this was established our focus turned to addressing specific aim two.

In order to answer specific aim two, we queried downstream effectors of mTORC2. Once we established that miRNA-99a had an effect on the overall expression of the active or phosphorylated form of mTORC1 and mTORC2 we wished to see what effect this down-regulation had on the proteins that mTORC1 directly targets. Initially we investigated the effect of miRNA-99a on S6K1.

One of the key roles of mTORC1 and its interaction with S6K1 is the regulation of cell growth and metabolism leading to its predictable role in aberrant cellular growth,

i.e. in cancer.¹²⁷ After we noted the effects that miRNA-99a had on the mTOR protein itself, it was key to study the phosphorylation or de-phosphorylation of S6K1. It has been shown in other cancers and disease states that when mTORC1 is active, it phosphorylates S6K1, which is thereby activated.

In our experiments, we would predict that if mTOR phosphorylation would be down-regulated as compared to the negative control, we would expect S6K1 to also to be down-regulated. This is what occurred in the HT-29 cell line as well as in CCD-841. In addition, in the HT-29 cell line total S6K1 was down-regulated as compared to the negative control. In our data, miRNA-99a down-regulates the active form of mTORC1 and this down-regulation directly affects the phosphorylation of S6K1. Thus by decreasing the amount of active mTORC1, the phosphorylation and thus the active form of S6K1 is reduced.

The behavior of the HCT-116 line is *opposite* that of the HT-29 and CCD 841 cell lines. Thus, when miRNA-99a mimic is introduced into the cells, we observed an up-regulation of the phosphorylation of S6K1 as compared to the negative controls. There are at least two possible explanations for this: there are multiple pathways that ultimately converge on mTORC1, thus in this particular cell line, another pathway could be the predominate regulator of mTOR and override the effects of miRNA-99a on S6K1 phosphorylation. In addition as seen in Figure 2, mTORC1 can directly phosphorylate S6K1, SGBP1 or 4EBP1. If mTOR predominantly phosphorylates IGBP1, this will then go on to dephosphorylate S6K1 via the PP2A catalytic pathway. One more possibility that could explain HCT-116's different behavior, in comparison to the other two cell lines, is that HCT-116 is a mismatch repair deficient (Hereditary Non-polyposis

Colorectal Cancer [HNPCC]) cell line. This means that the mutation that leads to CRC in this cell line is different from that seen in sporadic CRC and normal tissue (our HT-29 and CCD-841 cell lines). HNPCC is defective in DNA mismatch repair genes MSH2, MLH1, MSH6, PMS2, PMS1, TGFBR2 or MLH3, ultimately leading to microsatellite instability.^{117-120, 122} The fact that the pathology of this disease state is altered in comparison to sporadic CRC, could possibly lead to some of the different results observed with the HCT-116 cell line. The HCT-116 is a commonly utilized CRC cell-line, and the fact that it is mismatch repair deficient is not widely appreciated. This has great impact on much published literature.

We also wished to further investigate one other downstream protein of the mTOR pathway (4EBP1). We chose this protein since mTOR phosphorylation has the opposite effect on its function as compared to S6K1. The phosphorylation of 4EBP1 results in its deactivation. We would expect a similar phosphorylation trend to that seen with S6K1. This was, however, was not the case with all of the cell lines. With HT-29 and CCD-841 cell lines we saw the opposite outcome of what we would have predicted. In the HCT-116 cell line we observed what we would expect, i.e. when miRNA-99a mimic is introduced, phosphorylation of 4EBP1 is downregulated.

In conclusion, it is interesting that the HT-29 and normal epithelial cell line CCD-841 behave opposite of the HCT-116 cell line. Thus when miRNA-99a is introduced, in HT-29 and CCD-841 we observe downregulation of the S6K1 phosphorylation and upregulation of 4EBP1 phosphorylation. With HCT-116, the exact opposite is observed with both proteins. A possible explanation for this could be the fact that HCT-116 is a mismatch repair deficient cancer in contrast to HT-29 and CCD-841 which are both

mismatch repair proficient. To test this, further work is being done, which is not covered in this thesis, which will investigate a Dukes D CRC cell line that is mismatch repair proficient with a Dukes C CRC cell line that is mismatch repair deficient.

CHAPTER X

SPECIFIC AIM 3: TO DETERMINE IF TRANSFECTION OF HT-29, HCT-116 AND CCD841 CELL LINES WITH MIRNA-99A WILL INHIBIT CELL MIGRATION AND INVASION

A. INTRODUCTION

The motility of the cells lines was assessed to answer specific aim three. Since these cancer cell lines are classified by their metastatic potential, it is necessary to test the motility and invasion properties of each cell line. First, we needed to study the migration properties and once that was complete, we investigated the invasive nature of HT-29 and HCT-116.

Migration was tested first in HT-29 and HCT-116 utilizing the Boyden chamber method. The Boyden chamber assay allows us to compare migration between transfected cell lines and negative controls.¹²⁴ Once the transfection occurs, the transfected cell lines are then placed into the assay chambers and allowed to migrate into the bottom chamber. The technical specifications of these methods have been described previously in the Materials and Methods section (p. 70-72).

Transmigration assays allow us to observe the migration properties of specific cells in response to different chemoattractants.¹²⁴ In our case, it allows us to investigate the migration properties of cells that have undergone transfection. One possible

disadvantage of using this type of assay is that cells under study will only migrate if motivated. In our study we chose to use the cells' "food" FBS as a chemoattractant. By seeding the cells in an environment that is "starved," in theory we give the cells an incentive to migrate to a place where nourishment is available. To encourage this movement, our cell lines are originally seeded in a 1% FBS solution while the chamber that the cells would migrate to had a FBS solution of 20%. Disadvantages of the procedure are that it is technically challenging, and there is limited cell visualization while the assay is being performed.

1. MIGRATION DATA AND RESULTS

Initially we studied HT-29 to observe if transfection with miRNA-99a mimic would affect cell migration. Our sample size of five resulted in a reduced migration after miRNA-99a transfection equal to -0.045 ± 0.005 , yet this was not statistically significant ($p = 0.31$) compared to the negative control (Figure 30). Once again the 5 samples had a similar trend but was not statistically significant. Turning our attention to the cell lines transfected with miRNA-99a antagomir, the migration assay was essentially the same as the transfected negative control (Figure 30).

Figure 30. HT-29 Migration Assay after transfection with miRNA-99a Mimic (Blue) and Antagomir (Red). All data is normalized to the negative control.

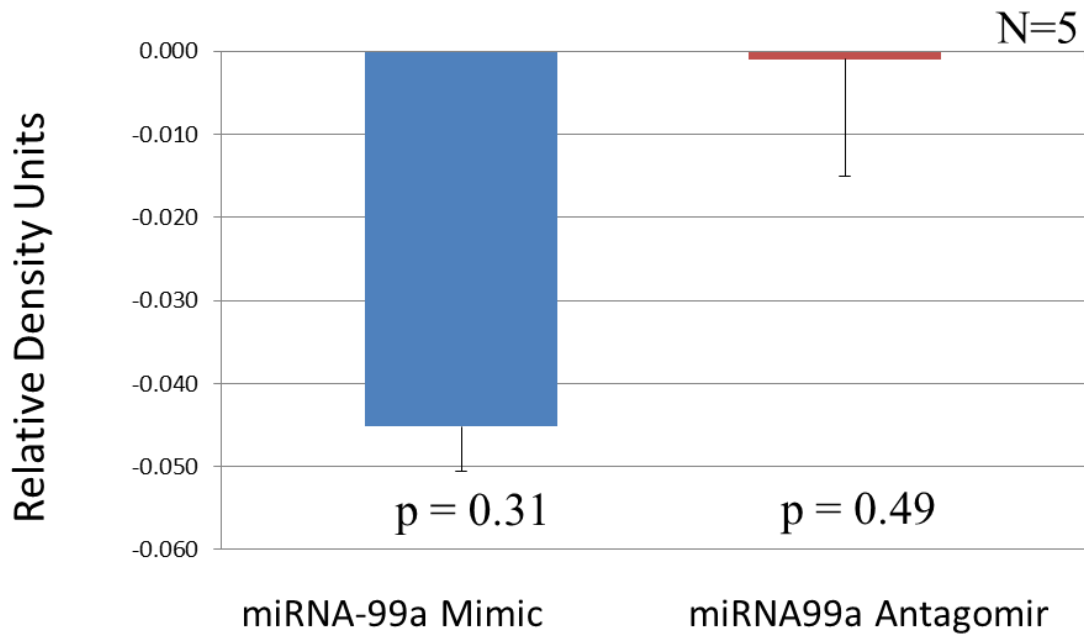


Figure 30b. Numerical Density Values for HT-29 migration assay

Normalized Migration (n=5)		
	99M	99A
Average	-0.045	-0.001
Standard Deviation	0.005	0.014
p-value (t-test)	0.312	0.496

We observed a similar pattern in HCT-116, yet the observed relative density values were larger in magnitude. After transfection with miRNA-99a mimic a relative density value after cell migration was equal to an average of -0.325 ± 0.379 which did approach statistical significance, $p = 0.064$ (Figure 31).

Similarly as with the HT29 (Dukes C cell line), HCT-116 antagomir assay studies were basically unchanged from their transfected negative control (Figure 31). This is not surprising as we did not have great success with the antagomir transfection being downregulated. Since the transfection was likely unsuccessful we did not expect there to be a significant influence on the pathway.

Figure 31. HCT-116 Migration Assay after transfection with miRNA-99a Mimic (Blue) and Antagomir (Red). All data is normalized to the negative control.

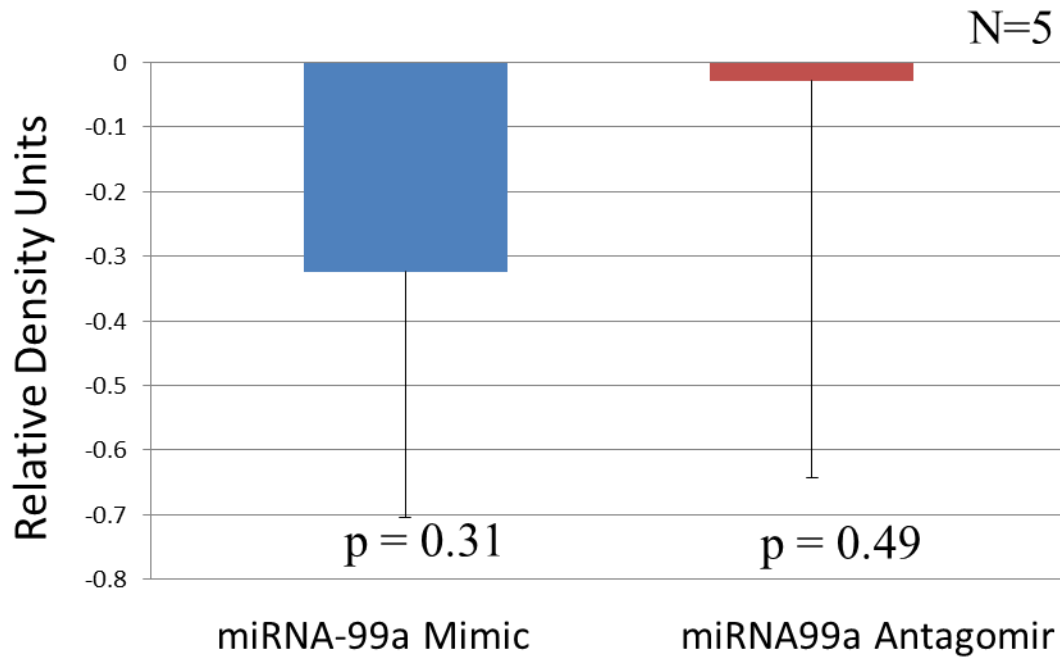


Figure 31b. Numerical Density Values for HCT-116 migration assay

Normalized Migration (n=5)		
	99M	99A
Average	-0.325	-0.029
Standard Deviation	0.379	0.613
p-value (t-test)	0.064	0.460

B. MIGRATION ASSAY DISCUSSION

Although the migration assays did not yield statistical significant in any of the studies, they did show promising results for further inquiry. After transfection in both cell lines we would predict that a decreased migration would occur when compared to the negative control. This was observed in all samples but not statistically significant. HCT-116 did approach statistical significance, which was promising for future studies.

The most likely reason we observed more migration in the Dukes D cell line compared to the Dukes C cell line is due to the fact that by definition the Dukes D cell line is a more aggressive cancer line. Another theory is that due to the fact that HCT-116 is able to replenish the cells that are lost after transfection occurs because of its aggressive nature, as it has been shown that transfection itself can have a cytotoxic effect on the cells themselves.¹²⁸

C. INVASION DATA AND RESULTS

The invasion assays once again utilize the Boyden chamber method and the specific details of experimental materials and method have been discussed previously.¹²⁴ The difference between the migration and the invasion assays is the membrane coating that is applied to the Boyden chambers. The migration assay has a non-coated polycarbonate membrane inserts with 8 μm pores. The invasion assay uses these same polycarbonate membranes with the same pore size yet it is coated with a dried basement membrane matrix solution to recreate a functional basement membrane. This is important because the ability of cells to invade through the basement membrane is essential to their metastatic potential.

Initially we evaluated the HT-29 cell line. We transfected HT-29 cells with miRNA-99a mimic and antagomir and then observed the amount of invasion at 48 hours. Cells transfected with miRNA-99a mimic exhibited minimal invasion. Our sample size of 6 resulted in an average relative density equal to -0.034 ± 0.030 , which was not significant as $p = 0.36$ (Figure 32). As expected from the migration studies, the transfected cells with miRNA-99a antagomir did not invade much and had an extremely wide standard deviation (Figure 32).

Figure 32. HT-29 Invasion Assay after transfection with miRNA-99a Mimic (Blue) and Antagomir (Red). All data is normalized to the negative control.

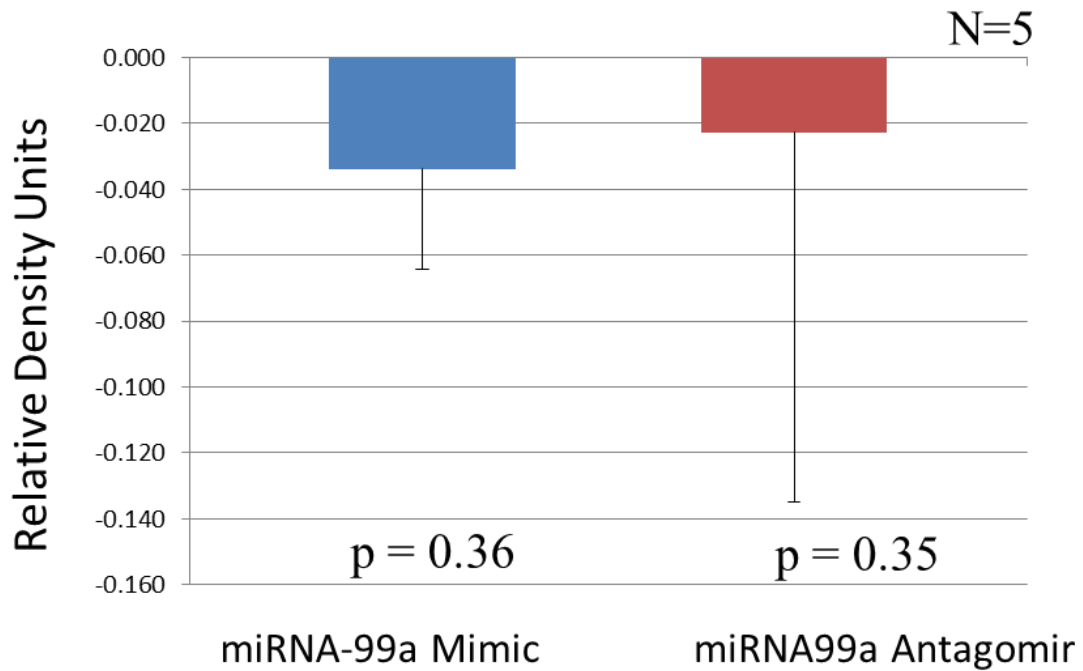


Figure 32b. Numerical Density Values for HCT-116 invasion assay

Normalized Invasion (n=5)		
	99M	99A
Average	-0.034	-0.023
Standard Deviation	0.030	0.112
p-value (t-test)	0.359	0.349

Next, we evaluated the invasive properties of HCT-116. The transfection of miRNA-99a mimic resulted in a relative density measurement of -0.041 ± 0.096 ($p = 0.20$, Figure 33). The transfection of the antagomir had a density measurement of -0.005 ± 0.111 ($p = 0.46$, Figure 33), as compared to the negative controls, i.e. there was basically no invasion with antagomir transfected cell lines as compared to the transfected negative control.

Overall data from the invasion assays were not as clear cut as those from the migration assays. Some possible explanations for this:

- Prior studies of the HT-29 cell line showed that it had minimal migration and invasive properties, which could account for the data we observed with this cell line.¹²⁹
- The motility of the antagomir transfected cell lines could be due to the lack of successful antagomir transfection.
- The effects of transfection itself can be cytotoxic after certain time periods.¹²⁸

Although Lipofectamine 3000[®] has not been tested for this to our knowledge, its predecessor Lipofectamine 2000[®] was thus tested and found to be cytotoxic.

Figure 33. HCT-116 Invasion Assay after transfection with miRNA-99a Mimic (Blue) and Antagomir (Red). All data is normalized to the negative control.

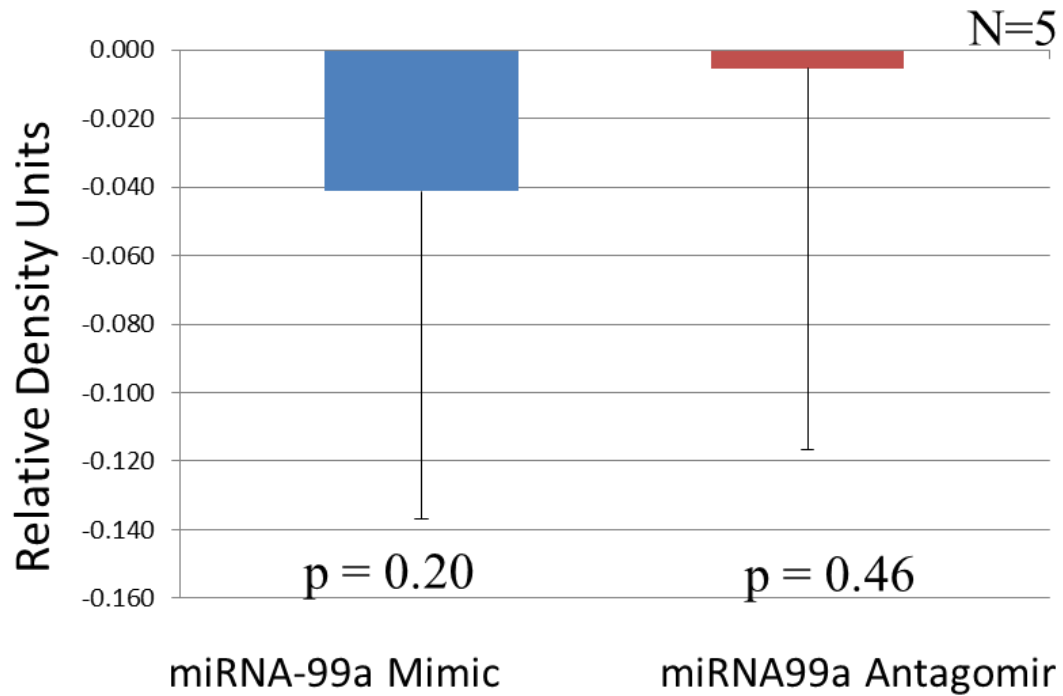


Figure 33b. Numerical values for HCT-116 Invasion Assay

Normalized Invasion (n=5)		
	99M	99A
Average	-0.041	-0.005
Standard Deviation	0.096	0.111
p-value (t-test)	0.195	0.459

D. DISCUSSION

The migration data are interesting in that HT-29 and HCT-116 had similar patterns of migration and invasion after transfection with miRNA-99a mimic. The more promising data with HCT-116 are not surprising as it has been previously reported that HT-29 cell lines have limited motility in migration assays.¹²⁹

The invasion data showed a similar trend as the migration data. Both cell lines exhibited reduced invasion after miRNA-99a transfection although this was not statistically significant. Invasion was not observed with either CRC cell line following antagomirs transfection. This could be due to the difficulty in antagomir transfection that was previously discussed.

CHAPTER XI

FINAL DISCUSSION AND OVERVIEW

Colorectal Cancer (CRC) is the third most common cancer in men and women in the United States.¹ According to the Centers for Disease Control and Prevention's most recent statistics in 2011 approximately 135,260 people were diagnosed with CRC in that year alone.¹ 51,783 reported deaths were credited to CRC, including 26,804 men and 24,979 women.¹ Out of all states, Kentucky ranked number one in incidence for male cases of CRC with 58.8 per 100,000 individuals. Females in the state of Kentucky ranked #3 out of all states with a rate of 40.6 per 100,000 individuals and combined Kentucky ranked #1 out of all states at a rate of 48.9 per 100,000 individuals.¹ All of these being well above the national average for new cases of CRC in individual states.

Although these might be daunting statistics, this poses a challenge from the researchers stand point, as it opens up an opportunity to focus on an area that potentially could change thousands of lives. CRC if caught early is potentially curable.

One pathway that has currently gained a large amount of attention because of its implication in cancer metastasis is the mechanistic target of rapamycin the mTOR pathway. The mTOR pathway is an extensive and complex pathway that has a great deal of control over the translation of many eukaryotic proteins.

Prior work shows that multiple upstream regulators control mTORC1, these are not limited to but include PI3K/Akt route to mTORC1.¹³⁰ It has been shown that the miRNA family of 99 and 100, which includes miRNA-99a, directly binds to mTORC2.¹²⁶

mTORC2 directly interacts with the AKT pathway which is one of the many upstream regulators of mTORC1.

Our work investigated the mTOR pathway and miRNA-99a's influence on CRC cell lines within this pathway. With better understanding of this pathway and the influence miRNA-99a on this pathway, many avenues of study for potential therapeutic intervention for metastatic CRC may become available.

A. SUMMARY OF FINDINGS

We initially needed to confirm successful cell line transfection of CCD-841 (normal colon epithelial cell line), HT-29 (Dukes C) and HCT-116 (Dukes D) cell lines. miRNA-99a mimic was successfully transfected in all three cell lines. This was shown with representative qRT-PCR transfection results of miRNA -99a indicating upregulation of expressed miRNA-99a after transfection with miRNA-99a mimic (Figure 9-11).

miRNA 99a antagomir transfection was not as successful (Figure 9-11). Three cell lines did show a miRNA-99a level close to baseline, however, not all cell lines were downregulated. Moving forward, we therefore focused our efforts on mimic transfection, especially when investigating the proteins in the mTOR pathway. We did pursue motility assays using both mimics and the antagomirs, although we did not expect much success for the antagomir motility studies due to our limited results with antagomir transfection.

To answer Specific Aim 2, we utilized Western blot analysis of mTOR protein, S6K1 and 4EBP1. Most data was in agreement to what one would predict after transfection with a miRNA-99a mimic. Our data showed HT-29 phosphorylated average relative density of 0.06 ± 0.02 compared to the negative control 0.15 ± 0.05 , although not

statistically significant ($p = 0.07$) it did have the same trend in all samples. This is what we would predict as miRNA-99a has been shown to directly bind to mTORC2 and to down-regulate this protein.¹²⁶

A similar pattern of mTOR was seen after transfection in HCT-116 and CCD-841. In HCT-116 an average relative density of phosphorylated antibodies was 0.03 ± 0.00 . This was compared to the negative controls average of 0.05 ± 0.04 . Which was a statistically significant difference ($p = 0.04$). The total antibody resulted an average density of 0.13 ± 0.13 compared to the negative control of 0.25 ± 0.23 , which was not a significant difference ($p = 0.23$). Finally, the CCD-841 cell lines, resulted in phosphorylated density average of 0.04 ± 0.01 compared to the negative control which was equal to 0.06 ± 0.01 . This was not statistically significant, $p = 0.19$. Probing for the total antibody resulted in an average of 0.02 ± 0.01 compared to the negative control which was equal to 0.08 ± 0.05 ($p = 0.14$).

S6K1 phosphorylated only Western blot analysis resulted in a relative density measurement of 0.19 ± 0.04 . This was compared to the transfected negative control which resulted in a relative density of 0.22 ± 0.07 , which was not statistically significant ($p = 0.15$) but all samples had the same trend. mTOR total probe resulted in a significant difference ($p = 0.02$) between miRNA-99a mimic and its transfected negative control. The average density after transfection was 0.09 ± 0.07 compared to the negative control, 0.10 ± 0.07 .

Then 4EBP1 was elucidated under Western blot analysis. HT-29 cell line shows the results of phosphorylated only 4EBP1, which is 0.46 ± 0.11 for miRNA-99a mimic

compared to the negative control, 0.42 ± 0.09 . This difference was not statistically significant with $p = 0.28$. Next, total expression of 4EBP1 shows a similar upregulation compared to negative control trend, with the relative density average being 1.17 ± 0.87 compared to the negative control average of 0.87 ± 0.60 , which was not significantly different.

Our attention next shifted to HCT-116, the Dukes' D cell line. Western blot analysis showed a relative density of 0.21 ± 0.11 compared to the negative control 0.24 ± 0.04 . Similarly, the total protein was downregulated (1.61 ± 0.27) compared to the negative control (1.78 ± 0.36). Neither were statistically significant with p values equal to 0.31, 0.25 respectively.

Finally CCD-841 phosphorylated only versus negative control Western blots basically showed no difference, 0.16 ± 0.09 compared to 0.16 ± 0.11 respectively. 4EBP1 total expression showed upregulation after transfection with miRNA-99a compared to negative control. A relative density of 0.14 ± 0.12 was compared to the negative control equal to 0.18 ± 0.14 . Once again the p value was not statistically significant but it was approaching significance ($p = 0.06$)

Out of all the Western Blots only three showed statistical significance compared to the negative control. When HCT-116 was evaluated for phosphorylated only mTOR. Next when HT-29 was evaluated for total S6K1. Finally, when CCD841 was evaluated for phosphorylated only S6K1.

The migration data for HT-29 and HCT-116 were similar to what was predicted. With the introduction of miRNA-99a mimic a decrease in motility was observed in both

cell lines. Although this was the appropriate trend, neither of these data sets was statistically significant. The antagomir transfection assays did not show much difference compared to the non-transfected cells.

The invasion data showed a similar trend after miRNA-99a mimic transfection. HT-29 and HCT-116 both exhibit decreased invasion following miRNA-99a transfection, but once again neither were statistically significant compared to negative control but all samples had a similar trend. Similar to the migration data the antagomir studies showed no difference. This was predicted due to the unsuccessful transfection of the antagomirs that was observed.

Overall, our data are promising for future studies. They highlight the role of miRNA-99a and its effect in the up and down-regulation of colorectal cancer cell lines. This is promising as it could open up avenues of possible therapeutic intervention. This thesis was limited only to cell lines of have a high degree of metastatic potential. Future studies would need to be done to delineate the impact of miRNA-99a on cancer cell lines of lesser metastatic potential. In addition future studies need to be undertaken to examine the difference between mismatch repair proficient and deficient CRC.

REFERENCES

1. Group USCSW. United States Cancer Statistics : 1999-2011 Incidence and Mortality Web-based Report. Atlanta, GA: Department of Health and Human Services, Centers for Disease Control and Prevention, and National Cancer Institute; 2014.
2. Senore C, Ederle A, Fantin A, Andreoni B, Bisanti L, Grazzini G, et al. Acceptability and side-effects of colonoscopy and sigmoidoscopy in a screening setting. *Journal of medical screening*. 2011;18:128-34.
3. Force USPST. Screening for colorectal cancer: U.S. Preventive Services Task Force recommendation statement. *Annals of internal medicine*. 2008;149:627-37.
4. Fakhri MG, Padmanabhan A. CEA monitoring in colorectal cancer. What you should know. *Oncology (Williston Park)*. 2006;20:579-87; discussion 88, 94, 96 passim.
5. Wang WS, Lin JK, Chiou TJ, Liu JH, Fan FS, Yen CC, et al. CA19-9 as the most significant prognostic indicator of metastatic colorectal cancer. *Hepatogastroenterology*. 2002;49:160-4.
6. Jin P, Kang Q, Wang X, Yang L, Yu Y, Li N, et al. Performance of a second generation methylated SEPT9 test in detecting colorectal neoplasm. *Journal of gastroenterology and hepatology*. 2014.
7. Pawa N, Arulampalam T, Norton JD. Screening for colorectal cancer: established and emerging modalities. *Nature reviews Gastroenterology & hepatology*. 2011;8:711-22.
8. Kramer BS. The Early Detection Research Network. National Cancer Institute, Division of Cancer Prevention. Conducting Research to Identify, Test, and Validate Cancer Biomarkers. 2011.
9. Billeter AT, Barnett RE, Druen D, Polk HC, Jr., van Berkel VH. MicroRNA as a new factor in lung and esophageal cancer. *Seminars in thoracic and cardiovascular surgery*. 2012;24:155-65.
10. Billeter AT, Druen D, Kanaan ZM, Polk HC, Jr. MicroRNAs: new helpers for surgeons? *Surgery*. 2012;151:1-5.
11. Kanaan Z, Rai SN, Eichenberger MR, Roberts H, Keskey B, Pan J, et al. Plasma miR-21: a potential diagnostic marker of colorectal cancer. *Annals of surgery*. 2012;256:544-51.
12. Kanaan Z, Roberts H, Eichenberger MR, Billeter A, Ocheretner G, Pan J, et al. A Plasma MicroRNA Panel for Detection of Colorectal Adenomas: A Step Toward More Precise Screening for Colorectal Cancer. *Annals of surgery*. 2013;258:400-8.

13. Stefanie Sassen EM, Carlos Caldas. MicroRNA-implications for cancer. *Virchows Arch.* 2008;452:1-10.
14. Aaron J. Schetter HO, Curtis C. Harris. The Role of microRNAs in Colorectal Cancer. *Cancer J.* 2012;18:244-52.
15. Dong Y, Wu WK, Wu CW, Sung JJ, Yu J, Ng SS. MicroRNA dysregulation in colorectal cancer: a clinical perspective. *Br J Cancer.* 2011;104:893-8.
16. Cho WC. Great potential of miRNAs as predictive and prognostic markers for cancer. *Expert Rev Mol Diagn.* 2012;12:315-8.
17. Cho WC. Circulating MicroRNAs as Minimally Invasive Biomarkers for Cancer Theragnosis and Prognosis. *Front Genet.* 2011;2:7.
18. Ichikawa M, Akiyama H. A combination of extraction reagent and DNA microarray that allows for the detection of global miRNA profiles from serum/plasma. *Methods Mol Biol.* 2013;1024:247-53.
19. Cheng L, Sharples RA, Scicluna BJ, Hill AF. Exosomes provide a protective and enriched source of miRNA for biomarker profiling compared to intracellular and cell-free blood. *Journal of extracellular vesicles.* 2014;3.
20. Ganepola GA, Rutledge JR, Suman P, Yiengpruksawan A, Chang DH. Novel blood-based microRNA biomarker panel for early diagnosis of pancreatic cancer. *World journal of gastrointestinal oncology.* 2014;6:22-33.
21. Bhatnagar S, Chertkow H, Schipper HM, Yuan Z, Shetty V, Jenkins S, et al. Increased microRNA-34c abundance in Alzheimer's disease circulating blood plasma. *Frontiers in molecular neuroscience.* 2014;7:2.
22. Westermann AM, Schmidt D, Holdenrieder S, Moritz R, Semjonow A, Schmidt M, et al. Serum microRNAs as biomarkers in patients undergoing prostate biopsy: results from a prospective multi-center study. *Anticancer research.* 2014;34:665-9.
23. Tsukamoto O, Miura K, Mishima H, Abe S, Kaneuchi M, Higashijima A, et al. Identification of endometrioid endometrial carcinoma-associated microRNAs in tissue and plasma. *Gynecologic oncology.* 2014;132:715-21.
24. Zanutto S, Pizzamiglio S, Ghilotti M, Bertan C, Ravagnani F, Perrone F, et al. Circulating miR-378 in plasma: a reliable, haemolysis-independent biomarker for colorectal cancer. *British journal of cancer.* 2014;110:1001-7.
25. Sozzi G, Boeri M, Rossi M, Verri C, Suatoni P, Bravi F, et al. Clinical utility of a plasma-based miRNA signature classifier within computed tomography lung cancer screening: a correlative MILD trial study. *Journal of clinical oncology : official journal of the American Society of Clinical Oncology.* 2014;32:768-73.
26. Yu H, Jiang L, Sun C, Li Guo L, Lin M, Huang J, et al. Decreased circulating miR-375: a potential biomarker for patients with non-small-cell lung cancer. *Gene.* 2014;534:60-5.
27. Teixeira AL, Ferreira M, Silva J, Gomes M, Dias F, Santos JI, et al. Higher circulating expression levels of miR-221 associated with poor overall survival in renal cell carcinoma patients. *Tumour biology : the journal of the International Society for Oncodevelopmental Biology and Medicine.* 2014;35:4057-66.
28. Achberger S, Aldrich W, Tubbs R, Crabb JW, Singh AD, Triozzi PL. Circulating immune cell and microRNA in patients with uveal melanoma developing metastatic disease. *Molecular immunology.* 2014;58:182-6.
29. Shapira I, Oswald M, Lovecchio J, Khalili H, Menzin A, Whyte J, et al. Circulating biomarkers for detection of ovarian cancer and predicting cancer outcomes. *British journal of cancer.* 2014;110:976-83.

30. Szabo DR, Luconi M, Szabo PM, Toth M, Szucs N, Horanyi J, et al. Analysis of circulating microRNAs in adrenocortical tumors. *Laboratory investigation; a journal of technical methods and pathology*. 2014;94:331-9.
31. Lu J, Xu X, Liu X, Peng Y, Zhang B, Wang L, et al. Predictive value of miR-9 as a potential biomarker for nasopharyngeal carcinoma metastasis. *British journal of cancer*. 2014;110:392-8.
32. Quackenbush JF, Cassidy PB, Pfeffer LM, Boucher KM, Hawkes JE, Pfeffer SR, et al. Isolation of circulating microRNAs from microvesicles found in human plasma. *Methods in molecular biology*. 2014;1102:641-53.
33. Li H, Ge Q, Guo L, Lu Z. Maternal plasma miRNAs expression in preeclamptic pregnancies. *BioMed research international*. 2013;2013:970265.
34. Roncarati R, Viviani Anselmi C, Losi MA, Papa L, Cavarretta E, Da Costa Martins P, et al. Circulating miR-29a, among other up-regulated microRNAs, is the only biomarker for both hypertrophy and fibrosis in patients with hypertrophic cardiomyopathy. *Journal of the American College of Cardiology*. 2014;63:920-7.
35. Aushev VN, Zborovskaya IB, Laktionov KK, Girard N, Cros MP, Herceg Z, et al. Comparisons of microRNA patterns in plasma before and after tumor removal reveal new biomarkers of lung squamous cell carcinoma. *PloS one*. 2013;8:e78649.
36. Kishimoto T, Eguchi H, Nagano H, Kobayashi S, Akita H, Hama N, et al. Plasma miR-21 is a novel diagnostic biomarker for biliary tract cancer. *Cancer science*. 2013;104:1626-31.
37. Tian Q, Jia J, Ling S, Liu Y, Yang S, Shao Z. A causal role for circulating miR-34b in osteosarcoma. *European journal of surgical oncology : the journal of the European Society of Surgical Oncology and the British Association of Surgical Oncology*. 2014;40:67-72.
38. Xiao B, Wang Y, Li W, Baker M, Guo J, Corbet K, et al. Plasma microRNA signature as a noninvasive biomarker for acute graft-versus-host disease. *Blood*. 2013;122:3365-75.
39. Rong Y, Bao W, Shan Z, Liu J, Yu X, Xia S, et al. Increased microRNA-146a levels in plasma of patients with newly diagnosed type 2 diabetes mellitus. *PloS one*. 2013;8:e73272.
40. Garcia R, Villar AV, Cobo M, Llano M, Martin-Duran R, Hurler MA, et al. Circulating levels of miR-133a predict the regression potential of left ventricular hypertrophy after valve replacement surgery in patients with aortic stenosis. *Journal of the American Heart Association*. 2013;2:e000211.
41. Cheng HH, Mitchell PS, Kroh EM, Dowell AE, Chery L, Siddiqui J, et al. Circulating microRNA profiling identifies a subset of metastatic prostate cancer patients with evidence of cancer-associated hypoxia. *PloS one*. 2013;8:e69239.
42. Kumar P, Dezso Z, MacKenzie C, Oestreicher J, Agoulnik S, Byrne M, et al. Circulating miRNA biomarkers for Alzheimer's disease. *PloS one*. 2013;8:e69807.
43. Benson EA, Skaar TC. Incubation of whole blood at room temperature does not alter the plasma concentrations of microRNA-16 and -223. *Drug metabolism and disposition: the biological fate of chemicals*. 2013;41:1778-81.
44. Murata K, Furu M, Yoshitomi H, Ishikawa M, Shibuya H, Hashimoto M, et al. Comprehensive microRNA analysis identifies miR-24 and miR-125a-5p as plasma biomarkers for rheumatoid arthritis. *PloS one*. 2013;8:e69118.
45. Zheng W, Di Y, Liu Y, Huang G, Zheng Y, Zhang Y, et al. Development and application of a novel reverse transcription real-time PCR method for miR-499 quantification. *Clinical biochemistry*. 2013;46:1566-71.

46. Leuenberger N, Schumacher YO, Pradervand S, Sander T, Saugy M, Pottgiesser T. Circulating microRNAs as biomarkers for detection of autologous blood transfusion. *PloS one*. 2013;8:e66309.
47. Cheng HH, Yi HS, Kim Y, Kroh EM, Chien JW, Eaton KD, et al. Plasma processing conditions substantially influence circulating microRNA biomarker levels. *PloS one*. 2013;8:e64795.
48. Marfella R, Di Filippo C, Potenza N, Sardu C, Rizzo MR, Siniscalchi M, et al. Circulating microRNA changes in heart failure patients treated with cardiac resynchronization therapy: responders vs. non-responders. *European journal of heart failure*. 2013;15:1277-88.
49. Du J, Cao X, Zou L, Chen Y, Guo J, Chen Z, et al. MicroRNA-21 and risk of severe acute kidney injury and poor outcomes after adult cardiac surgery. *PloS one*. 2013;8:e63390.
50. Ellis KL, Cameron VA, Troughton RW, Frampton CM, Ellmers LJ, Richards AM. Circulating microRNAs as candidate markers to distinguish heart failure in breathless patients. *European journal of heart failure*. 2013;15:1138-47.
51. Gourzones C, Ferrand FR, Amiel C, Verillaud B, Barat A, Guerin M, et al. Consistent high concentration of the viral microRNA BART17 in plasma samples from nasopharyngeal carcinoma patients--evidence of non-exosomal transport. *Virology journal*. 2013;10:119.
52. Shrivastava S, Petrone J, Steele R, Lauer GM, Di Bisceglie AM, Ray RB. Up-regulation of circulating miR-20a is correlated with hepatitis C virus-mediated liver disease progression. *Hepatology*. 2013;58:863-71.
53. Gorur A, Balci Fidanci S, Dogruer Unal N, Ayaz L, Akbayir S, Yildirim Yaroglu H, et al. Determination of plasma microRNA for early detection of gastric cancer. *Molecular biology reports*. 2013;40:2091-6.
54. Olivieri F, Antonicelli R, Lorenzi M, D'Alessandra Y, Lazzarini R, Santini G, et al. Diagnostic potential of circulating miR-499-5p in elderly patients with acute non ST-elevation myocardial infarction. *International journal of cardiology*. 2013;167:531-6.
55. Khoo SK, Petillo D, Kang UJ, Resau JH, Berryhill B, Linder J, et al. Plasma-based circulating MicroRNA biomarkers for Parkinson's disease. *Journal of Parkinson's disease*. 2012;2:321-31.
56. Ayaz L, Gorur A, Yaroglu HY, Ozcan C, Tamer L. Differential expression of microRNAs in plasma of patients with laryngeal squamous cell carcinoma: potential early-detection markers for laryngeal squamous cell carcinoma. *Journal of cancer research and clinical oncology*. 2013;139:1499-506.
57. Cai H, Yuan Y, Hao YF, Guo TK, Wei X, Zhang YM. Plasma microRNAs serve as novel potential biomarkers for early detection of gastric cancer. *Medical oncology*. 2013;30:452.
58. De Rosa S, Fichtlscherer S, Lehmann R, Assmus B, Dimmeler S, Zeiher AM. Transcoronary concentration gradients of circulating microRNAs. *Circulation*. 2011;124:1936-44.
59. Fan KL, Zhang HF, Shen J, Zhang Q, Li XL. Circulating microRNAs levels in Chinese heart failure patients caused by dilated cardiomyopathy. *Indian heart journal*. 2013;65:12-6.
60. Fayyad-Kazan H, Bitar N, Najjar M, Lewalle P, Fayyad-Kazan M, Badran R, et al. Circulating miR-150 and miR-342 in plasma are novel potential biomarkers for acute myeloid leukemia. *Journal of translational medicine*. 2013;11:31.
61. Freedman JE, Ercan B, Morin KM, Liu CT, Tamer L, Ayaz L, et al. The distribution of circulating microRNA and their relation to coronary disease. *F1000Research*. 2012;1:50.

62. Gandhi R, Healy B, Gholipour T, Egorova S, Musallam A, Hussain MS, et al. Circulating microRNAs as biomarkers for disease staging in multiple sclerosis. *Annals of neurology*. 2013;73:729-40.
63. Ge Q, Li H, Yang Q, Lu J, Tu J, Bai Y, et al. Sequencing circulating miRNA in maternal plasma with modified library preparation. *Clinica chimica acta; international journal of clinical chemistry*. 2011;412:1989-94.
64. Gidlof O, Smith JG, Miyazu K, Gilje P, Spencer A, Blomquist S, et al. Circulating cardio-enriched microRNAs are associated with long-term prognosis following myocardial infarction. *BMC cardiovascular disorders*. 2013;13:12.
65. Giraldez MD, Lozano JJ, Ramirez G, Hijona E, Bujanda L, Castells A, et al. Circulating microRNAs as biomarkers of colorectal cancer: results from a genome-wide profiling and validation study. *Clinical gastroenterology and hepatology : the official clinical practice journal of the American Gastroenterological Association*. 2013;11:681-8 e3.
66. Hirajima S, Komatsu S, Ichikawa D, Takeshita H, Konishi H, Shiozaki A, et al. Clinical impact of circulating miR-18a in plasma of patients with oesophageal squamous cell carcinoma. *British journal of cancer*. 2013;108:1822-9.
67. Huang JJ, Yu J, Li JY, Liu YT, Zhong RQ. Circulating microRNA expression is associated with genetic subtype and survival of multiple myeloma. *Medical oncology*. 2012;29:2402-8.
68. Huang X, Yuan T, Tschannen M, Sun Z, Jacob H, Du M, et al. Characterization of human plasma-derived exosomal RNAs by deep sequencing. *BMC genomics*. 2013;14:319.
69. Jia SZ, Yang Y, Lang J, Sun P, Leng J. Plasma miR-17-5p, miR-20a and miR-22 are down-regulated in women with endometriosis. *Human reproduction*. 2013;28:322-30.
70. Kawano Y, Iwata S, Kawada J, Gotoh K, Suzuki M, Torii Y, et al. Plasma viral microRNA profiles reveal potential biomarkers for chronic active Epstein-Barr virus infection. *The Journal of infectious diseases*. 2013;208:771-9.
71. Kin K, Miyagawa S, Fukushima S, Shirakawa Y, Torikai K, Shimamura K, et al. Tissue- and plasma-specific MicroRNA signatures for atherosclerotic abdominal aortic aneurysm. *Journal of the American Heart Association*. 2012;1:e000745.
72. Kumar S, Keerthana R, Pazhanimuthu A, Perumal P. Overexpression of circulating miRNA-21 and miRNA-146a in plasma samples of breast cancer patients. *Indian journal of biochemistry & biophysics*. 2013;50:210-4.
73. Laterza OF, Scott MG, Garrett-Engele PW, Korenblat KM, Lockwood CM. Circulating miR-122 as a potential biomarker of liver disease. *Biomarkers in medicine*. 2013;7:205-10.
74. Leidner RS, Li L, Thompson CL. Dampening enthusiasm for circulating microRNA in breast cancer. *PloS one*. 2013;8:e57841.
75. Li C, Li JF, Cai Q, Qiu QQ, Yan M, Liu BY, et al. MiRNA-199a-3p: A potential circulating diagnostic biomarker for early gastric cancer. *Journal of surgical oncology*. 2013;108:89-92.
76. Li YQ, Zhang MF, Wen HY, Hu CL, Liu R, Wei HY, et al. Comparing the diagnostic values of circulating microRNAs and cardiac troponin T in patients with acute myocardial infarction. *Clinics*. 2013;68:75-80.
77. Luo X, Stock C, Burwinkel B, Brenner H. Identification and evaluation of plasma MicroRNAs for early detection of colorectal cancer. *PloS one*. 2013;8:e62880.
78. Moldovan L, Batte K, Wang Y, Wisler J, Piper M. Analyzing the circulating microRNAs in exosomes/extracellular vesicles from serum or plasma by qRT-PCR. *Methods in molecular biology*. 2013;1024:129-45.

79. Nair N, Kumar S, Gongora E, Gupta S. Circulating miRNA as novel markers for diastolic dysfunction. *Molecular and cellular biochemistry*. 2013;376:33-40.
80. Ng EK, Li R, Shin VY, Jin HC, Leung CP, Ma ES, et al. Circulating microRNAs as specific biomarkers for breast cancer detection. *PloS one*. 2013;8:e53141.
81. Ouyang L, Liu P, Yang S, Ye S, Xu W, Liu X. A three-plasma miRNA signature serves as novel biomarkers for osteosarcoma. *Medical oncology*. 2013;30:340.
82. Parikh VN, Chan SY. Analysis of microRNA niches: techniques to measure extracellular microRNA and intracellular microRNA in situ. *Methods in molecular biology*. 2013;1024:157-72.
83. Prats-Puig A, Ortega FJ, Mercader JM, Moreno-Navarrete JM, Moreno M, Bonet N, et al. Changes in circulating microRNAs are associated with childhood obesity. *The Journal of clinical endocrinology and metabolism*. 2013;98:E1655-60.
84. Sanfiorenzo C, Ilie MI, Belaid A, Barlesi F, Mouroux J, Marquette CH, et al. Two panels of plasma microRNAs as non-invasive biomarkers for prediction of recurrence in resectable NSCLC. *PloS one*. 2013;8:e54596.
85. Shimizu C, Kim J, Stepanowsky P, Trinh C, Lau HD, Akers JC, et al. Differential expression of miR-145 in children with Kawasaki disease. *PloS one*. 2013;8:e58159.
86. Soeda S, Ohyashiki JH, Ohtsuki K, Umezu T, Setoguchi Y, Ohyashiki K. Clinical relevance of plasma miR-106b levels in patients with chronic obstructive pulmonary disease. *International journal of molecular medicine*. 2013;31:533-9.
87. Suryawanshi S, Vlad AM, Lin HM, Mantia-Smaldone G, Laskey R, Lee M, et al. Plasma microRNAs as novel biomarkers for endometriosis and endometriosis-associated ovarian cancer. *Clinical cancer research : an official journal of the American Association for Cancer Research*. 2013;19:1213-24.
88. Takahashi K, Yokota S, Tatsumi N, Fukami T, Yokoi T, Nakajima M. Cigarette smoking substantially alters plasma microRNA profiles in healthy subjects. *Toxicology and applied pharmacology*. 2013;272:154-60.
89. Wang E, Nie Y, Zhao Q, Wang W, Huang J, Liao Z, et al. Circulating miRNAs reflect early myocardial injury and recovery after heart transplantation. *Journal of cardiothoracic surgery*. 2013;8:165.
90. Winther TN, Bang-Berthelsen CH, Heiberg IL, Pociot F, Høgh B. Differential plasma microRNA profiles in HBeAg positive and HBeAg negative children with chronic hepatitis B. *PloS one*. 2013;8:e58236.
91. Yamamoto M, Singh A, Sava F, Pui M, Tebbutt SJ, Carlsten C. MicroRNA expression in response to controlled exposure to diesel exhaust: attenuation by the antioxidant N-acetylcysteine in a randomized crossover study. *Environmental health perspectives*. 2013;121:670-5.
92. Zeng RC, Zhang W, Yan XQ, Ye ZQ, Chen ED, Huang DP, et al. Down-regulation of miRNA-30a in human plasma is a novel marker for breast cancer. *Medical oncology*. 2013;30:477.
93. Zhao J, Lei T, Xu C, Li H, Ma W, Yang Y, et al. MicroRNA-187, down-regulated in clear cell renal cell carcinoma and associated with lower survival, inhibits cell growth and migration through targeting B7-H3. *Biochemical and biophysical research communications*. 2013;438:439-44.
94. Rice J, Roberts H, Burton J, Pan J, States V, Rai SN, et al. Assay Reproducibility in Clinical Studies of Plasma miRNA. *PloS one*. 2015;10:e0121948.
95. Rice JR, Henry. Rai, Shesh. Galandiuk, Susan. Housekeeping Genes for Studies of Plasma microRNA: A Need for More Precise Standardization. *Surgery*. 2015.

96. SAS 9.3 Product Documentation. SAS Institute Inc. ; 2014.
97. Schoen RE, Pinsky PF, Weissfeld JL, Yokochi LA, Church T, Laiyemo AO, et al. Colorectal-cancer incidence and mortality with screening flexible sigmoidoscopy. *The New England journal of medicine*. 2012;366:2345-57.
98. Rai SN RH, Yuan X, Pan J, Hamid T, Prabhu SD. Statistical Analysis of Repeated MicroRNA High Throughput Data with Application to Human Heart Failure: A Methodology Review. *Open Access Medical Statistics* 2012;2:21-31.
99. Gonen M. Receiver Operating Characteristics (ROC) Curves. Thirty-first Annual SAS Users Group International Conference: Proceedings of the Thirty-first Annual SAS Users Group International Conference, Paper 210-31. Cary, NC: SAS Institute Inc. ; 2006
100. Technologies L. TRizol LS Reagent. http://tools.lifetechnologies.com/content/sfs/manuals/trizol_ls_reagent.pdf; Life Technologies; 2010.
101. Moret I, Sanchez-Izquierdo D, Iborra M, Tortosa L, Navarro-Puche A, Nos P, et al. Assessing an improved protocol for plasma microRNA extraction. *PLoS One*. 2013;8:e82753.
102. Fleiss JL. Design and Analysis of Clinical Experiments. New York: John Wiley and Sons; 1986.
103. Dmitrienko A MG, Chuang-Stein, C and Offen W. Analysis of Clinical Trials Using SAS®: A practical Guide. Cary, NC, USA: SAS Institute Inc.; 2005.
104. Cambon AC BK BG, Cooper NGF, Wu D, Rai SN. Classification of Clinical Outcomes Using High-throughput Informatics: Part 1-Nonparametric Method Reviews. *Model Assisted Statistics and Applications*. 2014.
105. Cambon AC BK BG, Cooper NGF, Wu D, Rai SN. Classification of Clinical Outcomes Using High-throughput Informatics: Part 2-Parametric Method Reviews. . *Model Assisted Statistics and Applications*. 2014.
106. Pepe MS, Etzioni R, Feng Z, Potter JD, Thompson ML, Thornquist M, et al. Phases of biomarker development for early detection of cancer. *J Natl Cancer Inst*. 2001;93:1054-61.
107. Pepe MS. *The Statistical Evaluation of Medical Tests for Classification and Prediction*: Oxford; 2003.
108. Mitchell PS, Parkin RK, Kroh EM, Fritz BR, Wyman SK, Pogosova-Agadjanyan EL, et al. Circulating microRNAs as stable blood-based markers for cancer detection. *Proceedings of the National Academy of Sciences of the United States of America*. 2008;105:10513-8.
109. Wang K, Yuan Y, Cho JH, McClarty S, Baxter D, Galas DJ. Comparing the MicroRNA spectrum between serum and plasma. *PloS one*. 2012;7:e41561.
110. Wedge DC, Allwood JW, Dunn W, Vaughan AA, Simpson K, Brown M, et al. Is serum or plasma more appropriate for intersubject comparisons in metabolomic studies? An assessment in patients with small-cell lung cancer. *Analytical chemistry*. 2011;83:6689-97.
111. Kirschner MB, Kao SC, Edelman JJ, Armstrong NJ, Valley MP, van Zandwijk N, et al. Haemolysis during sample preparation alters microRNA content of plasma. *PloS one*. 2011;6:e24145.
112. Sun D, Lee YS, Malhotra A, Kim HK, Matecic M, Evans C, et al. miR-99 family of MicroRNAs suppresses the expression of prostate-specific antigen and prostate cancer cell proliferation. *Cancer research*. 2011;71:1313-24.
113. Laplante M, Sabatini DM. mTOR signaling in growth control and disease. *Cell*. 2012;149:274-93.

114. Sarbassov DD, Guertin DA, Ali SM, Sabatini DM. Phosphorylation and regulation of Akt/PKB by the rictor-mTOR complex. *Science*. 2005;307:1098-101.
115. Guertin DA, Stevens DM, Thoreen CC, Burds AA, Kalaany NY, Moffat J, et al. Ablation in mice of the mTORC components raptor, rictor, or mLST8 reveals that mTORC2 is required for signaling to Akt-FOXO and PKCalpha, but not S6K1. *Developmental cell*. 2006;11:859-71.
116. Jacinto E, Facchinetti V, Liu D, Soto N, Wei S, Jung SY, et al. SIN1/MIP1 maintains rictor-mTOR complex integrity and regulates Akt phosphorylation and substrate specificity. *Cell*. 2006;127:125-37.
117. Fishel R, Lescoe MK, Rao MR, Copeland NG, Jenkins NA, Garber J, et al. The human mutator gene homolog MSH2 and its association with hereditary nonpolyposis colon cancer. *Cell*. 1993;75:1027-38.
118. Papadopoulos N, Nicolaides NC, Wei YF, Ruben SM, Carter KC, Rosen CA, et al. Mutation of a mutL homolog in hereditary colon cancer. *Science*. 1994;263:1625-9.
119. Miyaki M, Konishi M, Tanaka K, Kikuchi-Yanoshita R, Muraoka M, Yasuno M, et al. Germline mutation of MSH6 as the cause of hereditary nonpolyposis colorectal cancer. *Nat Genet*. 1997;17:271-2.
120. Nicolaides NC, Papadopoulos N, Liu B, Wei YF, Carter KC, Ruben SM, et al. Mutations of two PMS homologues in hereditary nonpolyposis colon cancer. *Nature*. 1994;371:75-80.
121. Lu SL, Kawabata M, Imamura T, Akiyama Y, Nomizu T, Miyazono K, et al. HNPCC associated with germline mutation in the TGF-beta type II receptor gene. *Nat Genet*. 1998;19:17-8.
122. Ou J, Rasmussen M, Westers H, Andersen SD, Jager PO, Kooi KA, et al. Biochemical characterization of MLH3 missense mutations does not reveal an apparent role of MLH3 in Lynch syndrome. *Genes Chromosomes Cancer*. 2009;48:340-50.
123. Wei H, Zhang Z, Saha A, Peng S, Chandra G, Quezado Z, et al. Disruption of adaptive energy metabolism and elevated ribosomal p-S6K1 levels contribute to INCL pathogenesis: partial rescue by resveratrol. *Human molecular genetics*. 2011;20:1111-21.
124. Boyden S. The chemotactic effect of mixtures of antibody and antigen on polymorphonuclear leucocytes. *The Journal of experimental medicine*. 1962;115:453-66.
125. Lang SA, Gaumann A, Koehl GE, Seidel U, Bataille F, Klein D, et al. Mammalian target of rapamycin is activated in human gastric cancer and serves as a target for therapy in an experimental model. *International journal of cancer Journal international du cancer*. 2007;120:1803-10.
126. Jin Y, Tymen SD, Chen D, Fang ZJ, Zhao Y, Dragas D, et al. MicroRNA-99 family targets AKT/mTOR signaling pathway in dermal wound healing. *PloS one*. 2013;8:e64434.
127. Dann SG, Selvaraj A, Thomas G. mTOR Complex1-S6K1 signaling: at the crossroads of obesity, diabetes and cancer. *Trends in molecular medicine*. 2007;13:252-9.
128. Juckem L. Cellular Toxicity Caused by Transfection: Why is it important? <http://www.biocompare.com/Bench-Tips/121111-Cellular-Toxicity-Caused-by-Transfection-Why-is-it-important/2012>.
129. de Both NJ, Vermey M, Dinjens WN, Bosman FT. A comparative evaluation of various invasion assays testing colon carcinoma cell lines. *British journal of cancer*. 1999;81:934-41.
130. Mamane Y, Petroulakis E, LeBacquer O, Sonenberg N. mTOR, translation initiation and cancer. *Oncogene*. 2006;25:6416-22.

APPENDIX:
ABBREVIATIONS

99M	miRNA-99a mimic
99A	miRNA-99a antagomir
M-	miRNA-99a mimic negative control
A-	miRNA-99a antagomir negative control
AUC	Area Under the Curve
BC	Breast Cancer
BCA	Bicinchoninic acid
CA 19-9	Carbohydrate antigen 19-9
CAA	Colorectal Advanced Adenomas
CCSP	Colon-cancer-secreted-protein
CEA	Carcinoembryonic antigen
CRC	Colorectal Cancer
CSA	Colon cancer specific antigen
CT	Cycle threshold
DMSO	Dimethyl sulfoxide
eIF4EBP1	Eukaryotic translation initiation factor 4E-binding protein 1
EtOH	Ethanol
FBS	Fetal bovine serum
HKG	Housekeeping gene
LC	Lung Cancer
miRNA	micro-Ribonucleic acid
mTOR	Mechanistic target of rapamycin
mTORC1	mTOR Complex 1

mTORC2	mTOR Complex 2
PBS	Phosphate buffered saline
PC	Pancreatic Cancer
PVDF	Polyvinylidene difluoride
qRT-PCR	Real time polymerase chain reaction
RCF	Relative centrifugal force
RISC	RNA-induced silencing complex
ROC	Receiver operating characteristic
S6K1	Ribosomal protein S6 kinase beta-1

CURRICULUM VITAE

Jonathan David Rice, M.D.

Education PhD, Physiology and Biophysics

Department of Physiology, University of Louisville

Thesis: The influence of miR-99a on mTOR signaling regulation in colorectal cancer cell lines

Degree to be granted May 13, 2016

Doctor of Medicine

The University of Texas Medical Branch, Galveston, Texas

June 2011

Bachelor of Science, Deans Scholar degree in Chemistry with Honors

The University of Texas at Austin, Austin, Texas

May 2007

Bachelor of Science, Chemistry

The University of Oklahoma, Norman, Oklahoma

Transferred August 2003 to above

Training The University of Louisville, Louisville Kentucky

PGY-3 Categorical Resident in General Surgery 2011-present

Chairman: Kelly McMasters, MD, PhD

Program Director: William Cheadle, MD

Publications **Rice J**, Roberts H, Burton J, Pan J, States V, Rai SN, Galandiuk S. Assay Reproducibility in Clinical Studies of Plasma miRNA. PLOS One. 2015 Apr 8;10(4):e0121948. doi: 10.1371/journal.pone.0121948.

Rice J, Roberts H, Rai SN, Galandiuk S. Housekeeping genes for studies of plasma microRNA: A need for more precise standardization. Surgery. 2015 Nov;158(5):1345-51. doi: 10.1016/j.surg.2015.04.025. Epub 2015 Jun 18. PMID: 26094174

Billeter AT, **Rice J**, Druen D, Sklare S, Walker S, Gardner SA, Polk HC Jr. Warming to 39°C But Not to 37°C Ameliorates the Effects on the Monocyte Response by Hypothermia. Ann Surg. 2015 Feb 25. PMID: 25719808

Galandiuk S, **Rice J**, Deveaux P, Farmer R,. Chapter 69. Pneumstosis Cystoides Intestinales. Current Therapy in Colon and Rectal Surgery 3rd. Edition. Fazio VW, Delaney C, Church J, Ravi Kiran R (Eds.), Elsevier, London. In Press.

Galandiuk, S, Jordan J, **Rice J**, Deveaux P. Chapter 79. Acute and Chronic Mesenteric Ischemia. Current Therapy in Colon and Rectal Surgery 3rd. Edition. Fazio VW, Delaney C, Church J, Ravi Kiran R (Eds.), Elsevier, London. In Press.

Boydston, A. J.; **Rice, J. D.**; Sanderson, M. D.; Dykhno, O. L.; Bielawski, C. W. Synthesis and Study of Bidentate Benzimidazolylidene-Group 10 Metal Complexes and Related Main-Chain Organometallic Polymers. Organometallics 2006, 25, 6087.DOI: 10.1021/om060494u

Deans Scholar Senior Thesis (Advisor: Jason Shear, PhD)
“Chemotaxis Studies and Characterization of Laminar Flow Streams Created Using Laser-Induced Membrane Ablation” **Rice, J.D.**

Carter J, **Rice J**, Pan J, Roberts H, Eichenberger MR, Burton J, BA Galbraith N, Jordan J, Deveaux P, Farmer RW, Williford A, Kanaan Z, Rai S, Galandiuk S. A Highly Predictive Model for Diagnosis of Colorectal Neoplasms Using Plasma MicroRNA: Improving Specificity and Sensitivity. Ann. Surg. 2016. To be submitted April 2016.

Research **Price Institute of Surgical Research, The University of Louisville**

Price Research Fellow

Lab of Susan Galandiuk, M.D.

July 2013-present

The University of Texas Medical Branch at Galveston, Research Associate

Lab of Celeste C. Finnerty, PhD

December 2010-January 2011

Data base analysis of the genomic responses to burns

The University of Texas Medical Branch at Galveston, Research Associate

Lab of Vinod K. Panchbhavi, M.D.

May 2008-September 2008

Properties of Achilles tendon rupture and repair

The University of Texas at Austin, Research Associate

Lab of Jason Shear, PhD

August 2006-May 2007

Completed studies on laminar flow in micro fluidics to aid in the design of methods to study chemotaxis properties of neutrophil movement in a controlled environment

The University of Texas at Austin, Research Associate

Lab of Christopher Bielawski, PhD

January 2005- August 2006

Researched new methods in route to determine new tertiary oxidation methods.
Developed methods for use of Benzobis(imidazolylidene)s in the creation of novel fluorescence polymers.

Presented at 2006 Beckman Summer Research Symposium, Irvine California.

Presented at 2005, 2006 University of Texas at Austin Undergraduate Research Day.

Honors/ UTMB Humanism Award in Pediatrics, Spring 2010

Awards UTMB Honors in Pediatric Clerkship, Spring 2010

Arnold and Mabel Beckman Foundation Beckman Scholar, 2005-2006

UT Austin Dean's Scholar Honors, 2004-2007

UT Austin University Honors Spring, 2004-2007

UT Austin **Phi Beta Kappa** member, Inducted 2006

UT Austin Undergraduate Research Fellowship, 2005-2006

University of Oklahoma Presidential Honor Roll, 2002-2003

University of Oklahoma Outstanding Freshman Honor Roll, Spring 2003

University of Oklahoma Gamma Phi Beta member, Inducted Spring 2003

Valedictorian, Fossil Ridge High School Fort Worth, TX, May 2002

Professional American College of Surgeons

Memberships American Medical Association

American Chemical Society

Greater Louisville Medical Society

Presentations:

Local:

Rice, J. Roberts H, Eichenberger MR, Galandiuk S. Comparing colorectal cell lines miRNA profile. Research Louisville. Res-18. September 16, 2014.

Roberts H, **Rice R**, Eichenberger MR, Pan J, Rai S, Galandiuk S. Plasma-based micro-RNA panel specific for colorectal neoplasia. Research Louisville. UCE-66. September 16, 2014

Myers A, Roberts H, **Rice R**, Eichenberger MR, Galandiuk S. Identification of an internal reference microRNA from the plasma of multiple cancer types. Research Louisville. UCE-63. September, 2014

National:

Rice J, Roberts H, Eichenberger MR, Pan J, Rai S, Galandiuk S. Plasma housekeeping gene free for all: a need for standardization. Academic Surgical Congress. Las Vegas, NV February, 2015.

TRPA1 mediates the effects of hypothermia on the monocyte inflammatory response. Galbraith NJ, Billeter At, Lawson C, **Rice JD**, Polk HC. Academic Surgical Congress. Las Vegas, NV February, 2015.

International:

Rice J. miR-99a influence on mTOR signaling regulation in colorectal cancer cell lines. 50th meeting of the European Society of Surgical Research, Liverpool, UK. June 13, 2015

- Activities**
- UTMB Clinical Preceptorship in the Department of Orthopedic Surgery, Summer 2008
 - UTMB Research Preceptorship in the Department of Orthopedic Surgery, Summer 2008-Fall 2008
 - UTMB St. Vincent's Free Clinic volunteer, 2007-2009
 - UTMB Orthopedic Surgery Student Organization Member, 2007-2009
 - UTMB Student Surgical Society Member, 2007-2011
 - UT Austin Cycling Team member, 2006-2007
 - UT Austin Undergraduate Research Investigator 2004-2007

UT Austin, Texas Union Film Committee 2004-2007

Austin Children's Hospital Volunteer, Fall 2004, Fall 2005

Texas Union Theater Volunteer, Spring 2003-Spring 2007

UT Austin Undergraduate Research Focus Group member, Spring 2003-Spring 2007

University of Oklahoma Union Programming Board, 2002-2003

University of Oklahoma Honors College Council Member, 2002-2003

Interests Current events, hockey, vinyl record collecting, cycling, film, literature, percussion instruments, videogames and culinary arts